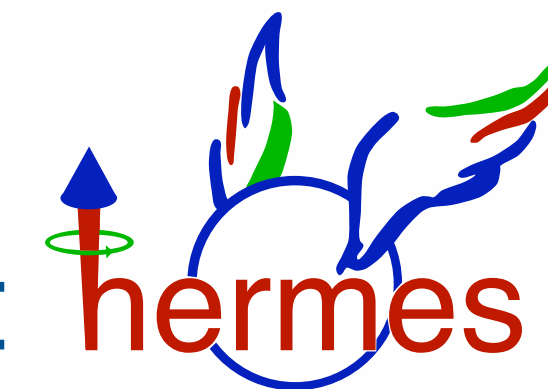




Exclusive processes at  hermes

Generalized parton distributions

- I believe Peter has done a good job this morning introducing generalized parton distributions (GPDs) ...



Generalized parton distributions

- I believe Peter has done a good job this morning introducing generalized parton distributions (GPDs) ...

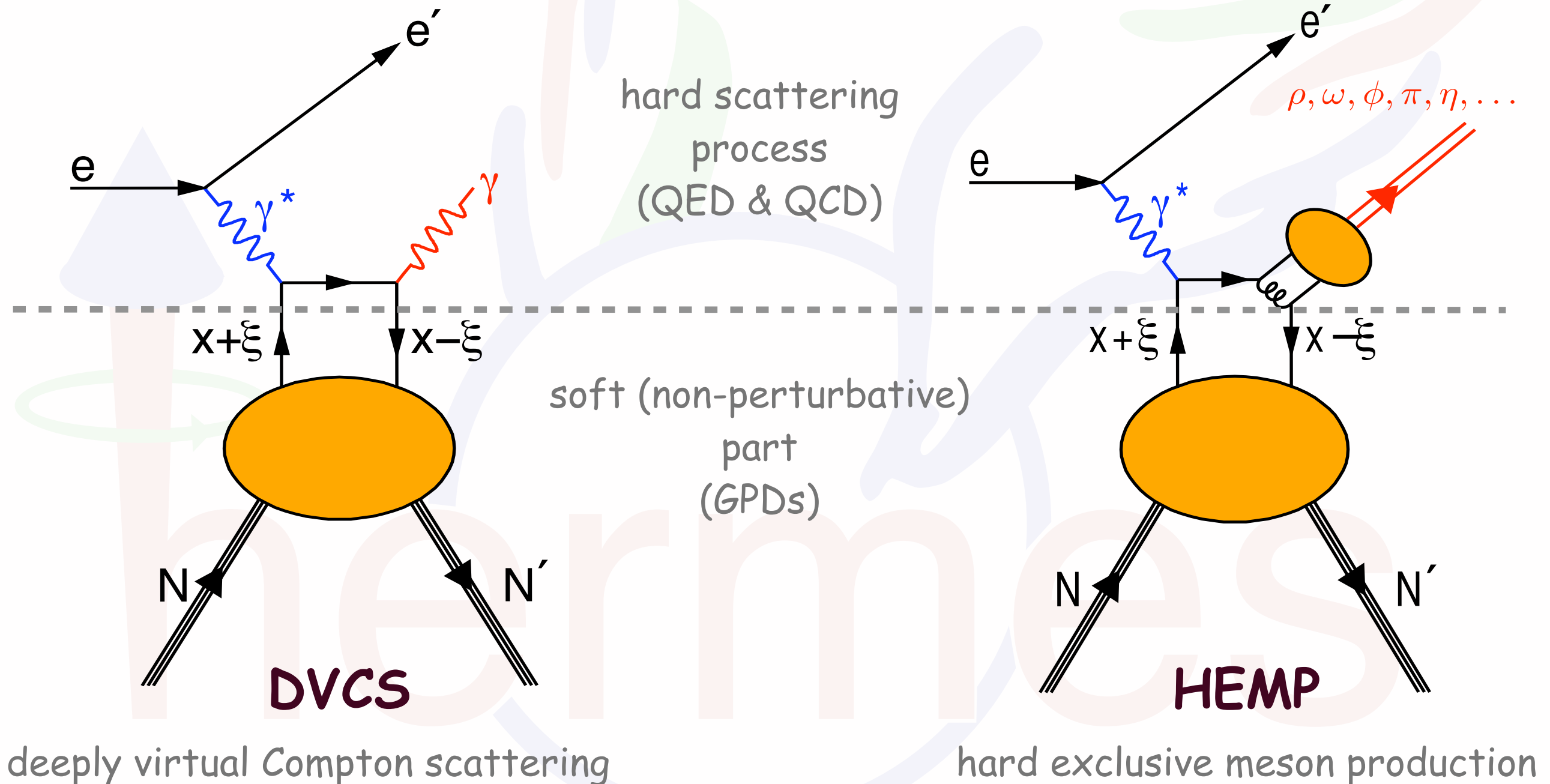
... thanks!

Generalized parton distributions

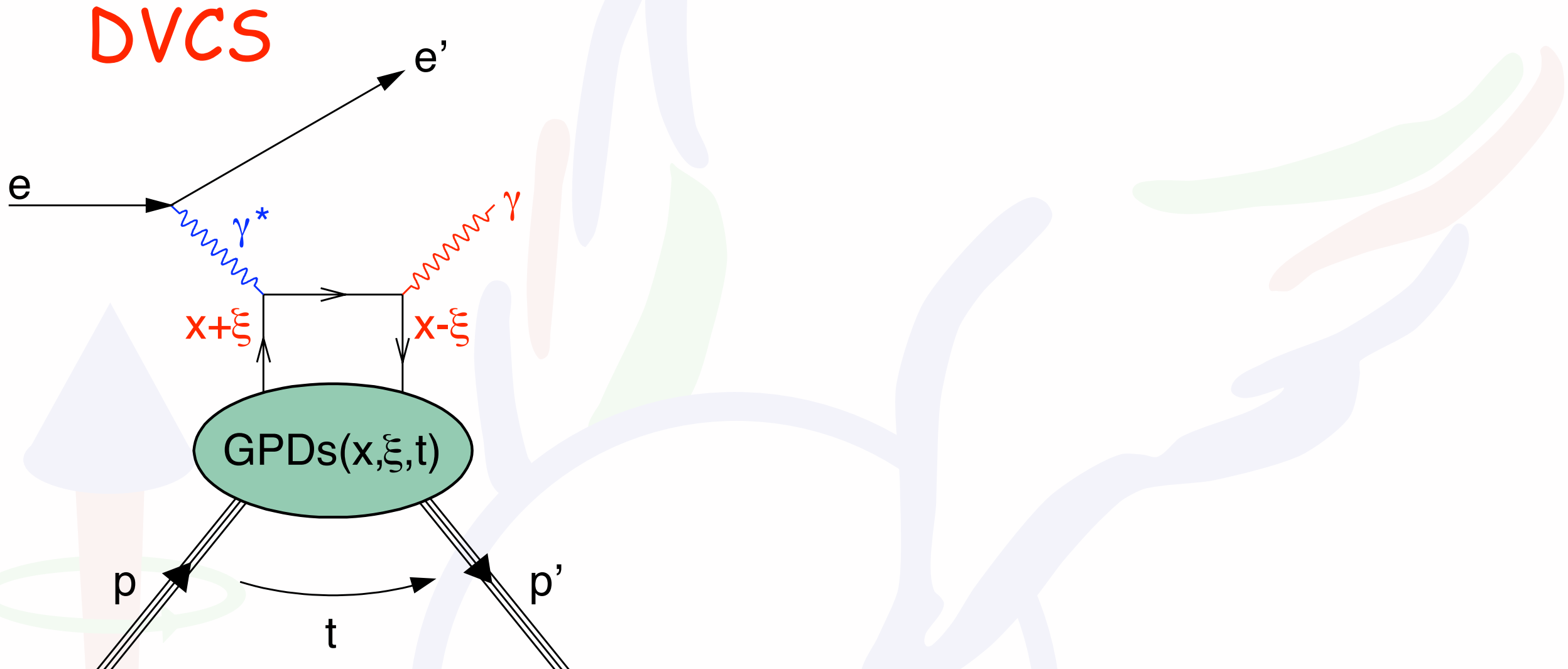
- I believe Peter has done a good job this morning introducing generalized parton distributions (GPDs) ...
- ... thanks!
- ... also to Erik Etzelmüller and Charlotte Van Hulse for "slides support"

GPDs in exclusive reactions

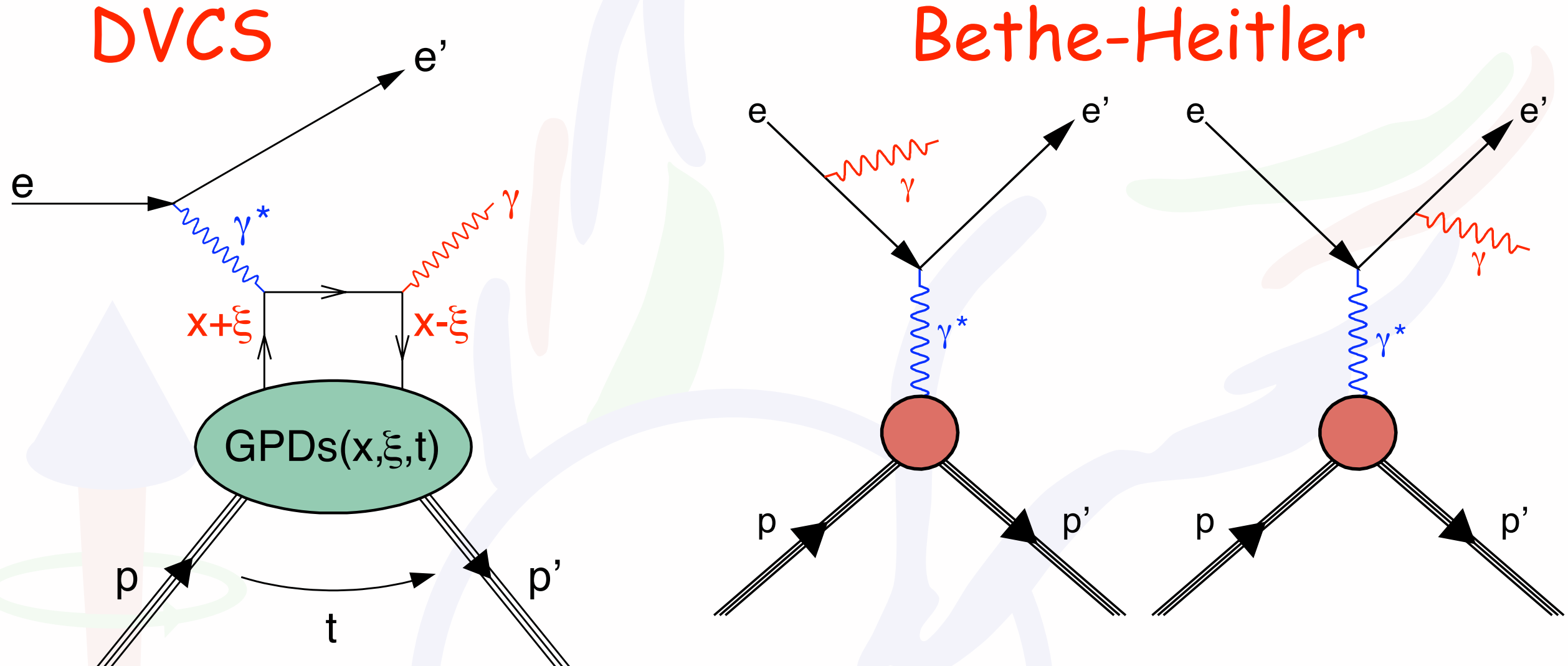
Experimentally GPDs can be accessed through measurements of hard exclusive lepton-nucleon scattering processes.



Real-photon production

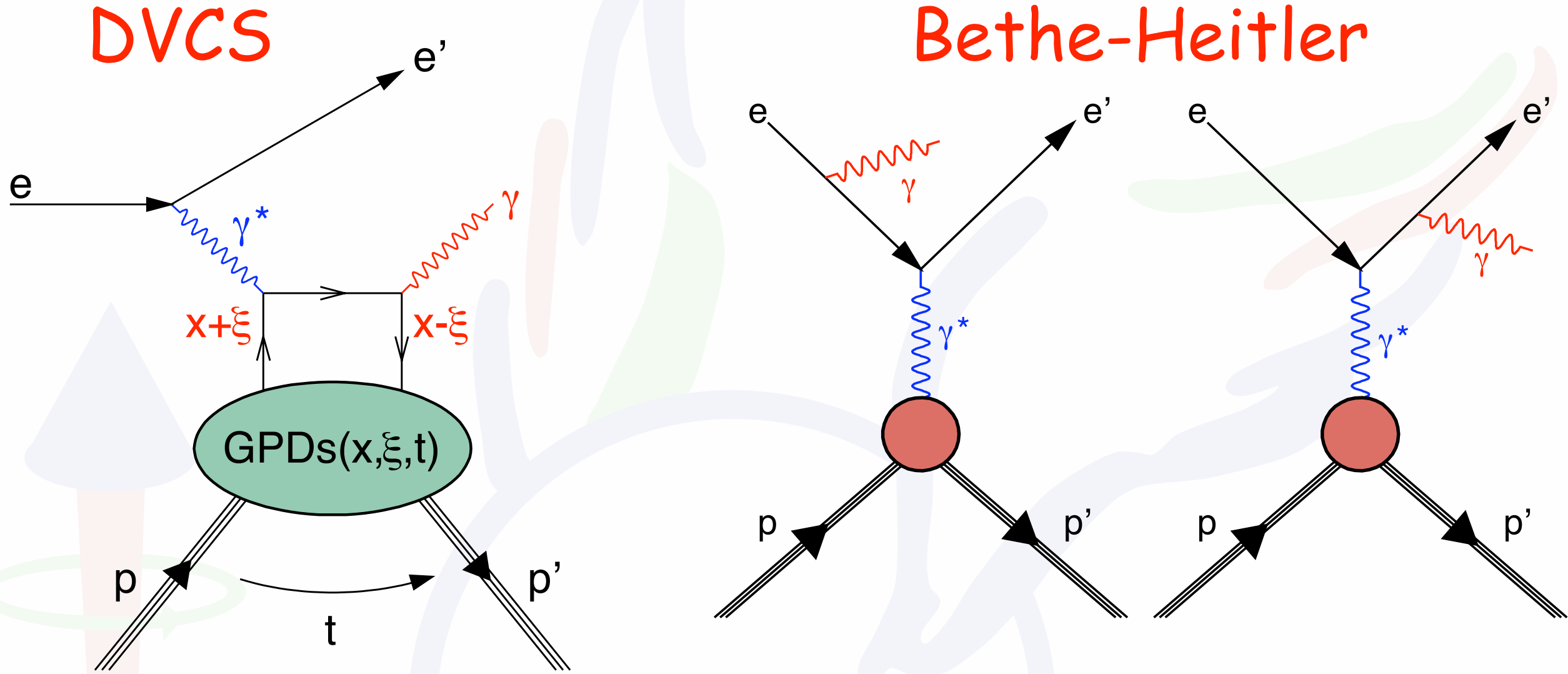


Real-photon production



$$\frac{d^4\sigma}{dQ^2 dx_B dt d\phi} = \frac{y^2}{32(2\pi)^4 \sqrt{1 + \frac{4M^2x_B^2}{Q^2}}} (|\mathcal{T}_{\text{DVCS}}|^2 + |\mathcal{T}_{\text{BH}}|^2 + \mathcal{I})$$

Real-photon production



Amplitude of Bethe-Heitler scattering is dominant at HERMES kinematics

$$\frac{d^4\sigma}{dQ^2 dx_B dt d\phi} = \frac{y^2}{32(2\pi)^4 \sqrt{1 + \frac{4M^2 x_B^2}{Q^2}}} (|\mathcal{T}_{\text{DVCS}}|^2 + |\mathcal{T}_{\text{BH}}|^2 + \boxed{\mathcal{I}})$$

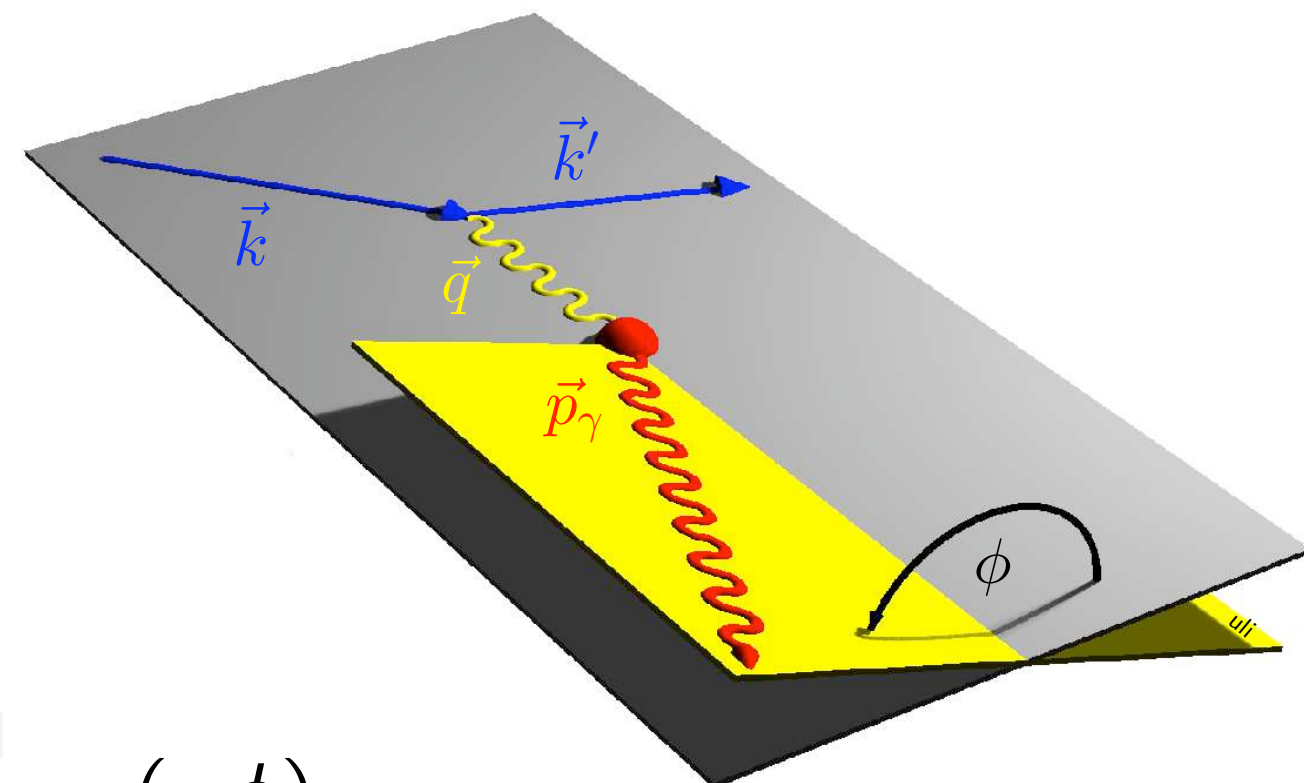
DVCS amplitude is amplified by BH in the interference term

Azimuthal dependences in DVCS/BH

- beam polarization P_B
- beam charge C_B
- here: unpolarized target

Fourier expansion for ϕ :

$$|\mathcal{T}_{\text{BH}}|^2 = \frac{K_{\text{BH}}}{\mathcal{P}_1(\phi)\mathcal{P}_2(\phi)} \sum_{n=0}^2 c_n^{\text{BH}} \cos(n\phi)$$



calculable in QED
(using form-factor measurements)

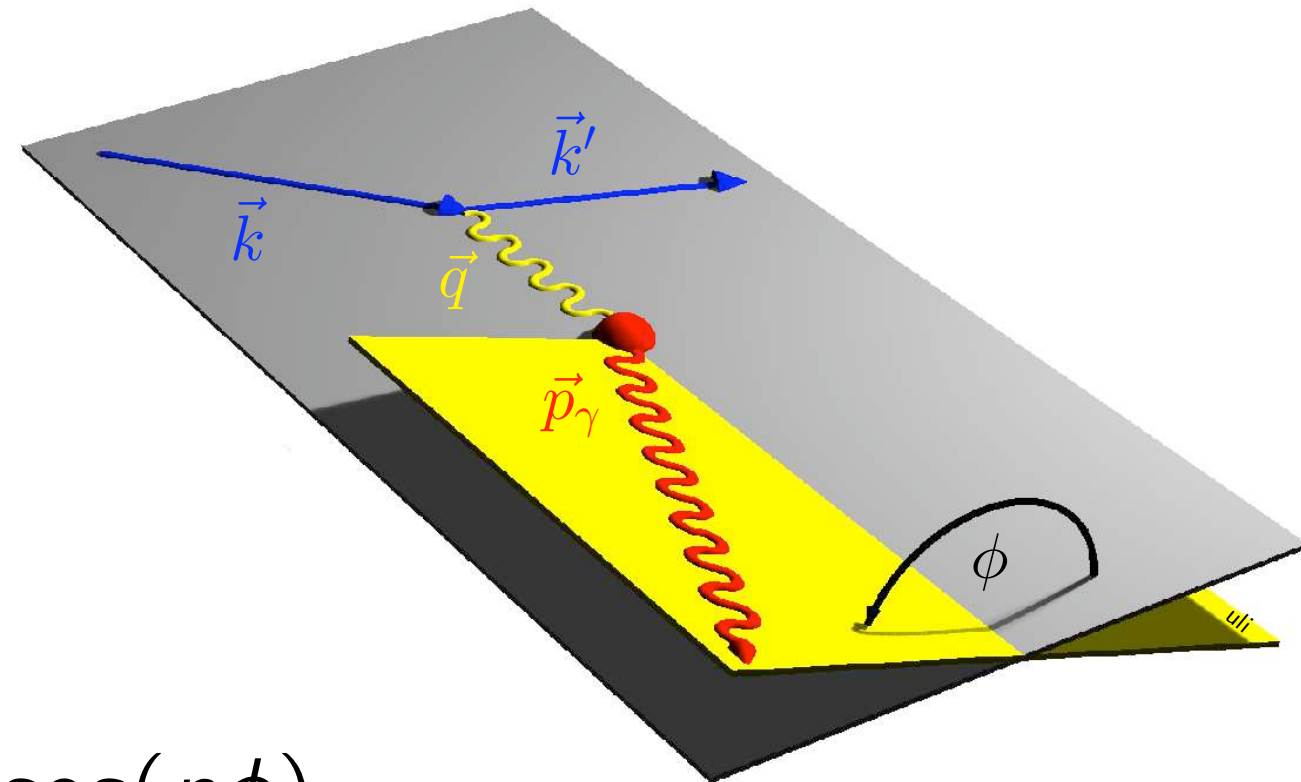
Azimuthal dependences in DVCS/BH

- beam polarization P_B
- beam charge C_B
- here: unpolarized target

Fourier expansion for ϕ :

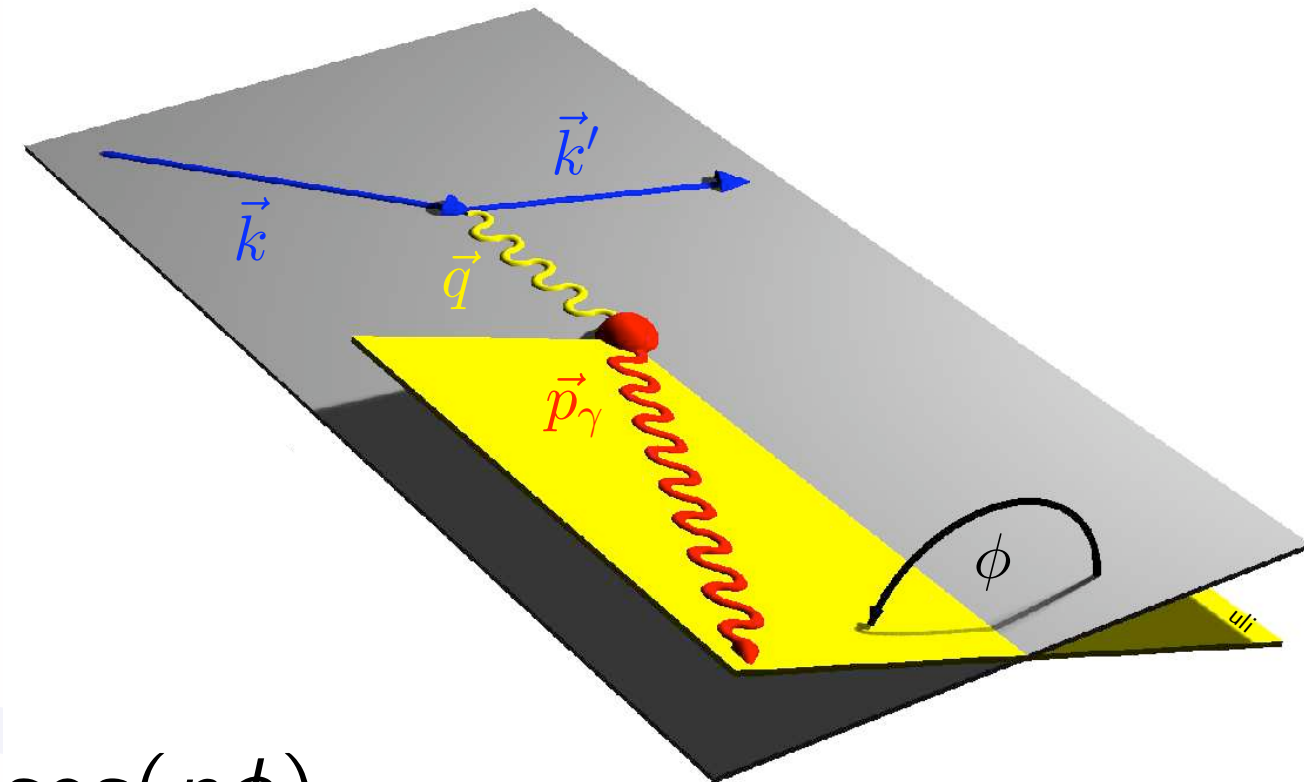
$$|\mathcal{T}_{\text{BH}}|^2 = \frac{K_{\text{BH}}}{\mathcal{P}_1(\phi)\mathcal{P}_2(\phi)} \sum_{n=0}^2 c_n^{\text{BH}} \cos(n\phi)$$

$$|\mathcal{T}_{\text{DVCS}}|^2 = K_{\text{DVCS}} \left[\sum_{n=0}^2 c_n^{\text{DVCS}} \cos(n\phi) + P_B \sum_{n=1}^1 s_n^{\text{DVCS}} \sin(n\phi) \right]$$



Azimuthal dependences in DVCS/BH

- beam polarization P_B
- beam charge C_B
- here: unpolarized target



Fourier expansion for ϕ :

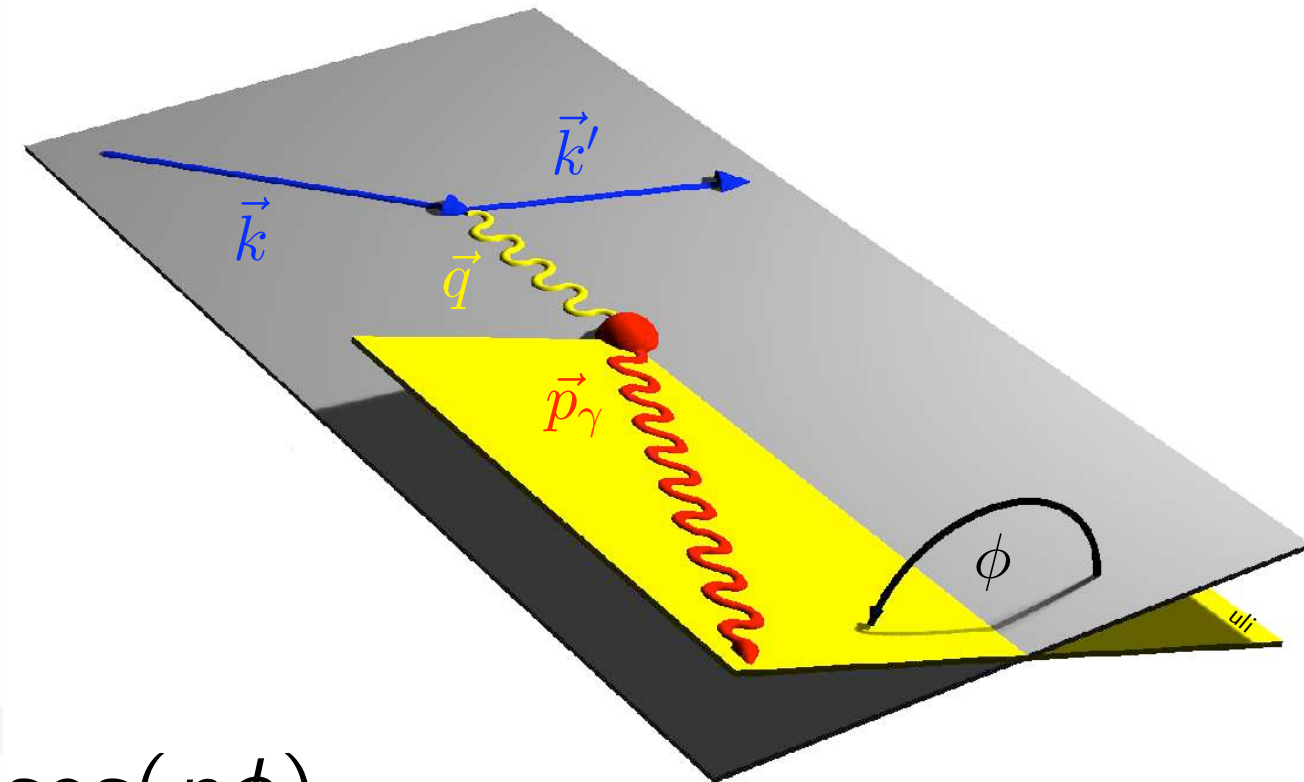
$$|\mathcal{T}_{\text{BH}}|^2 = \frac{K_{\text{BH}}}{\mathcal{P}_1(\phi)\mathcal{P}_2(\phi)} \sum_{n=0}^2 c_n^{\text{BH}} \cos(n\phi)$$

$$|\mathcal{T}_{\text{DVCS}}|^2 = K_{\text{DVCS}} \left[\sum_{n=0}^2 c_n^{\text{DVCS}} \cos(n\phi) + P_B \sum_{n=1}^1 s_n^{\text{DVCS}} \sin(n\phi) \right]$$

$$\mathcal{I} = \frac{C_B K_{\mathcal{I}}}{\mathcal{P}_1(\phi)\mathcal{P}_2(\phi)} \left[\sum_{n=0}^3 c_n^{\mathcal{I}} \cos(n\phi) + P_B \sum_{n=1}^2 s_n^{\mathcal{I}} \sin(n\phi) \right]$$

Azimuthal dependences in DVCS/BH

- beam polarization P_B
- beam charge C_B
- here: unpolarized target



Fourier expansion for ϕ :

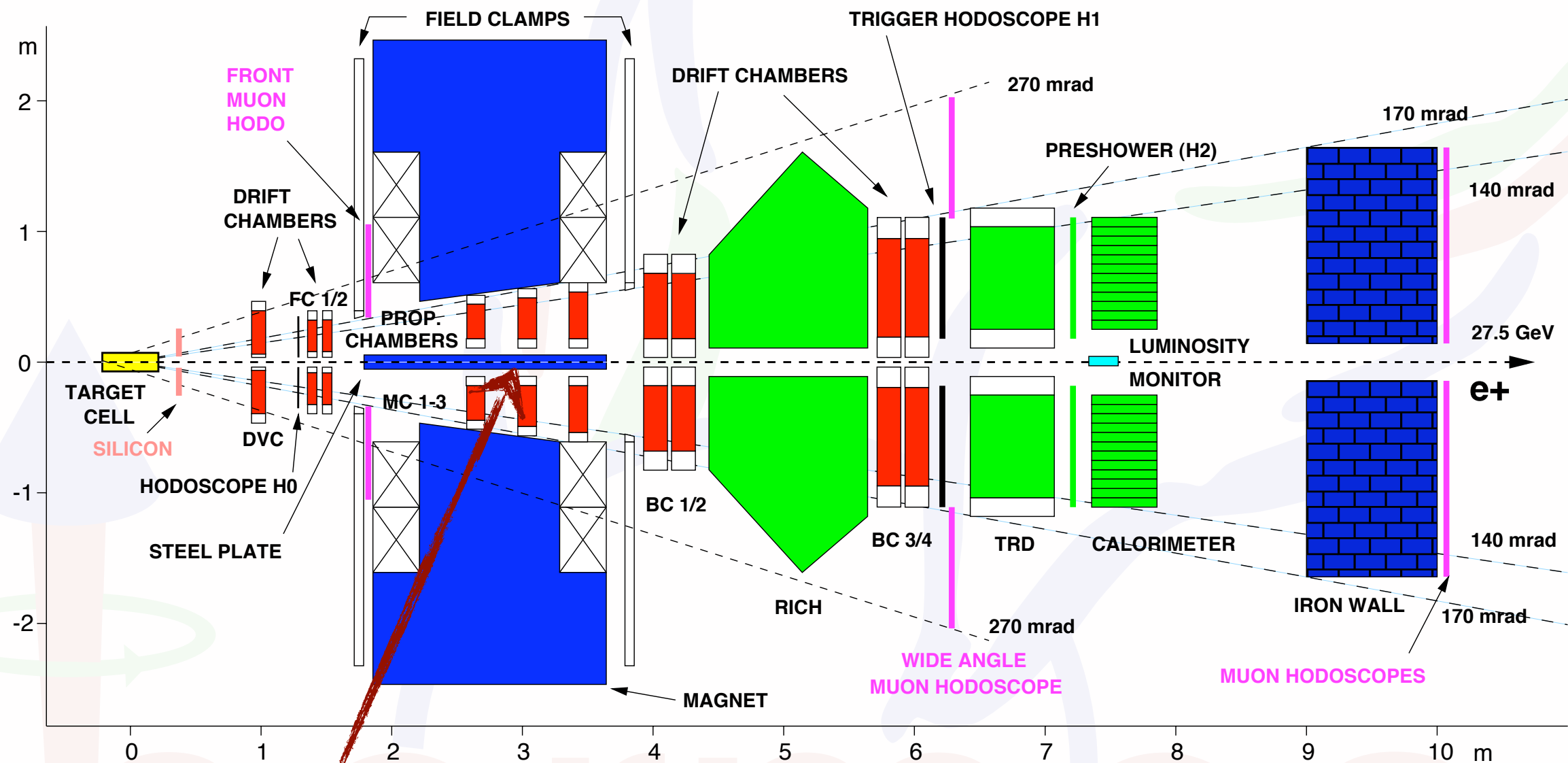
$$|\mathcal{T}_{\text{BH}}|^2 = \frac{K_{\text{BH}}}{\mathcal{P}_1(\phi)\mathcal{P}_2(\phi)} \sum_{n=0}^2 c_n^{\text{BH}} \cos(n\phi)$$

$$|\mathcal{T}_{\text{DVCS}}|^2 = K_{\text{DVCS}} \left[\sum_{n=0}^2 c_n^{\text{DVCS}} \cos(n\phi) + P_B \sum_{n=1}^1 s_n^{\text{DVCS}} \sin(n\phi) \right]$$

$$\mathcal{I} = \frac{C_B K_I}{\mathcal{P}_1(\phi)\mathcal{P}_2(\phi)} \left[\sum_{n=0}^3 c_n^I \cos(n\phi) + P_B \sum_{n=1}^2 s_n^I \sin(n\phi) \right]$$

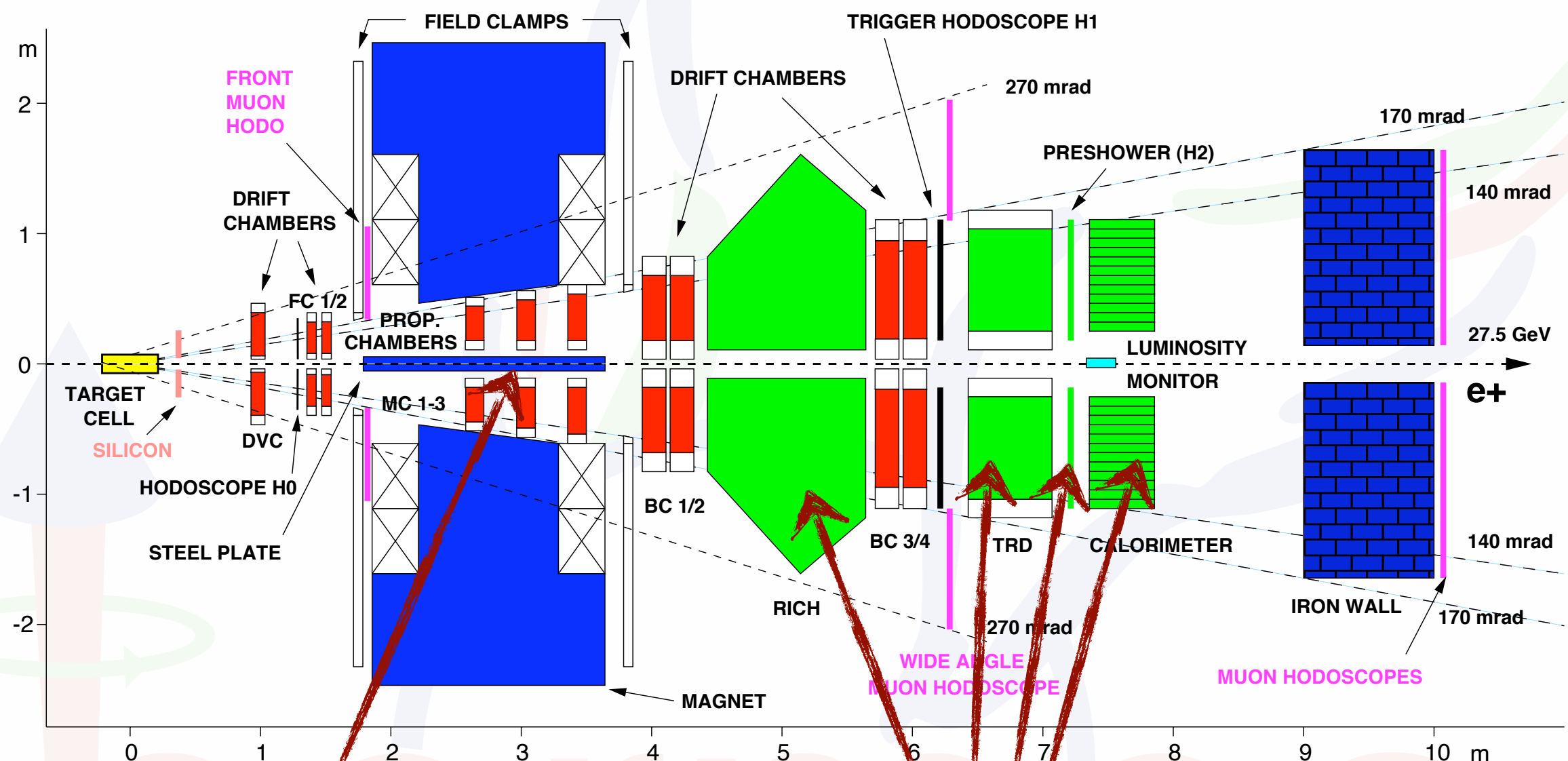
bilinear ("DVCS") or linear ("I") in GPDs

HERMES (1998-2005) schematically



two (mirror-symmetric) halves
 -> no homogenous azimuthal
 coverage

HERMES (1998-2005) schematically



two (mirror-symmetric) halves
-> no homogenous azimuthal
coverage

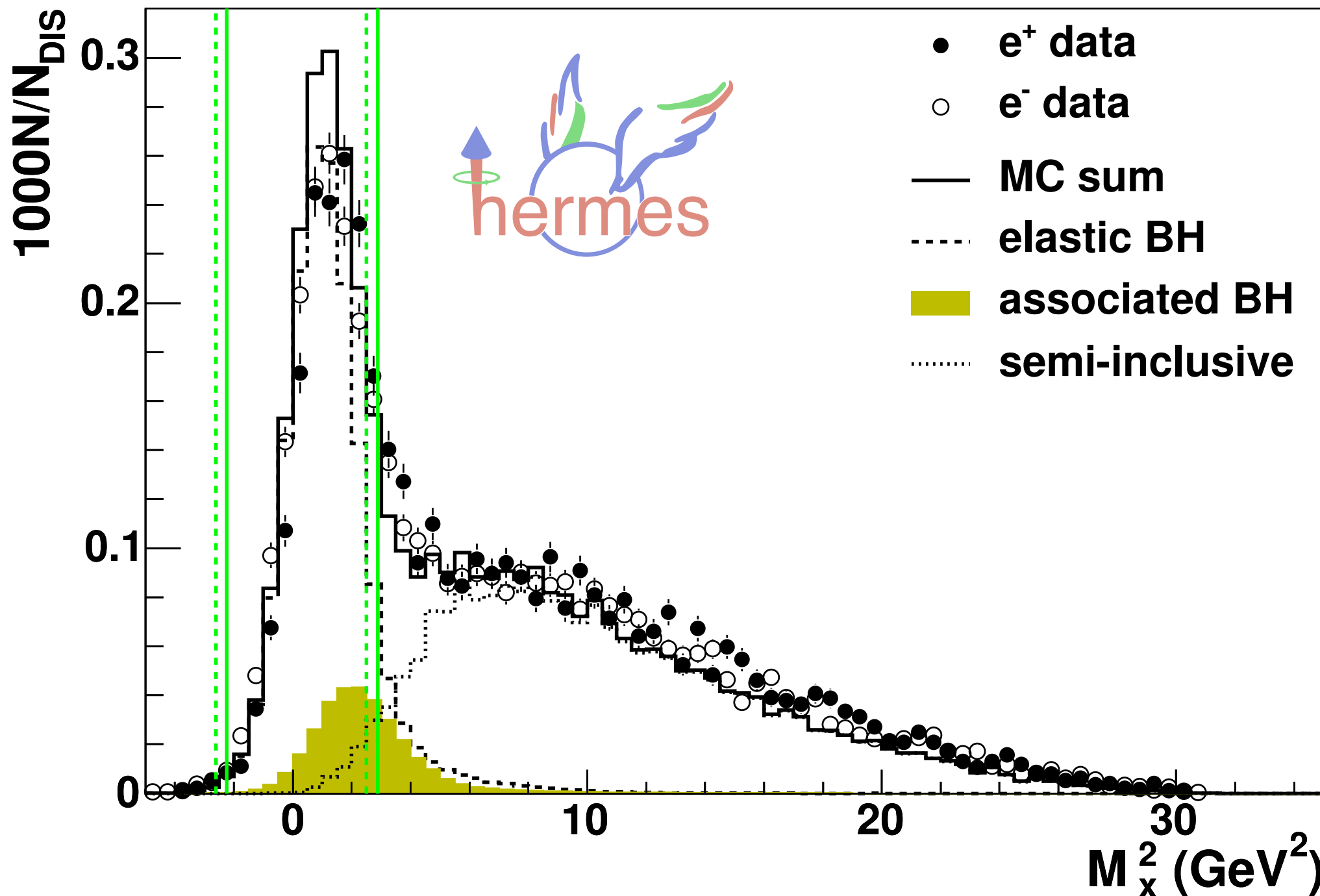
Particle ID detectors allow for

- lepton/hadron separation
- RICH: pion/kaon/proton discrimination $2\text{GeV} < p < 15\text{GeV}$

Exclusivity: missing-mass technique

$$M_x^2 = (k - k' + P_0 - P_\gamma)^2 = M^2 + 2M(\nu - E_\gamma) + t$$

ep $\rightarrow e \gamma X$

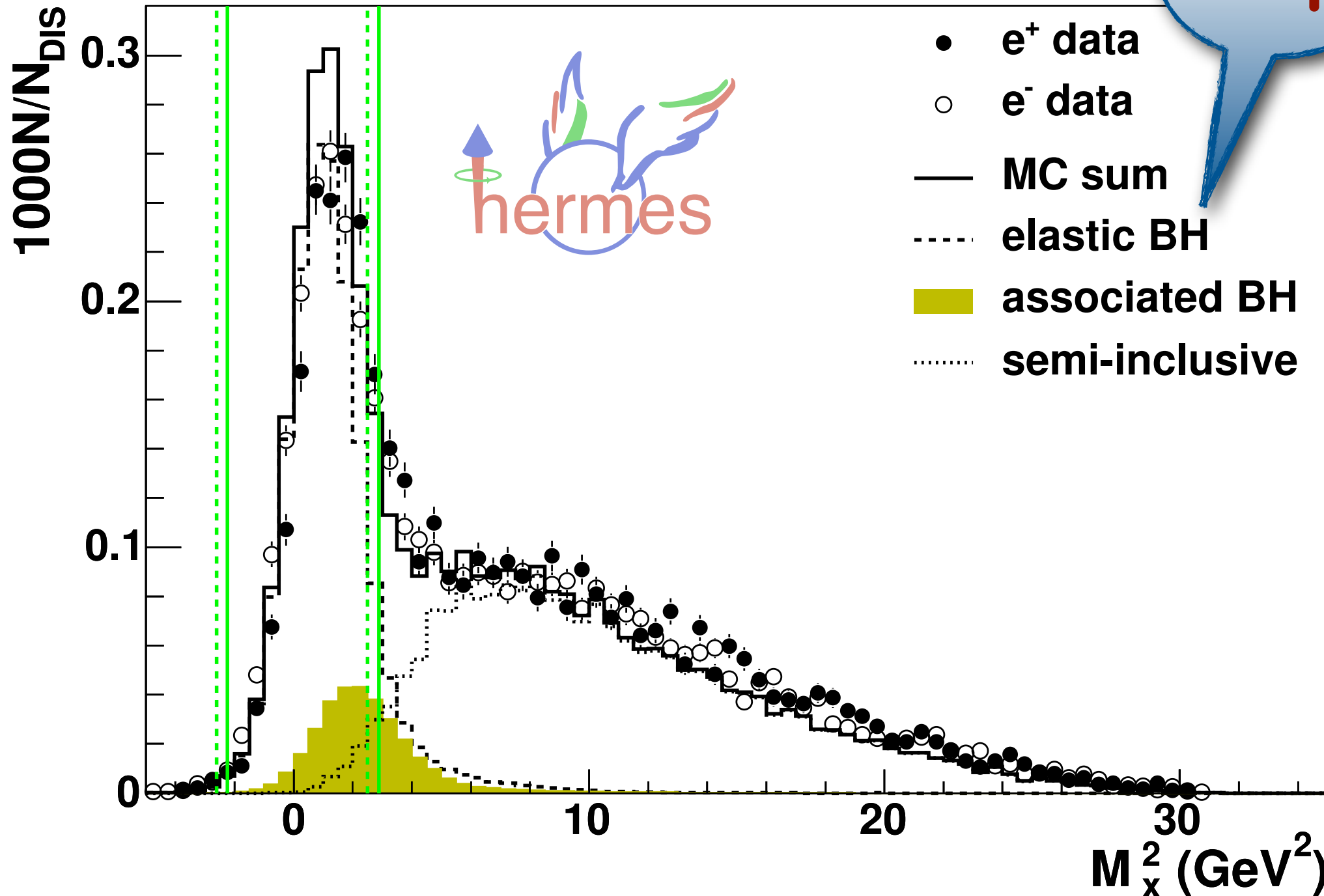


Exclusivity: missing-mass technique

$$M_x^2 = (k - k' + P_0 - P_\gamma)^2 = M^2 + 2M(\nu - E_\gamma) + t$$

$e p \rightarrow e \gamma X$

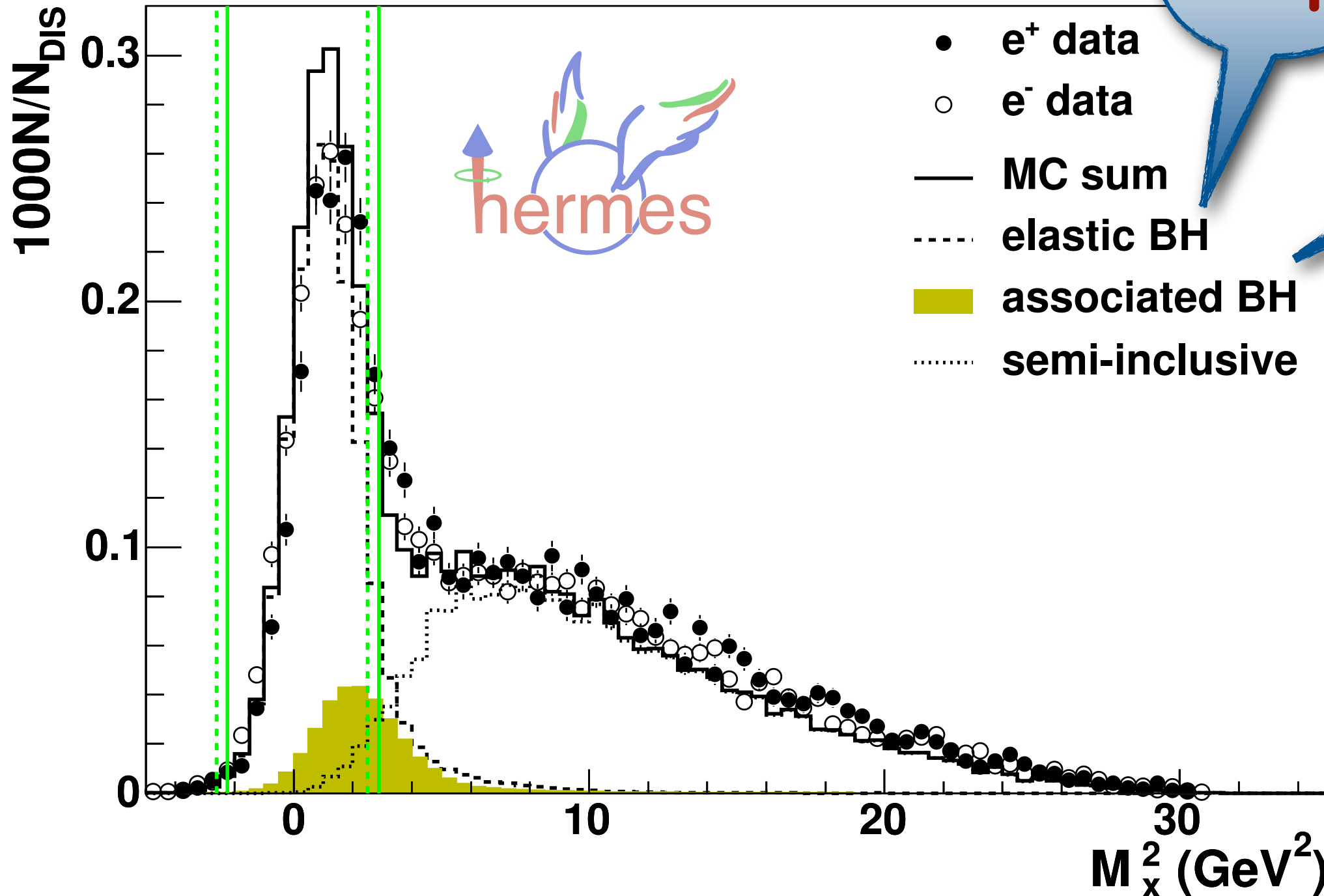
$X=p$



Exclusivity: missing-mass technique

$$M_x^2 = (k - k' + P_0 - P_\gamma)^2 = M^2 + 2M(\nu - E_\gamma) + t$$

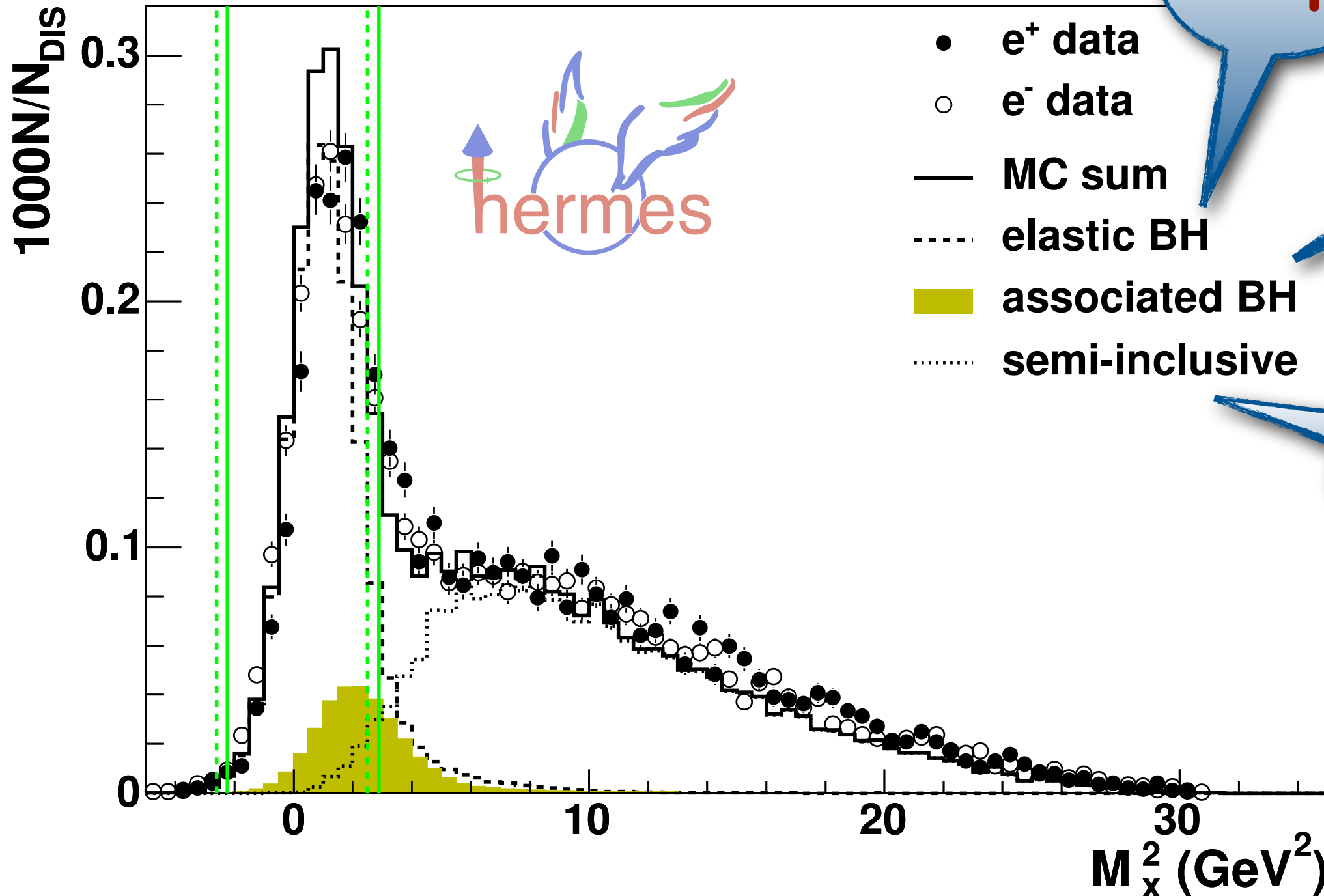
$e p \rightarrow e \gamma X$



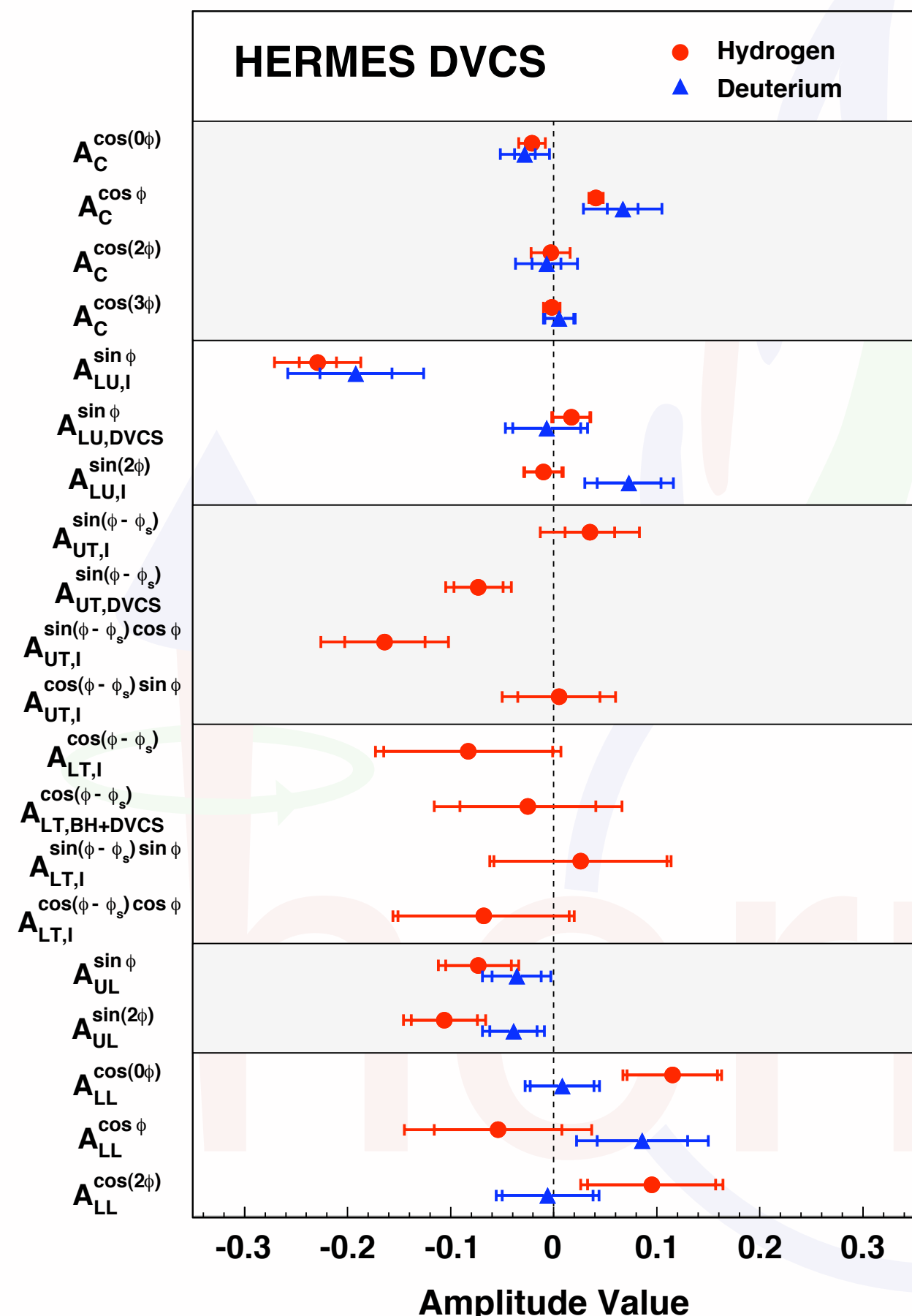
Exclusivity: missing-mass technique

$$M_x^2 = (k - k' + P_0 - P_\gamma)^2 = M^2 + 2M(\nu - E_\gamma) + t$$

$e p \rightarrow e \gamma X$



A wealth of azimuthal amplitudes



Beam-charge asymmetry:
GPD H

Beam-helicity asymmetry:
GPD H

Transverse target spin asymmetries:
GPD E from proton target

Longitudinal target spin asymmetry:

GPD \tilde{H}

Double-spin asymmetry:

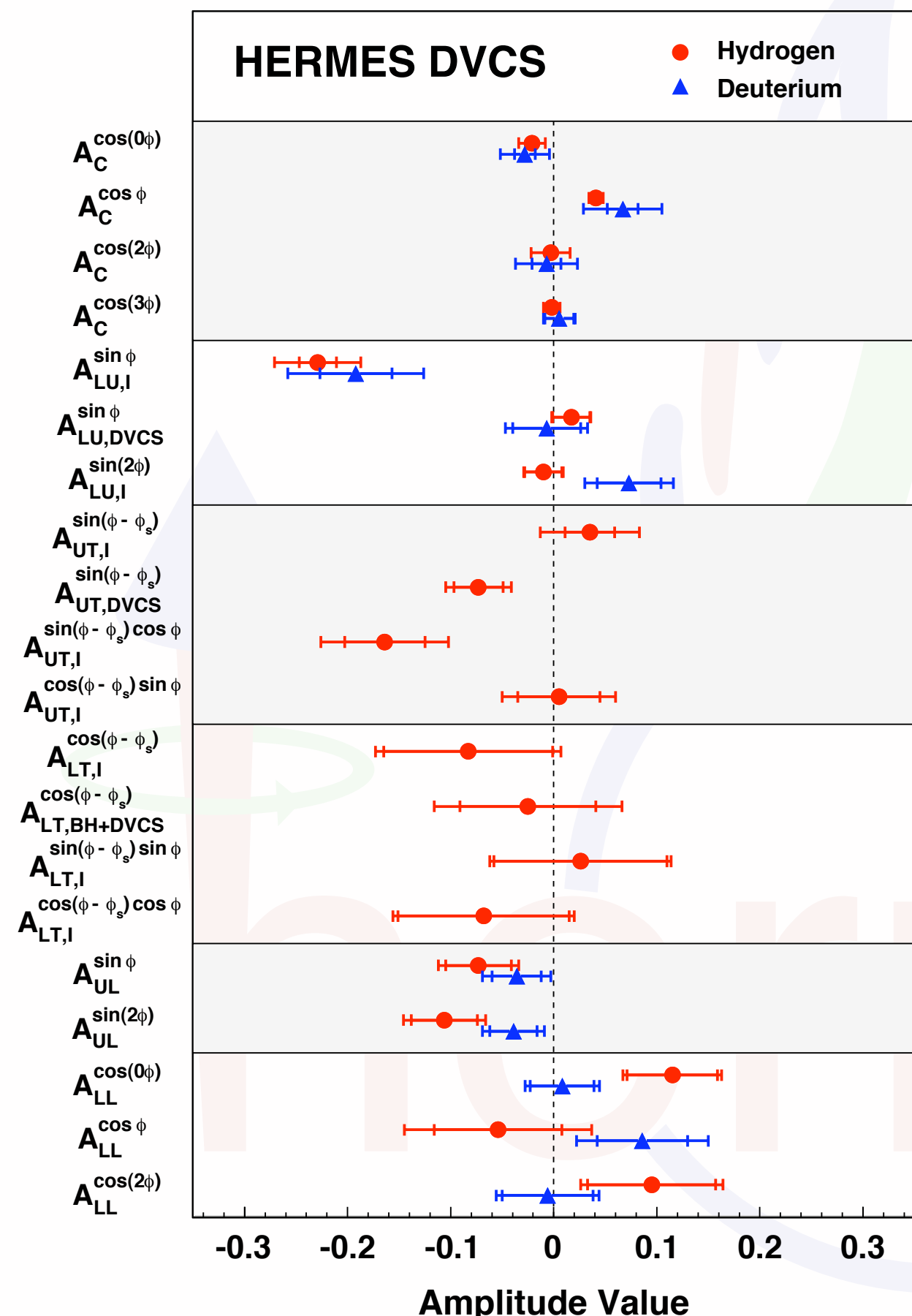
GPD \tilde{H}

- PRD 75 (2007) 011103
- NPB 829 (2010) 1
- JHEP 11 (2009) 083
- PRC 81 (2010) 035202
- PRL 87 (2001) 182001
- JHEP 07 (2012) 032

- JHEP 06 (2008) 066
- PLB 704 (2011) 15

- JHEP 06 (2010) 019
- NPB 842 (2011) 265

A wealth of azimuthal amplitudes



Beam-charge asymmetry:
GPD H

Beam-helicity asymmetry:
GPD H

Transverse target spin asymmetries:
GPD E from proton target

Longitudinal target spin asymmetry:

GPD \tilde{H}

Double-spin asymmetry:

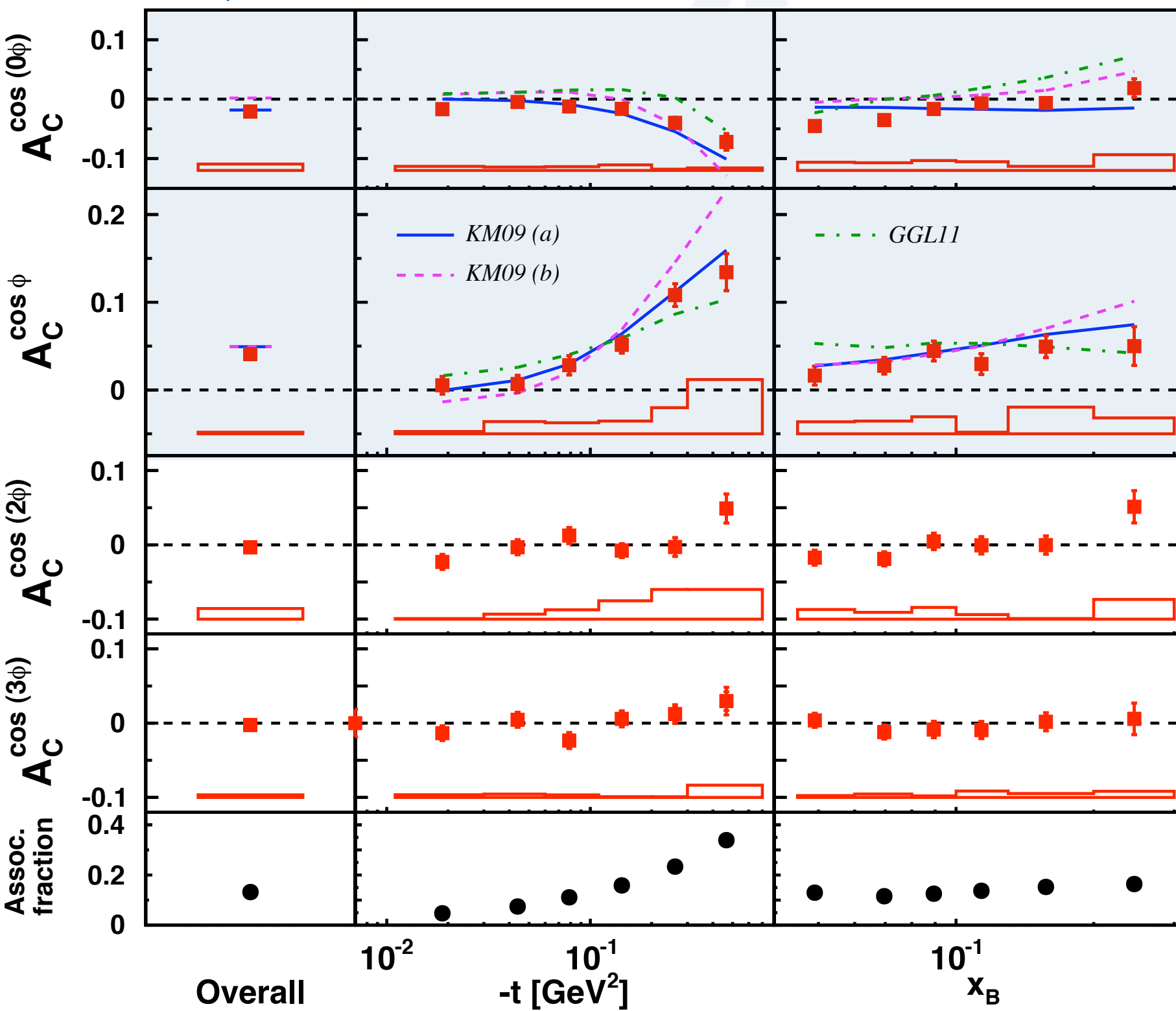
GPD \tilde{H}

- PRD 75 (2007) 011103
- NPB 829 (2010) 1
- JHEP 11 (2009) 083
- PRC 81 (2010) 035202
- PRL 87 (2001) 182001
- JHEP 07 (2012) 032

complete data set!

Beam-charge asymmetry

[Airapetian et al., JHEP 07 (2012) 032]



constant term:

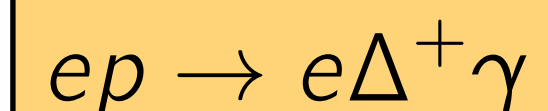
$$\propto -A_C^{\cos \phi}$$

$$\propto \text{Re}[F_1 \mathcal{H}]$$

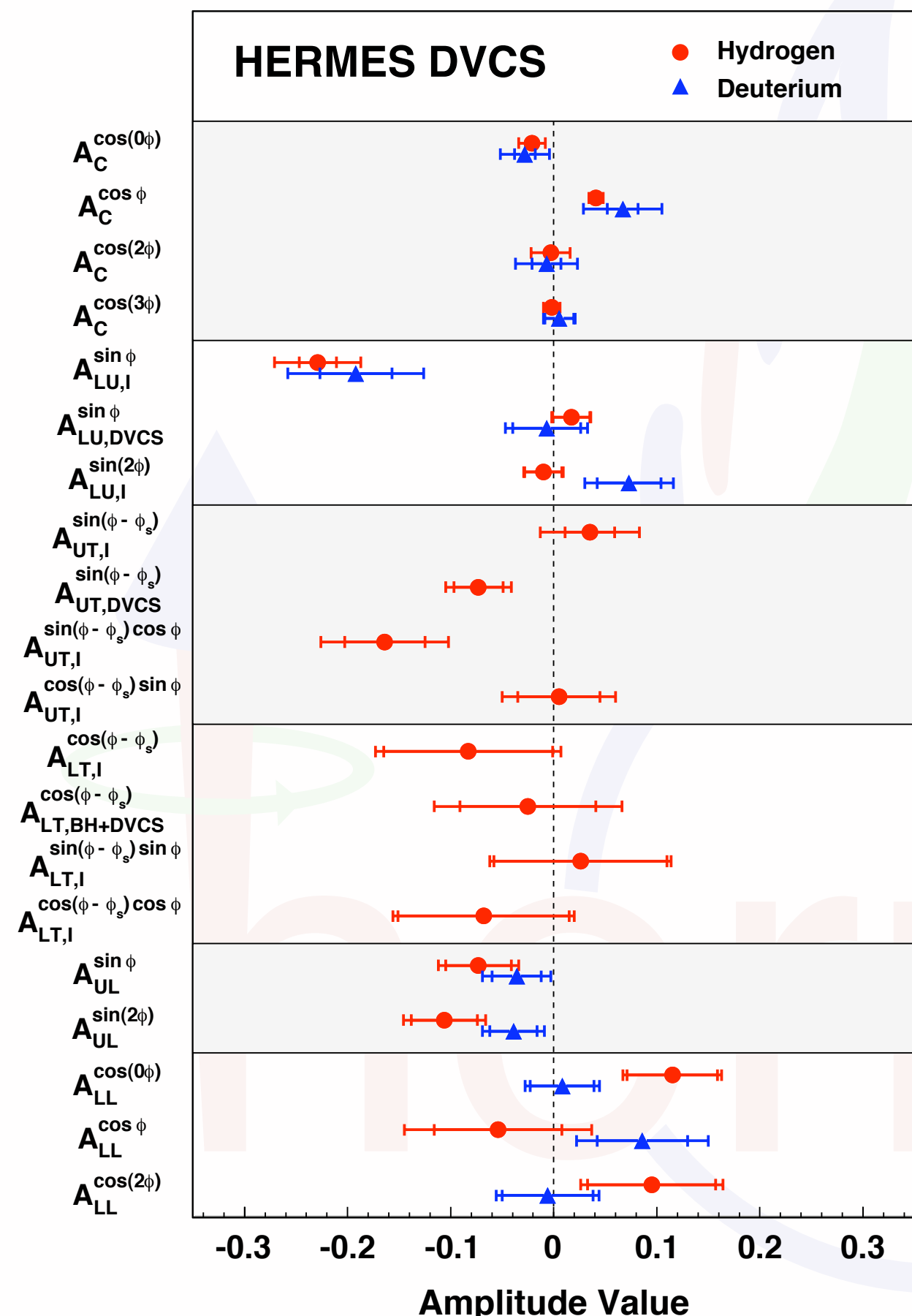
[higher twist]

[gluon leading twist]

Resonant fraction:



A wealth of azimuthal amplitudes



Beam-charge asymmetry:
GPD H

Beam-helicity asymmetry:
GPD H

Transverse target spin asymmetries:
GPD E from proton target

Longitudinal target spin asymmetry:

GPD \tilde{H}

Double-spin asymmetry:

GPD \tilde{H}

PRD 75 (2007) 011103

NPB 829 (2010) 1

JHEP 11 (2009) 083

PRC 81 (2010) 035202

PRL 87 (2001) 182001

JHEP 07 (2012) 032

JHEP 06 (2008) 066

PLB 704 (2011) 15

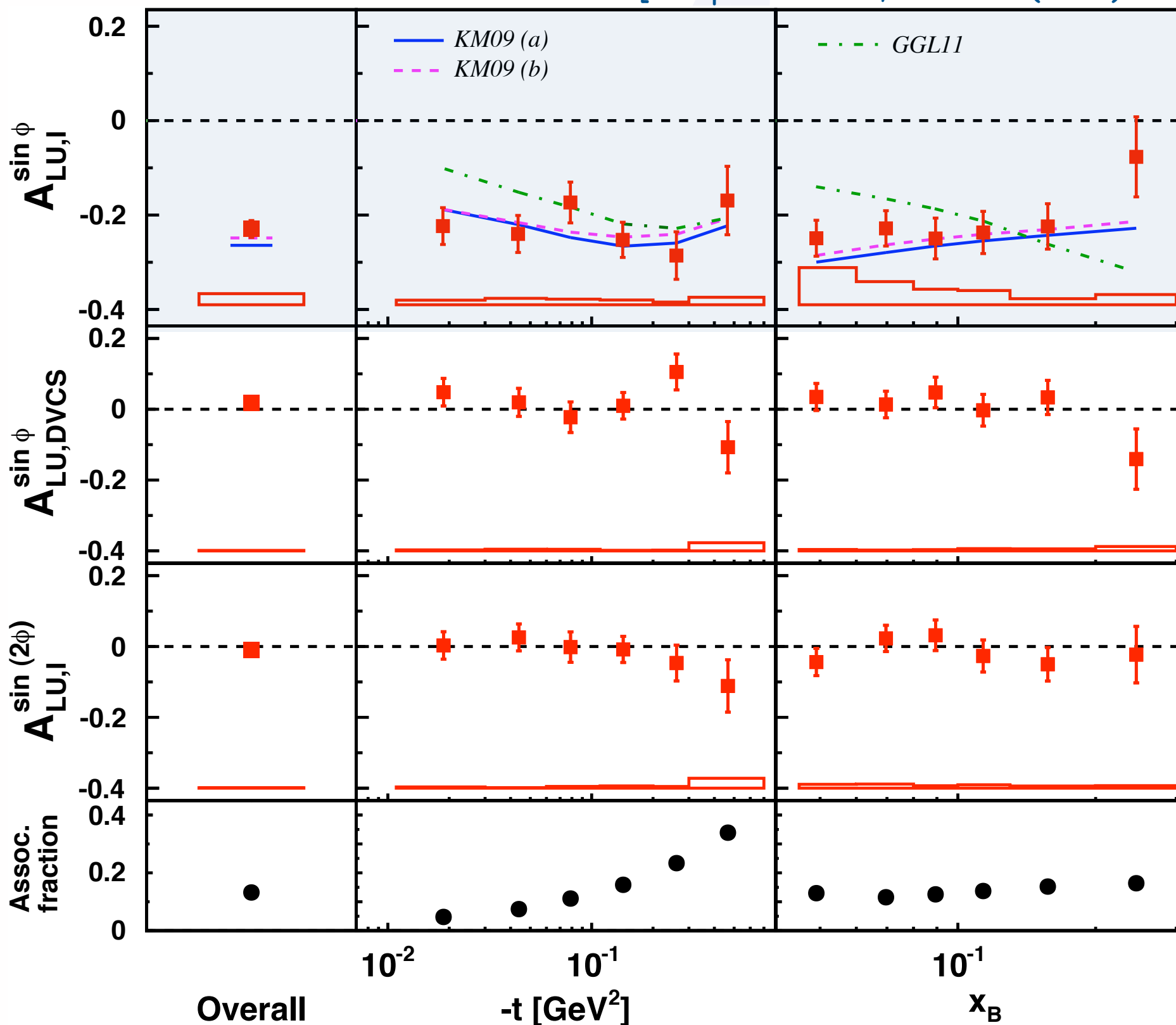
JHEP 06 (2010) 019

NPB 842 (2011) 265

complete data set!

Beam-spin asymmetry

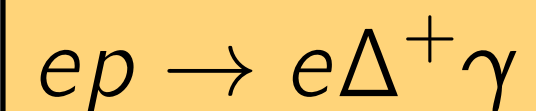
[Airapetian et al., JHEP 07 (2012) 032]



$$\propto \text{Im}[F_1 \mathcal{H}]$$

[higher twist]

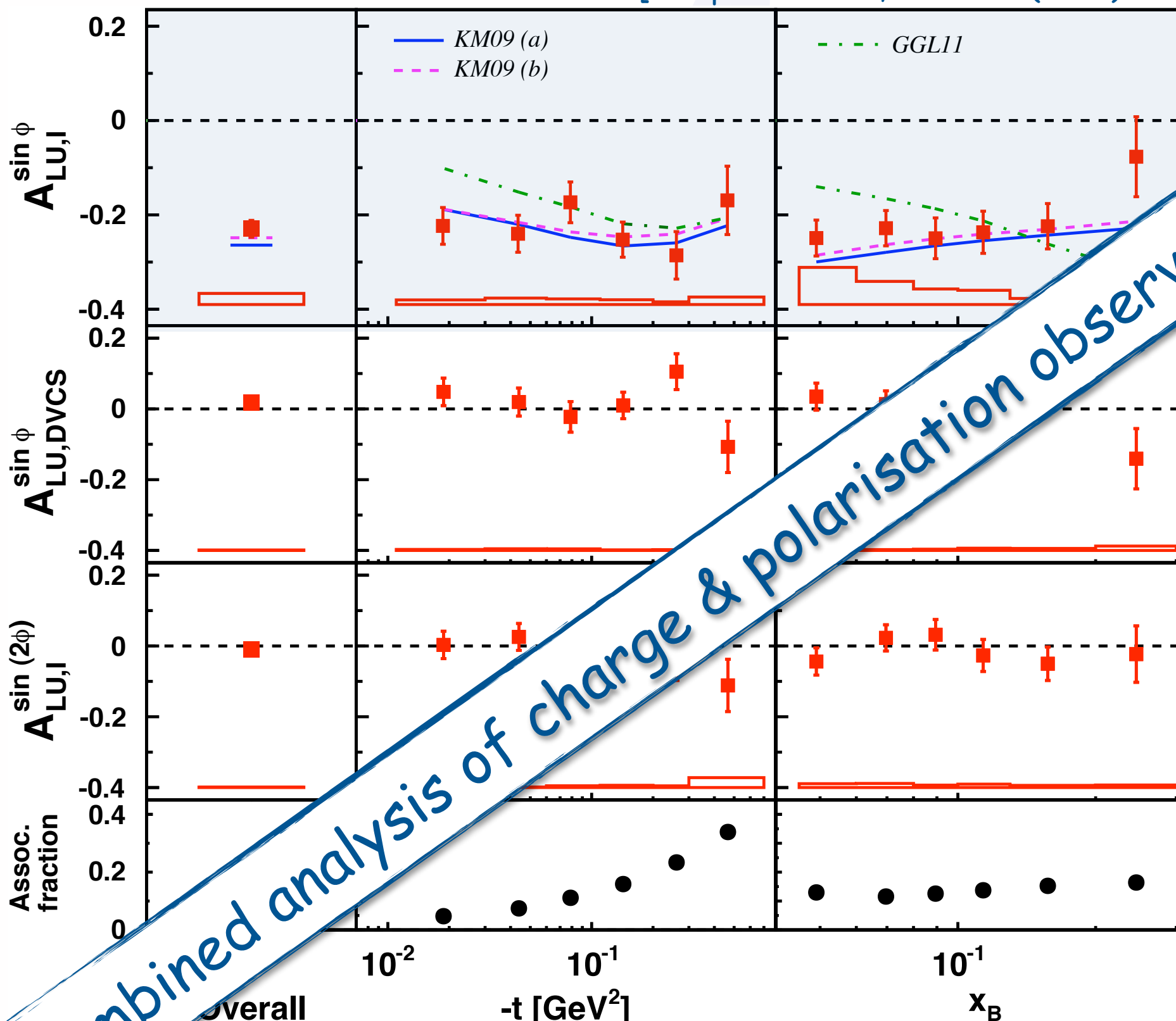
Resonant fraction:



complete data set!

Beam-spin asymmetries

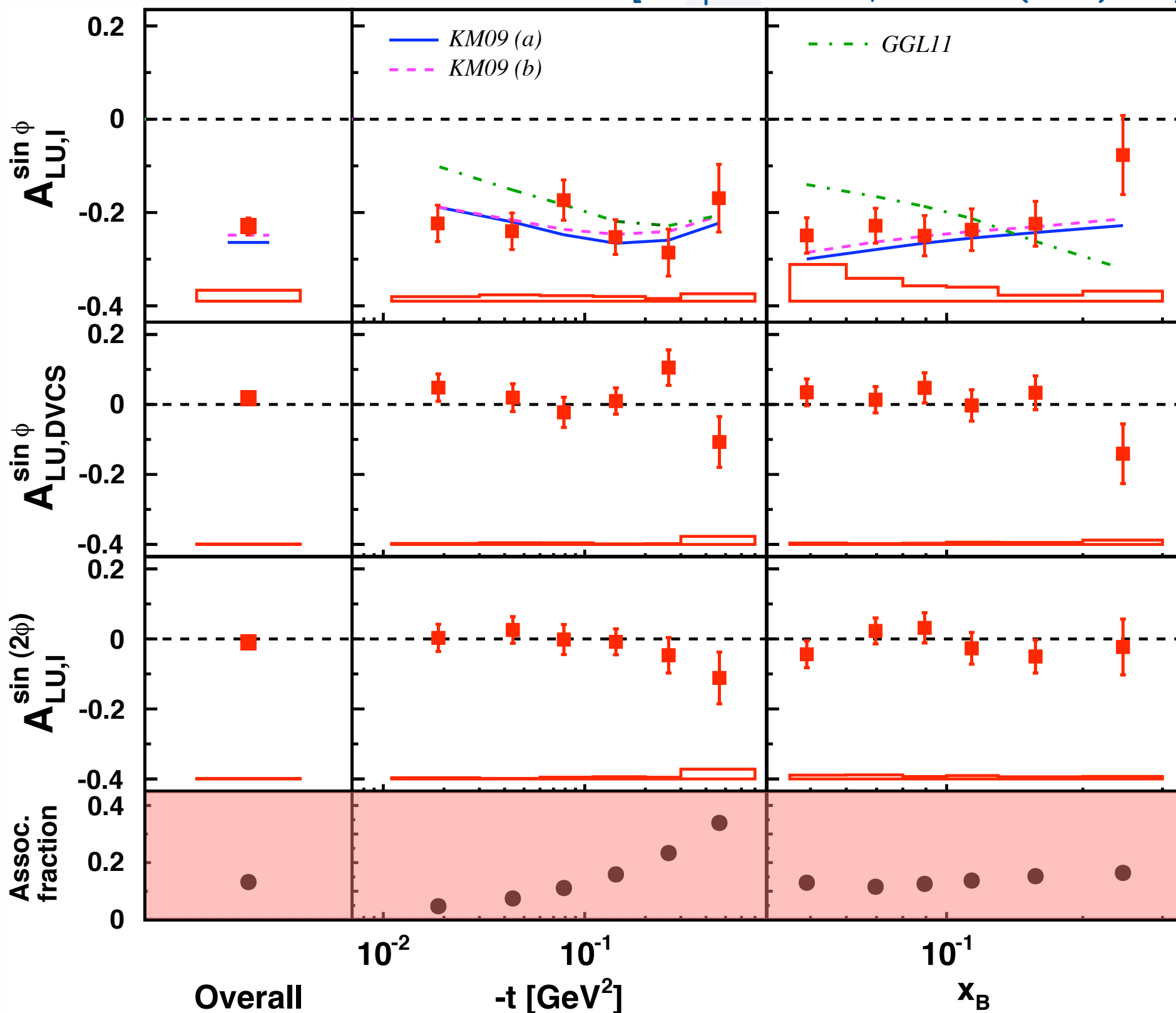
[Airapetian et al., JHEP 07 (2012) 032]



complete data set!

Beam-spin asymmetry

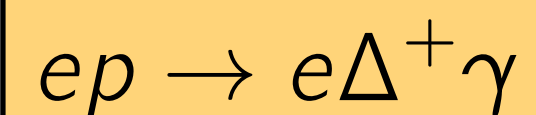
[Airapetian et al., JHEP 07 (2012) 032]



$$\propto \text{Im}[F_1 \mathcal{H}]$$

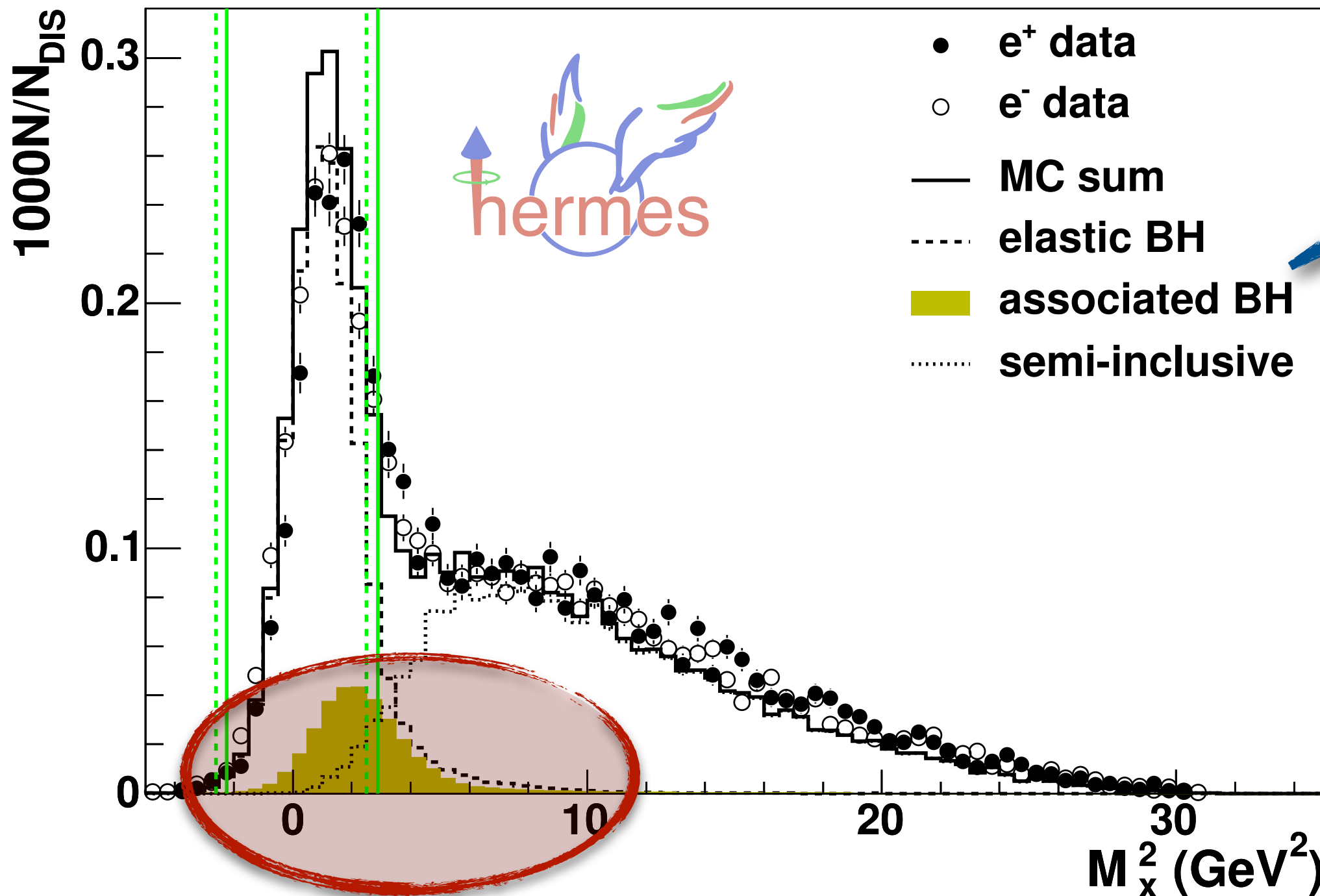
[higher twist]

Resonant fraction:



Exclusivity: missing-mass technique

$e p \rightarrow e \gamma X$

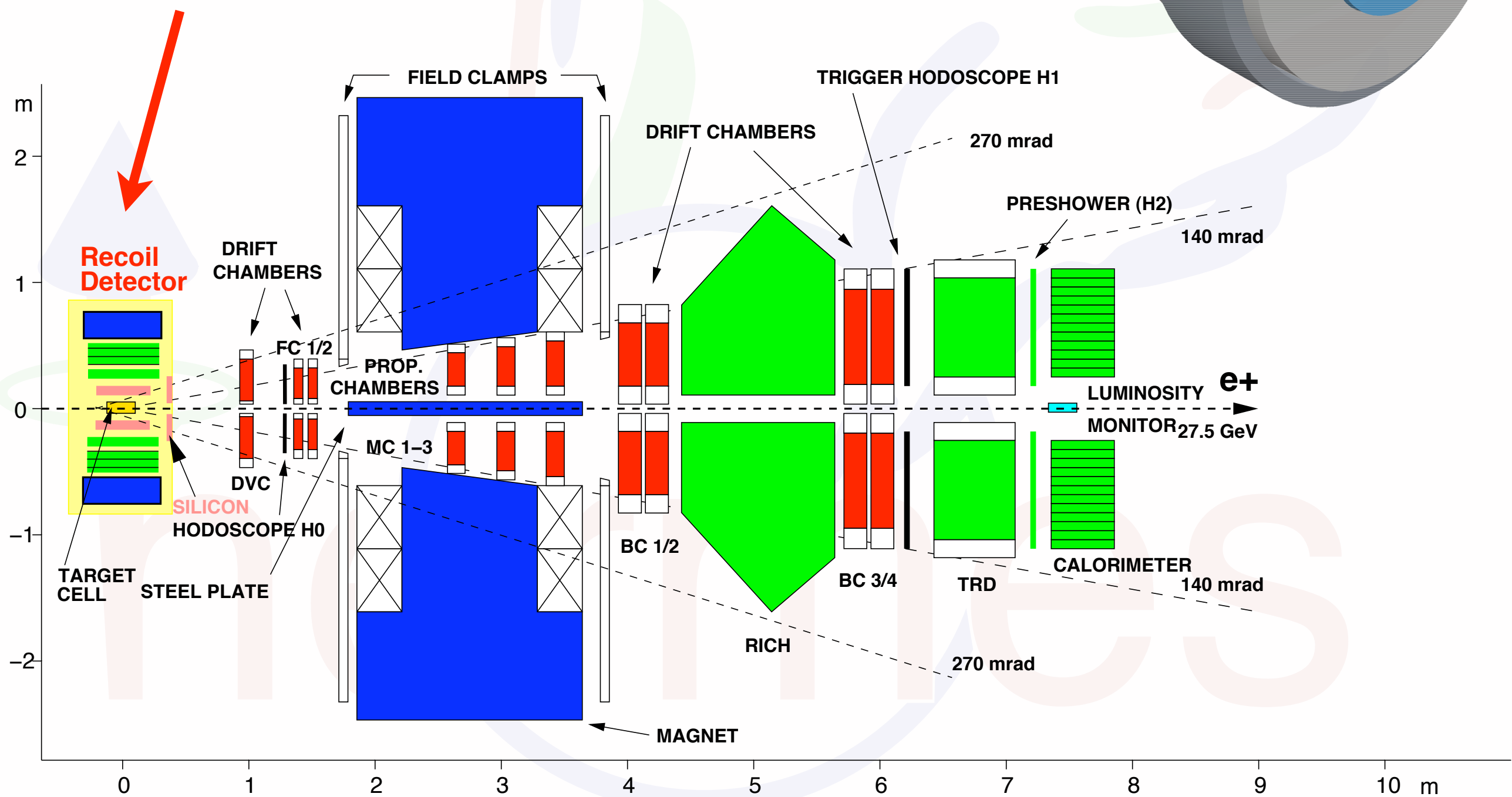


$X = \Delta^+, \dots$

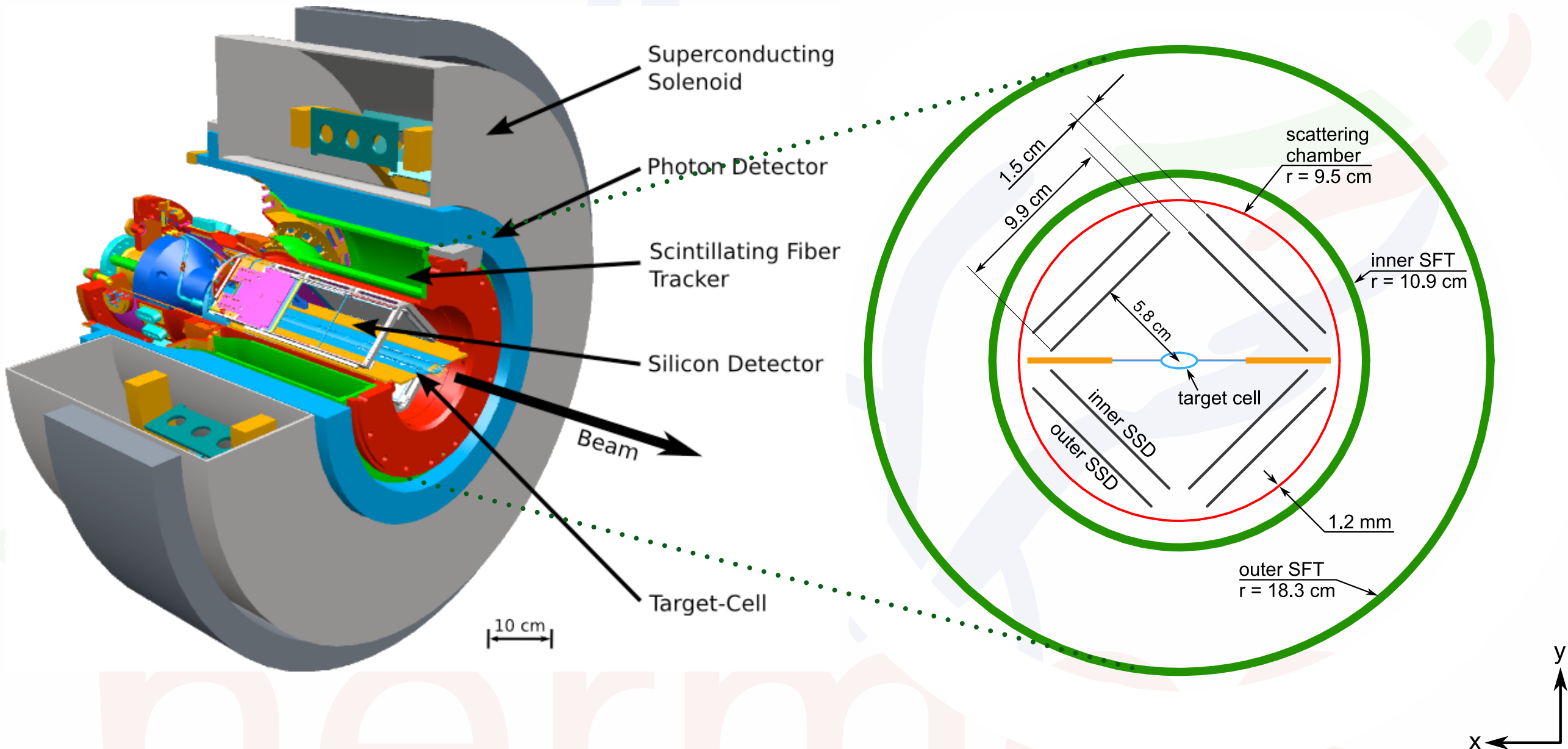
S

HERMES detector (2006/07)

detection of
recoiling proton



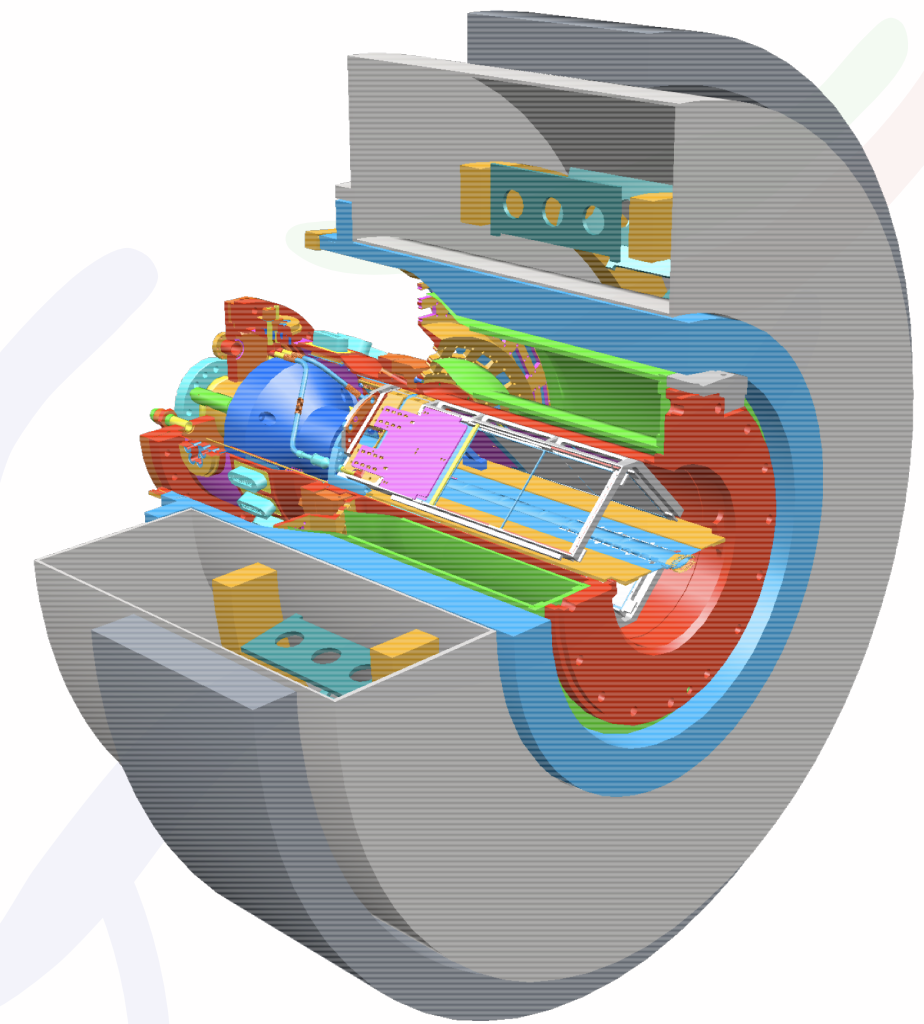
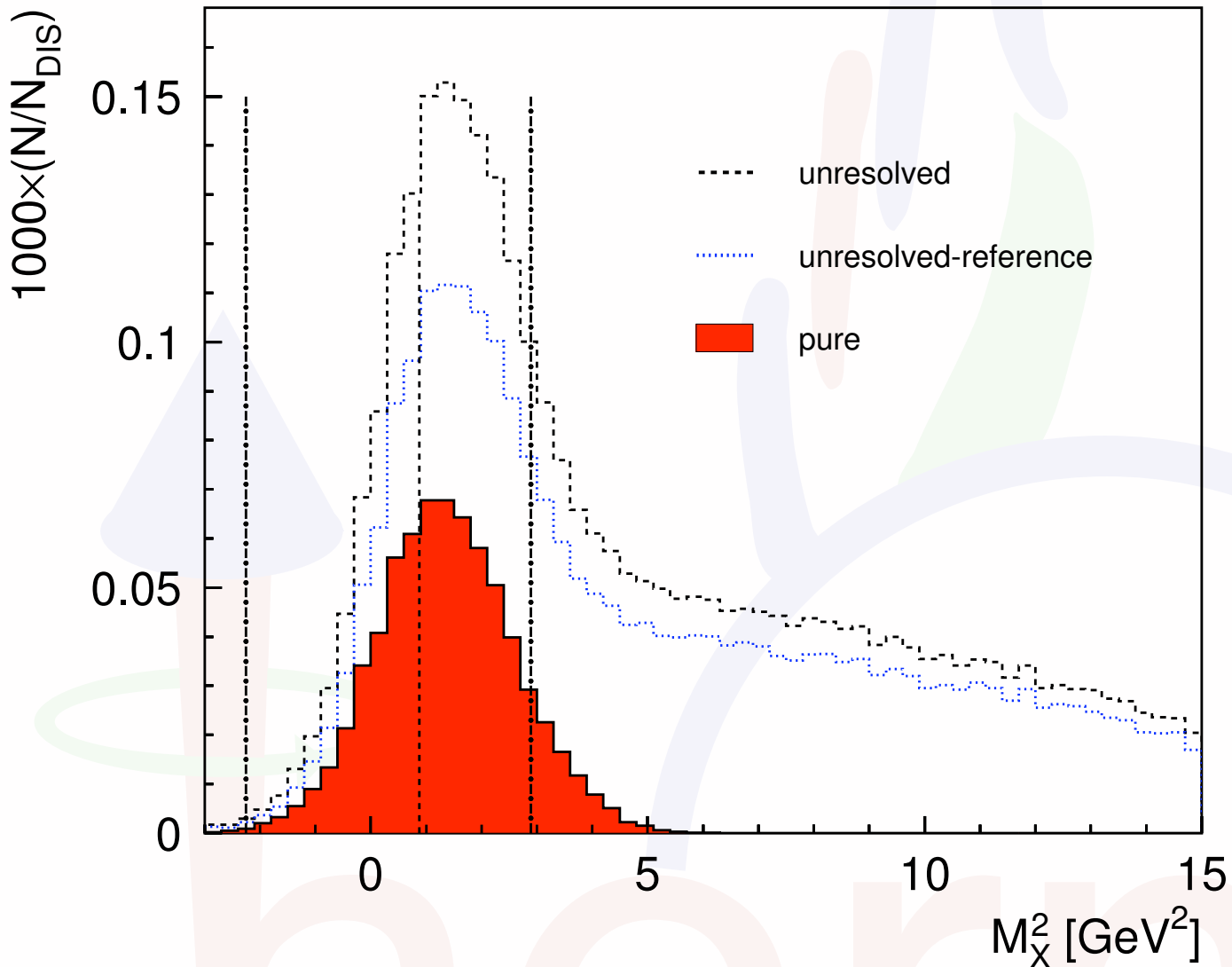
The HERMES Recoil detector



Enables the measurement of the recoiling charged particle and therefore full $e p \rightarrow e p \gamma$ event reconstruction

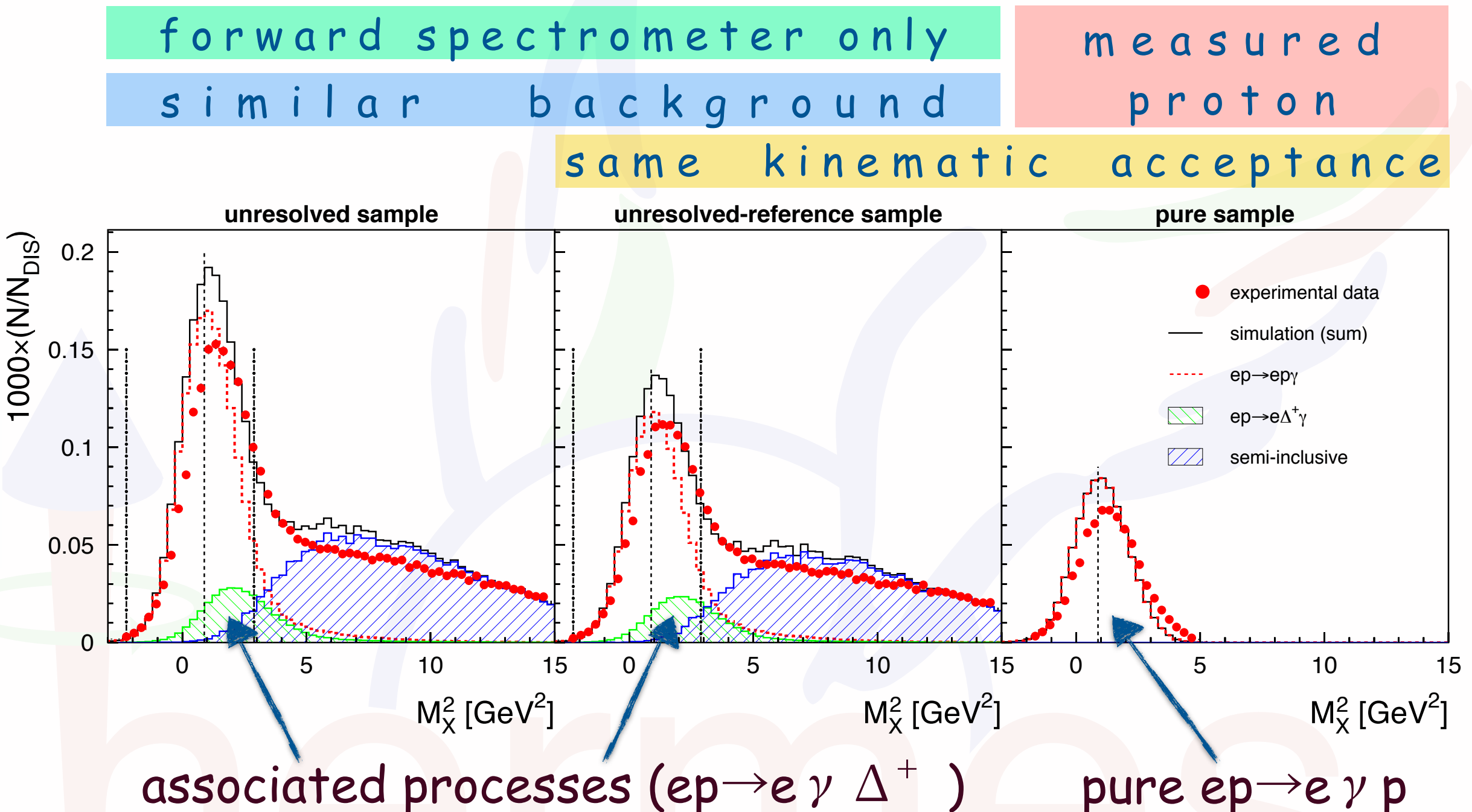
HERMES detector (2006/07)

kinematic fitting



- All particles in final state detected \rightarrow 4 constraints from energy-momentum conservation
- Selection of **pure BH/DVCS ($e p \rightarrow e p \gamma$)** with **high efficiency (~83%)**
- Allows to suppress background from associated and semi-inclusive processes to a negligible level (<0.2%)

Exclusivity with recoil detector

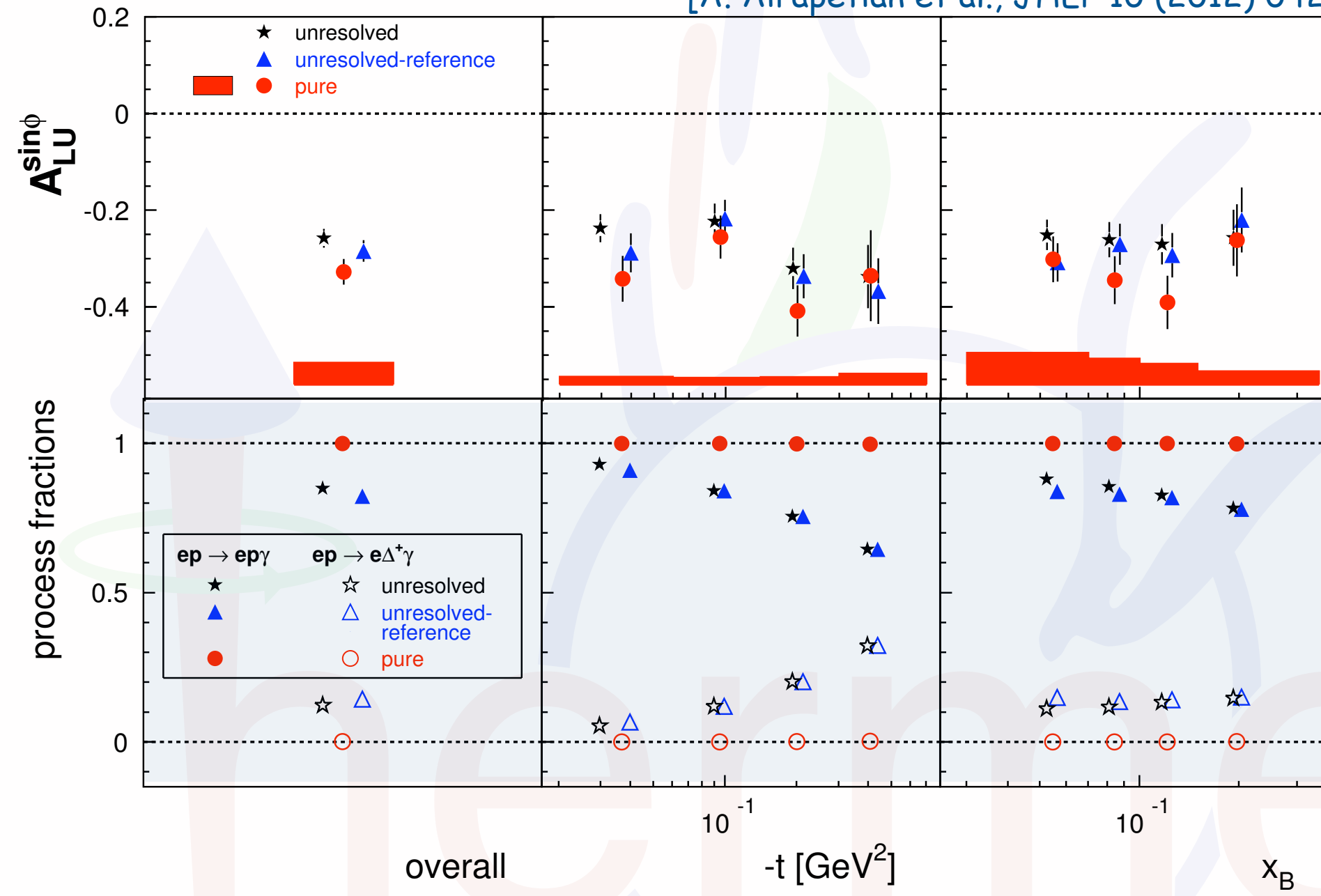


Missing mass:

$$M_x^2 = (k - k' + P_0 - P_\gamma)^2 = M^2 + 2M(\nu - E_\gamma) + t$$

Single-charge BSA with recoil proton

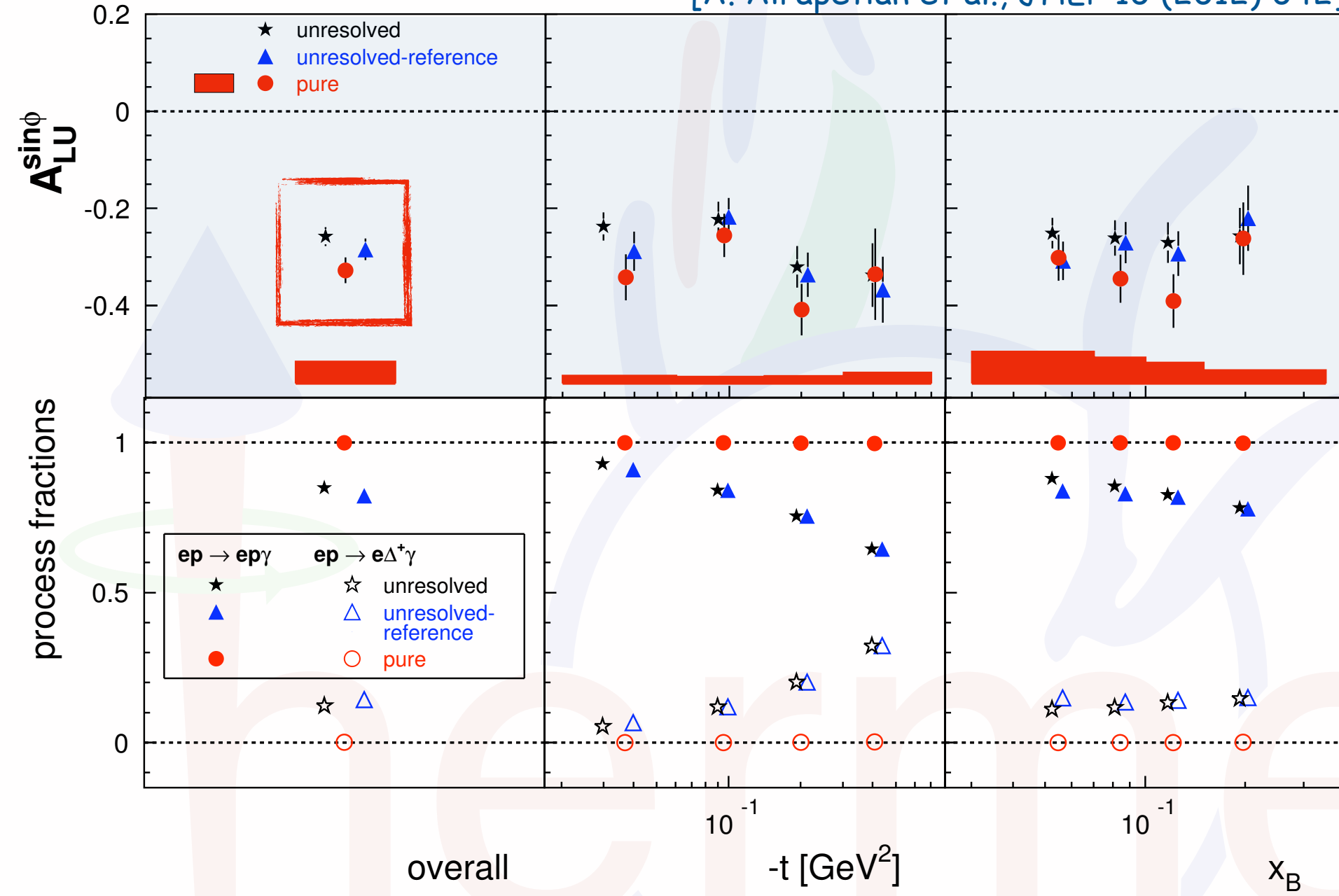
[A. Airapetian et al., JHEP 10 (2012) 042]



basically no
contamination
→ clear interpretation

Single-charge BSA with recoil proton

[A. Airapetian et al., JHEP 10 (2012) 042]

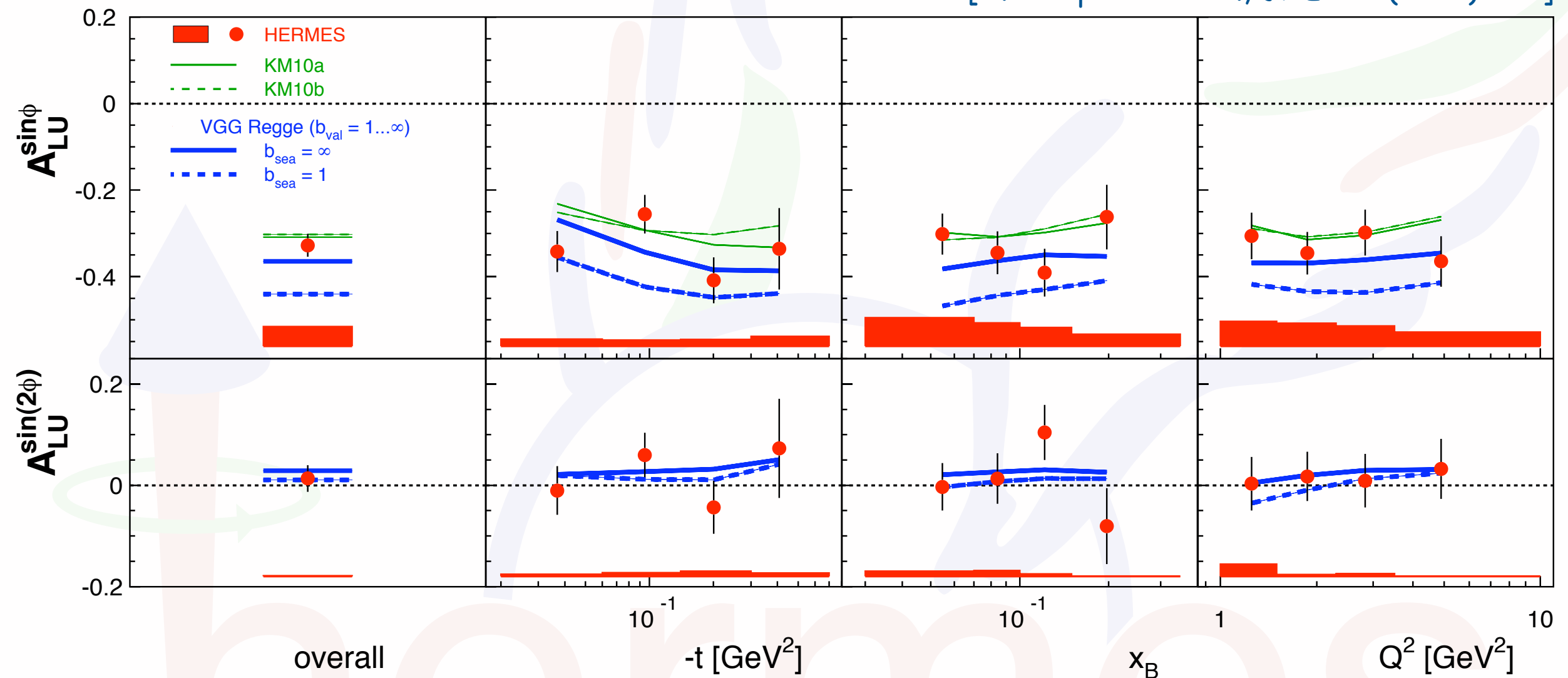


Magnitude of the leading asymmetry has increased by 0.054 ± 0.016
(-> assoc. in traditional analysis mainly dilution)

basically no contamination
-> clear interpretation

Single-charge BSA with recoil proton

[A. Airapetian et al., JHEP 10 (2012) 042]



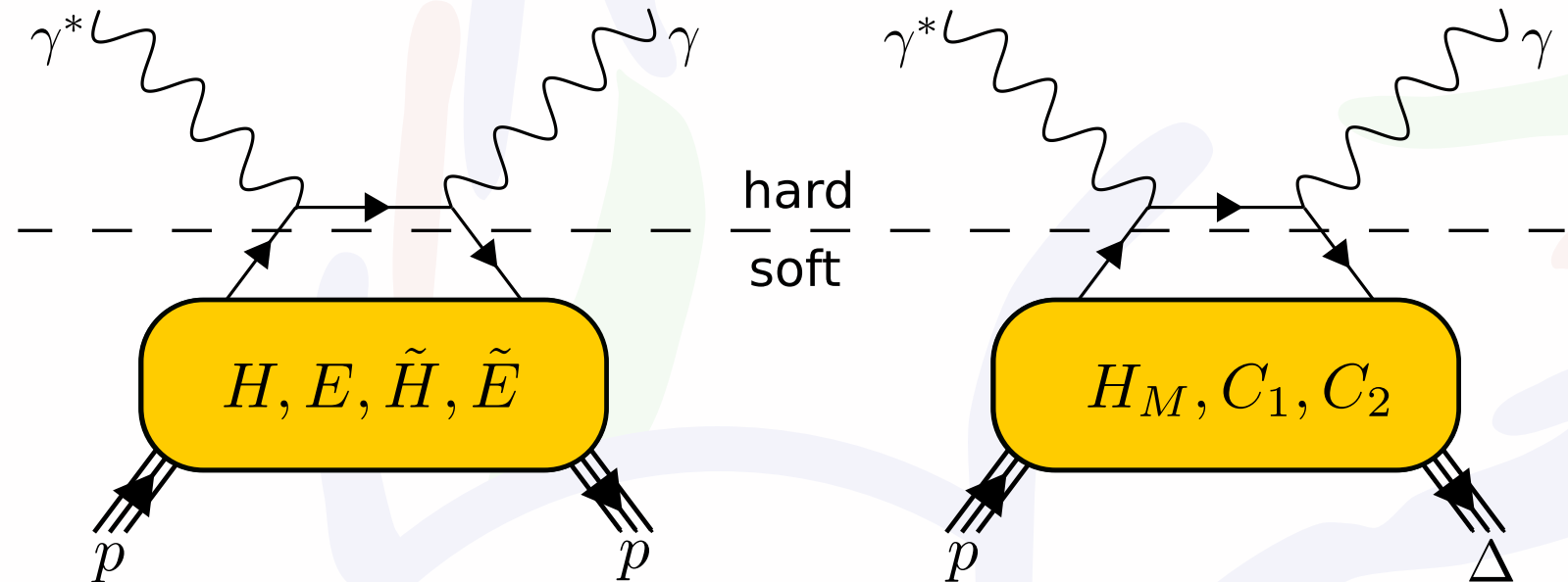
good agreement with models

KM10 - K. Kumericki and D. Müller, Nucl. Phys. B 841 (2010) 1

VGG - M. Vanderhaeghen et al., Phys. Rev. D 60 (1999) 094017

Beam-spin asymmetries $e p \rightarrow e \gamma N \pi$

Besides a better understanding of the unresolved sample, associated DVCS in principle also allows further access to GPDs.

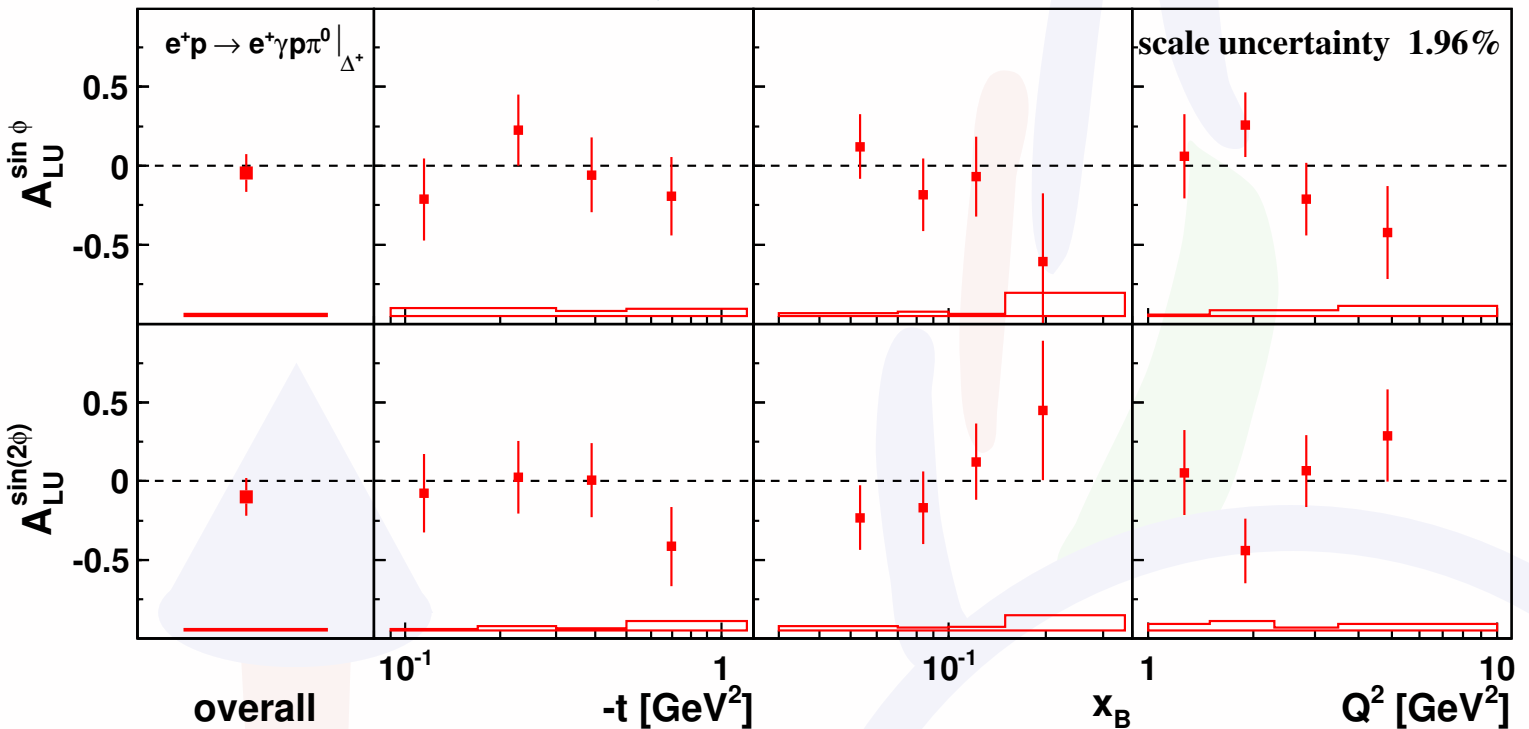


In the large- N_c limit the remaining $N \rightarrow \Delta$ GPDs can be related to the
N \rightarrow N iso-vector GPDs:

$$H_M(x, \xi, t) = \frac{2}{\sqrt{3}} [E^u(x, \xi, t) - E^d(x, \xi, t)],$$
$$C_1(x, \xi, t) = \sqrt{3} [\tilde{H}^u(x, \xi, t) - \tilde{H}^d(x, \xi, t)],$$
$$C_2(x, \xi, t) = \frac{\sqrt{3}}{4} [\tilde{E}^u(x, \xi, t) - \tilde{E}^d(x, \xi, t)]$$

Beam-spin asymmetries $e p \rightarrow e \gamma p \pi^0$

[A. Airapetian et al., JHEP 01 (2014) 077]

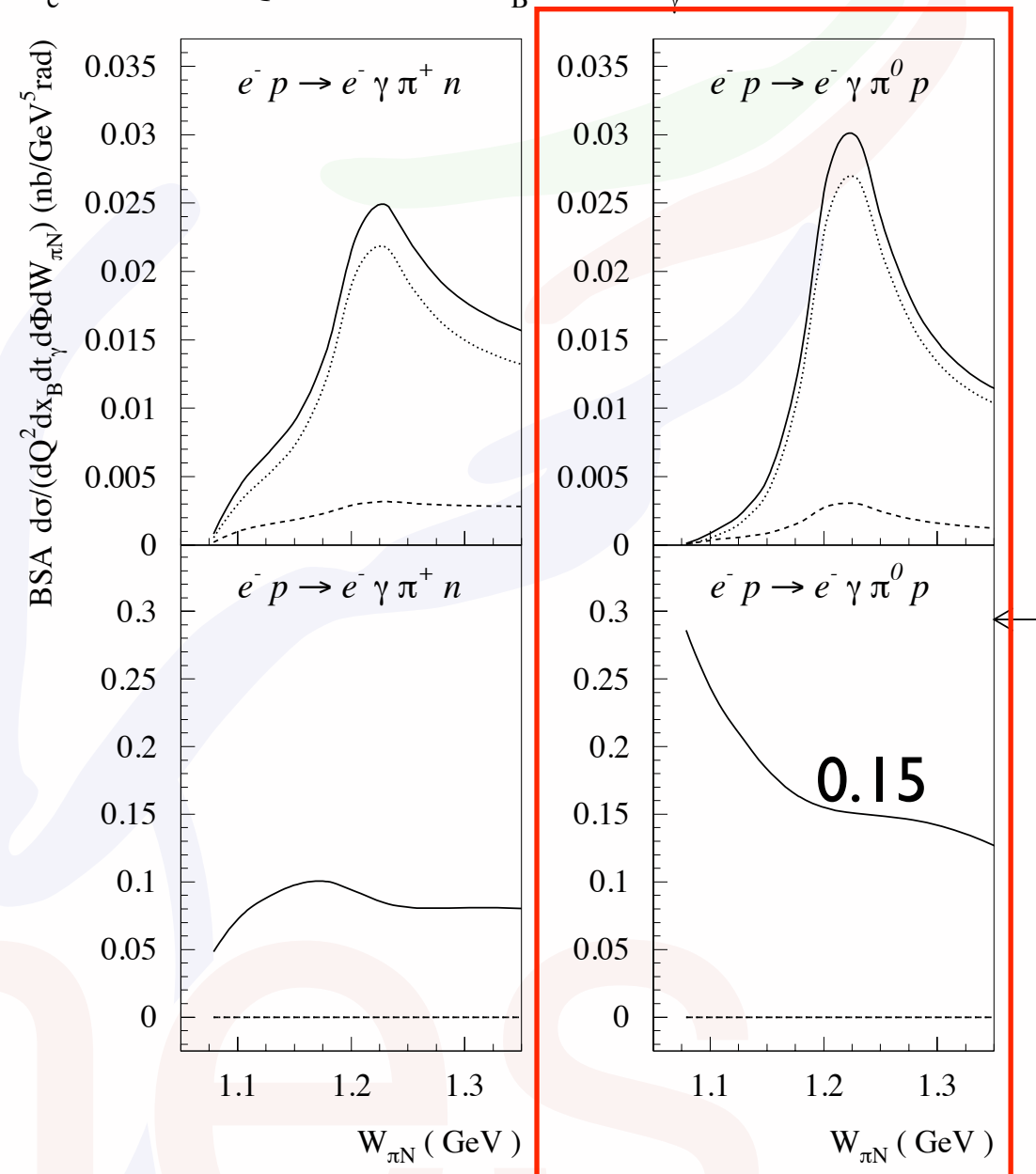


Shown amplitudes corrected for background
(only overall fractions are listed here):

Associated DVCS/BH ($e p \rightarrow e \gamma p \pi^0$)	85 ± 1
Elastic DVCS/BH ($e p \rightarrow e \gamma p$)	4.6 ± 0.1
SIDIS ($e p \rightarrow e X \pi^0$)	11 ± 1

[Guichon et al., PRD 68 (2003) 034018]

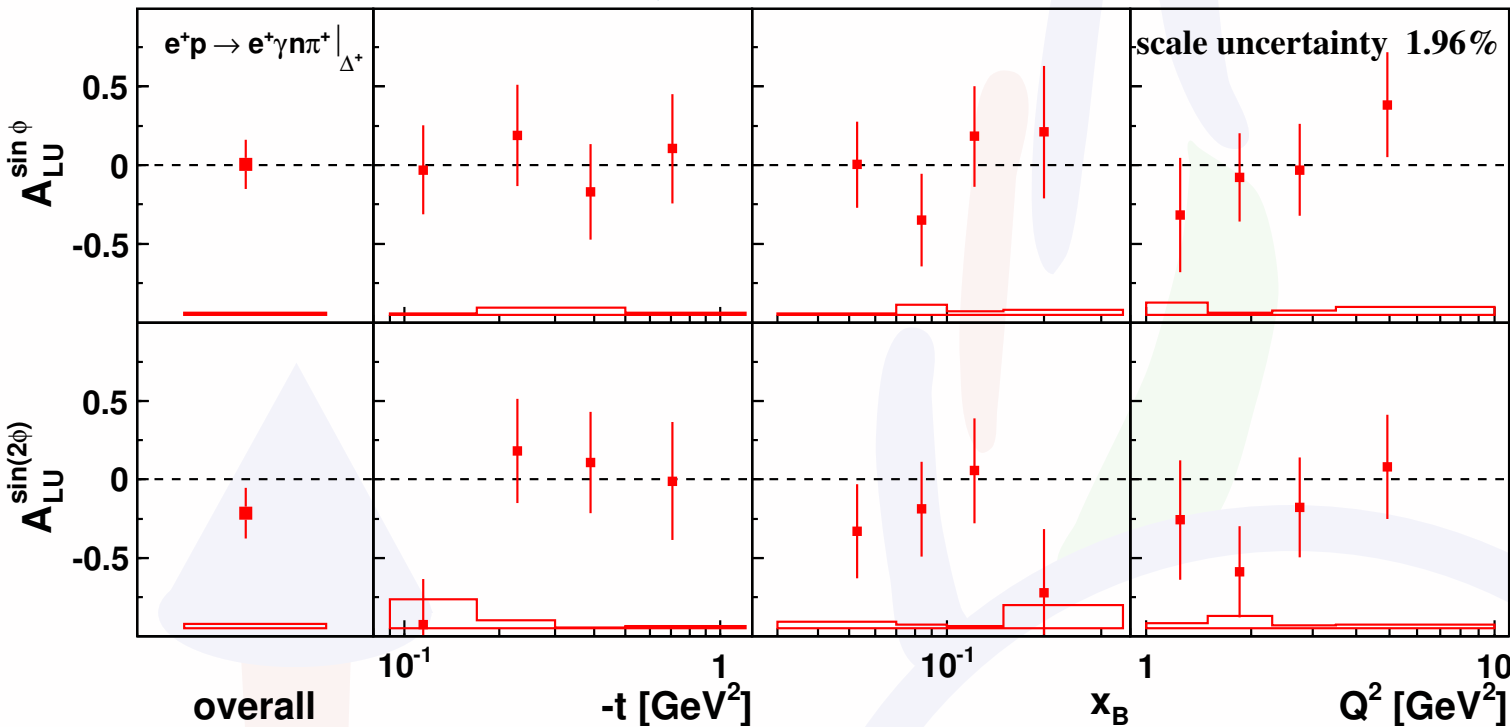
$E_e = 27$ GeV, $Q^2 = 2.5$ GeV 2 , $x_B = 0.15$, $t_\gamma = -0.25$ GeV 2 , $\Phi = 90^\circ$



opposite sign conventions!

Beam-spin asymmetries $e p \rightarrow e \gamma n \pi^+$

[A. Airapetian et al., JHEP 01 (2014) 077]

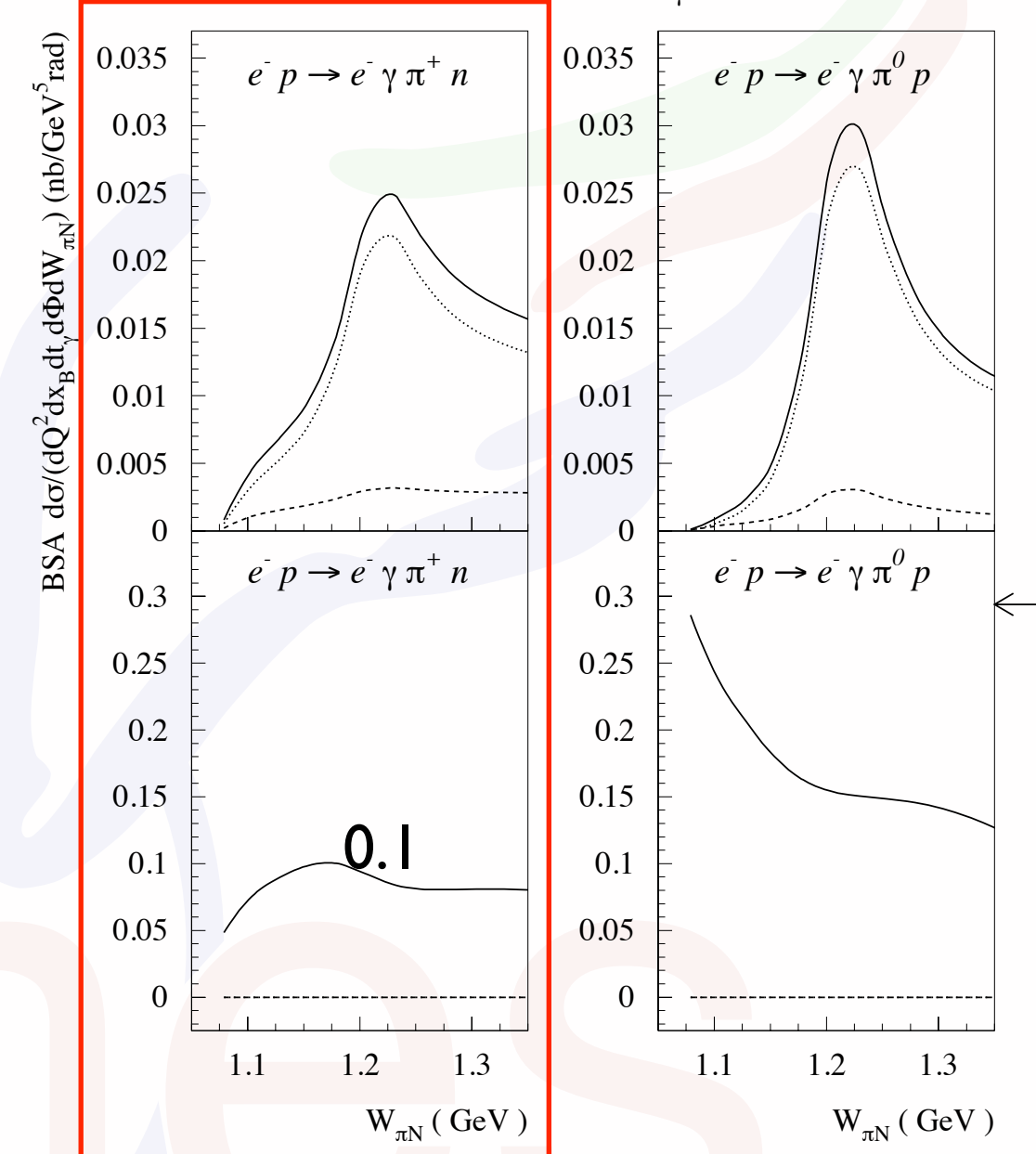


Shown amplitudes corrected for background
(only overall fractions are listed here):

Associated DVCS/BH ($e p \rightarrow e \gamma n \pi^+$)	77 ± 2
Elastic DVCS/BH ($e p \rightarrow e \gamma p$)	0.2 ± 0.1
SIDIS ($e p \rightarrow e X \pi^0$)	23 ± 3

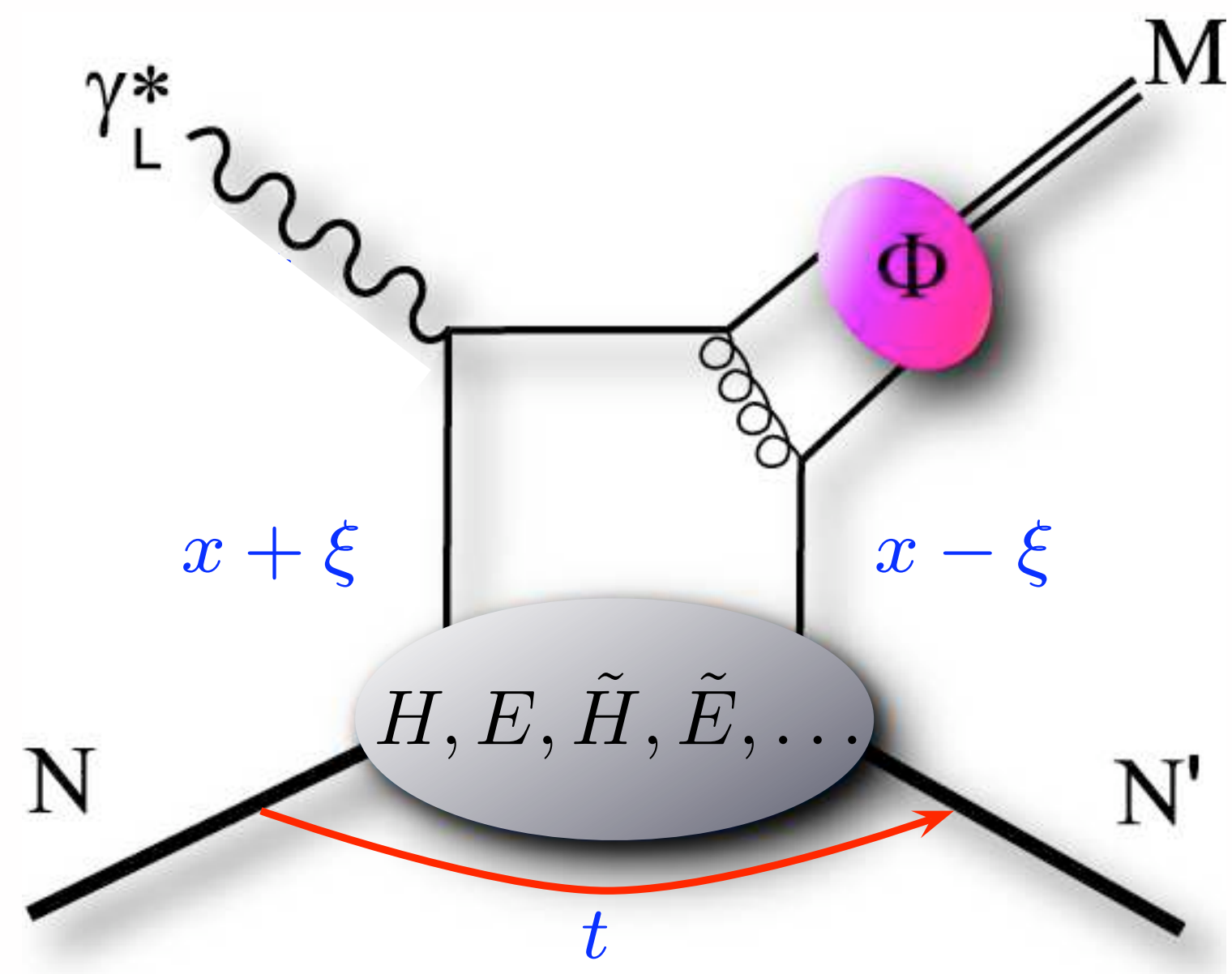
[Guichon et al., PRD 68 (2003) 034018]

$E_e = 27 \text{ GeV}, Q^2 = 2.5 \text{ GeV}^2, x_B = 0.15, t_\gamma = -0.25 \text{ GeV}^2, \Phi = 90^\circ$



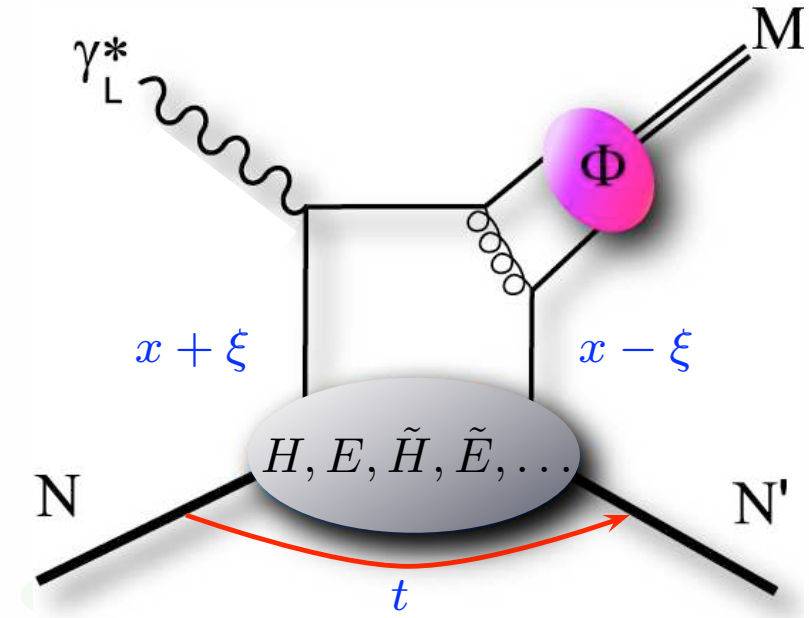
opposite sign convention!

Exclusive meson production



Exclusive meson production

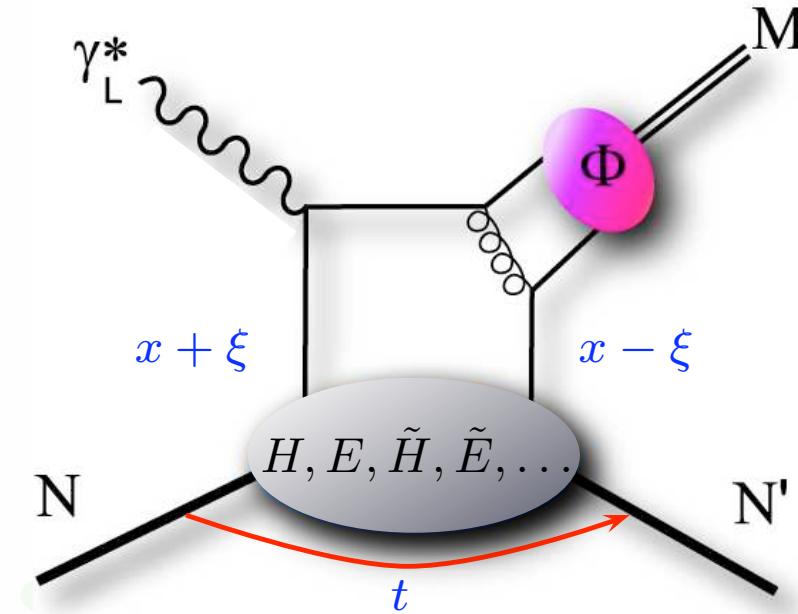
- GPDs convoluted with meson amplitude



hermes

Exclusive meson production

- GPDs convoluted with meson amplitude
- access to various quark-flavor combinations

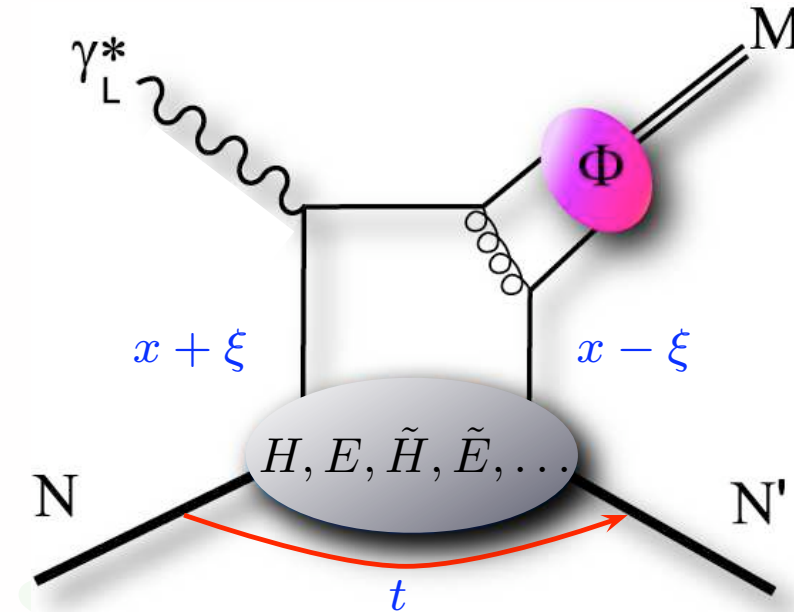


π^0	$2\Delta u + \Delta d$
η	$2\Delta u - \Delta d$
ρ^0	$2u+d, 9g/4$
ω	$2u-d, 3g/4$
ϕ	s, g
ρ^+	$u-d$
J/ψ	g

hermes

Exclusive meson production

- GPDs convoluted with meson amplitude
- access to various quark-flavor combinations
- factorization proven for longitudinal photons

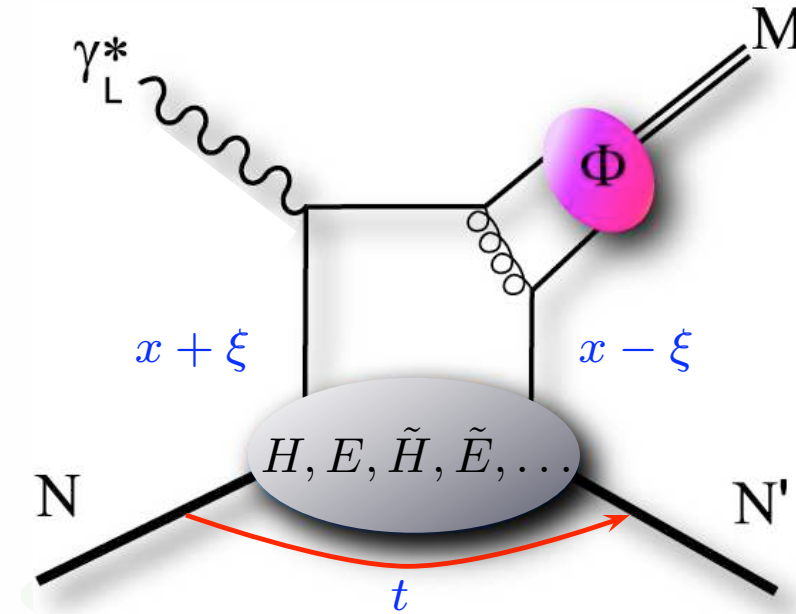


π^0	$2\Delta u + \Delta d$
η	$2\Delta u - \Delta d$
ρ^0	$2u+d$, $9g/4$
ω	$2u-d$, $3g/4$
ϕ	s , g
ρ^+	$u-d$
J/ψ	g

hermes

Exclusive meson production

- GPDs convoluted with meson amplitude
- access to various quark-flavor combinations
- factorization proven for longitudinal photons
- generalized to transverse photons in GK model



π^0	$2\Delta u + \Delta d$
η	$2\Delta u - \Delta d$
ρ^0	$2u+d, 9g/4$
ω	$2u-d, 3g/4$
ϕ	s, g
ρ^+	$u-d$
J/ψ	g

hermes

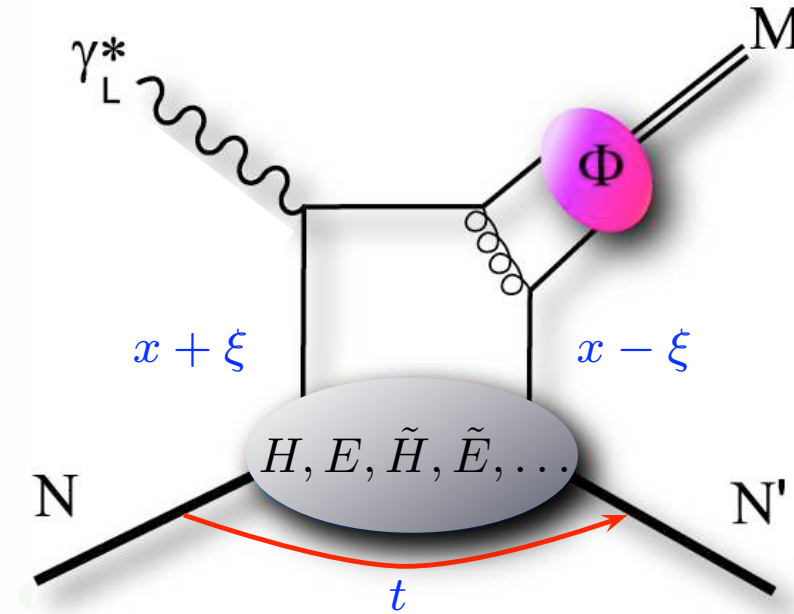
Exclusive meson production

- GPDs convoluted with meson amplitude
- access to various quark-flavor combinations
- factorization proven for longitudinal photons
- generalized to transverse photons in GK model
- vector-meson cross section:

$$\frac{d\sigma}{dx_B dQ^2 dt d\phi_S d\phi d\cos\theta d\varphi} = \frac{d\sigma}{dx_B dQ^2 dt} W(x_B, Q^2, t, \phi_S, \phi, \cos\theta, \varphi)$$

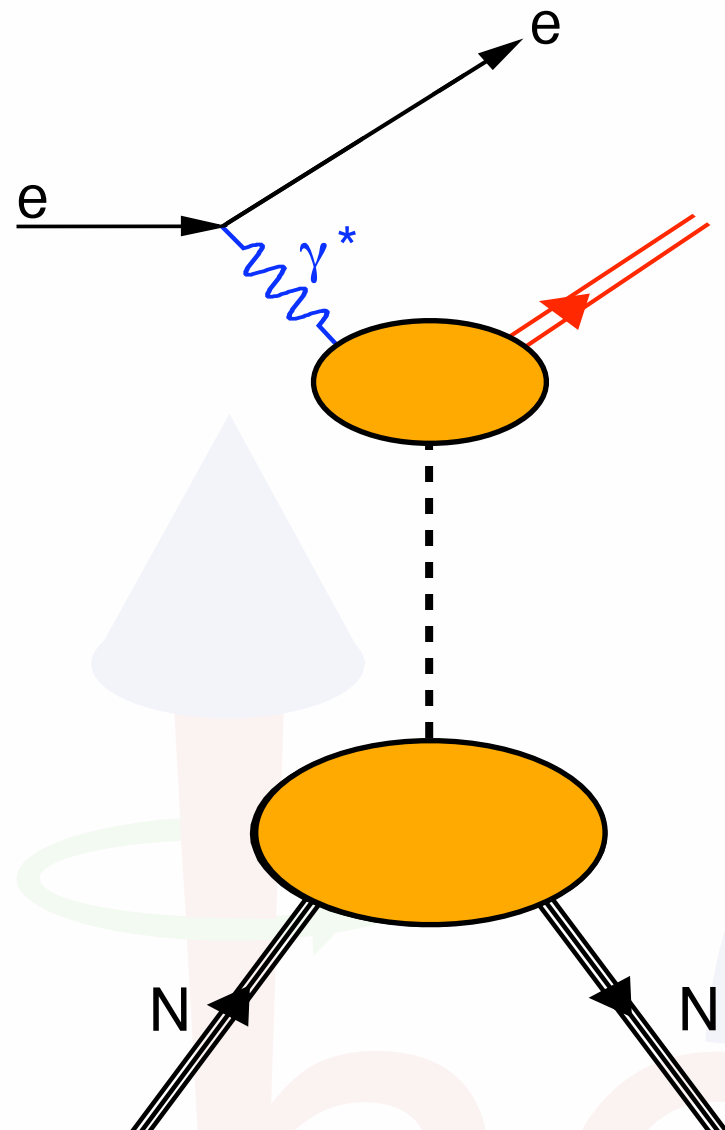
$$W = W_{UU} + P_B W_{LU} + S_L W_{UL} + P_B S_L W_{LL} + S_T W_{UT} + P_B S_T W_{LT}$$

look at various angular (decay) distributions to study helicity transitions ("spin-density matrix elements")



π^0	$2\Delta u + \Delta d$
η	$2\Delta u - \Delta d$
ρ^0	$2u+d$, $9g/4$
ω	$2u-d$, $3g/4$
ϕ	s , g
ρ^+	$u-d$
J/ψ	g

"Regge phenomenology"



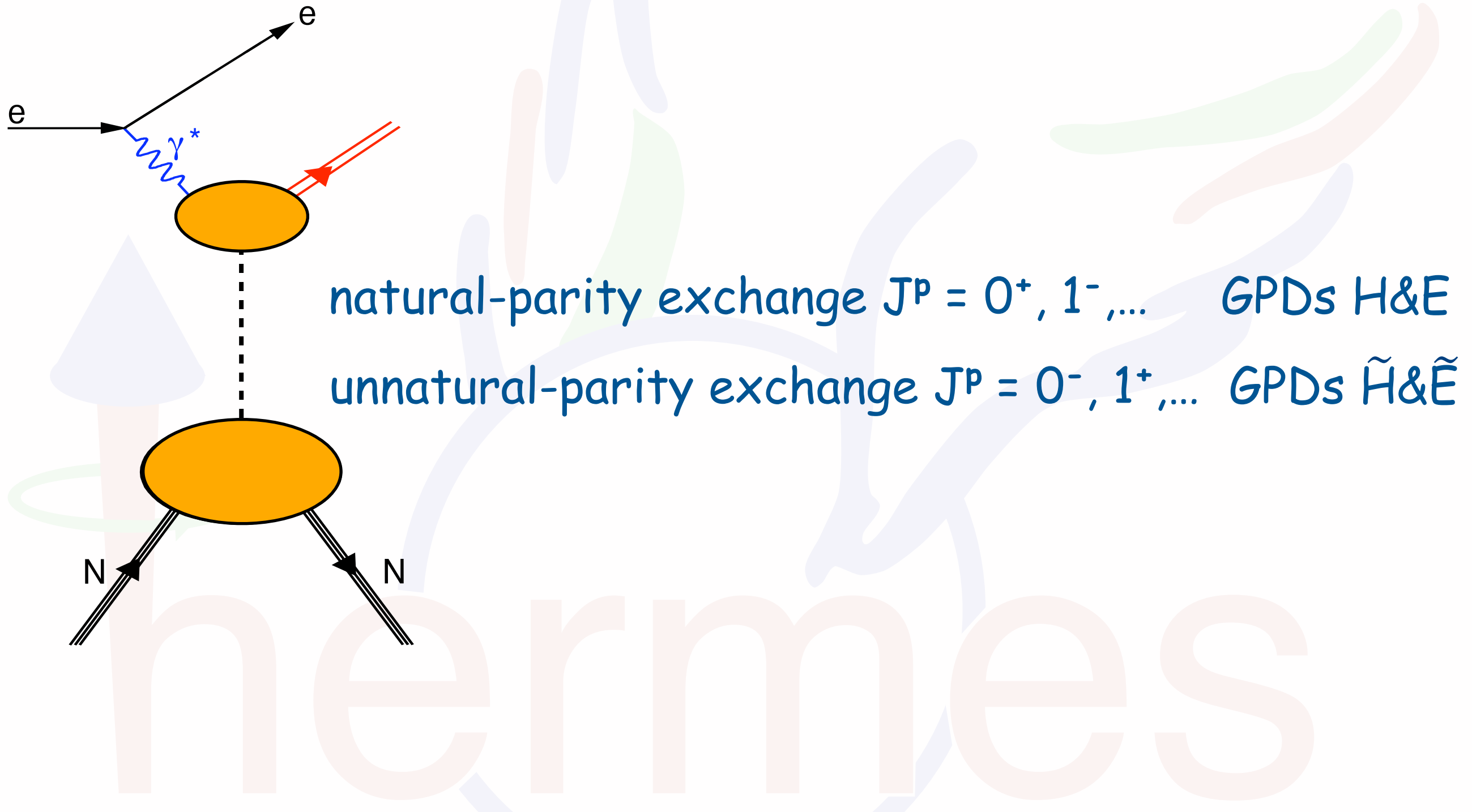
"Regge phenomenology"



GPDs H&E

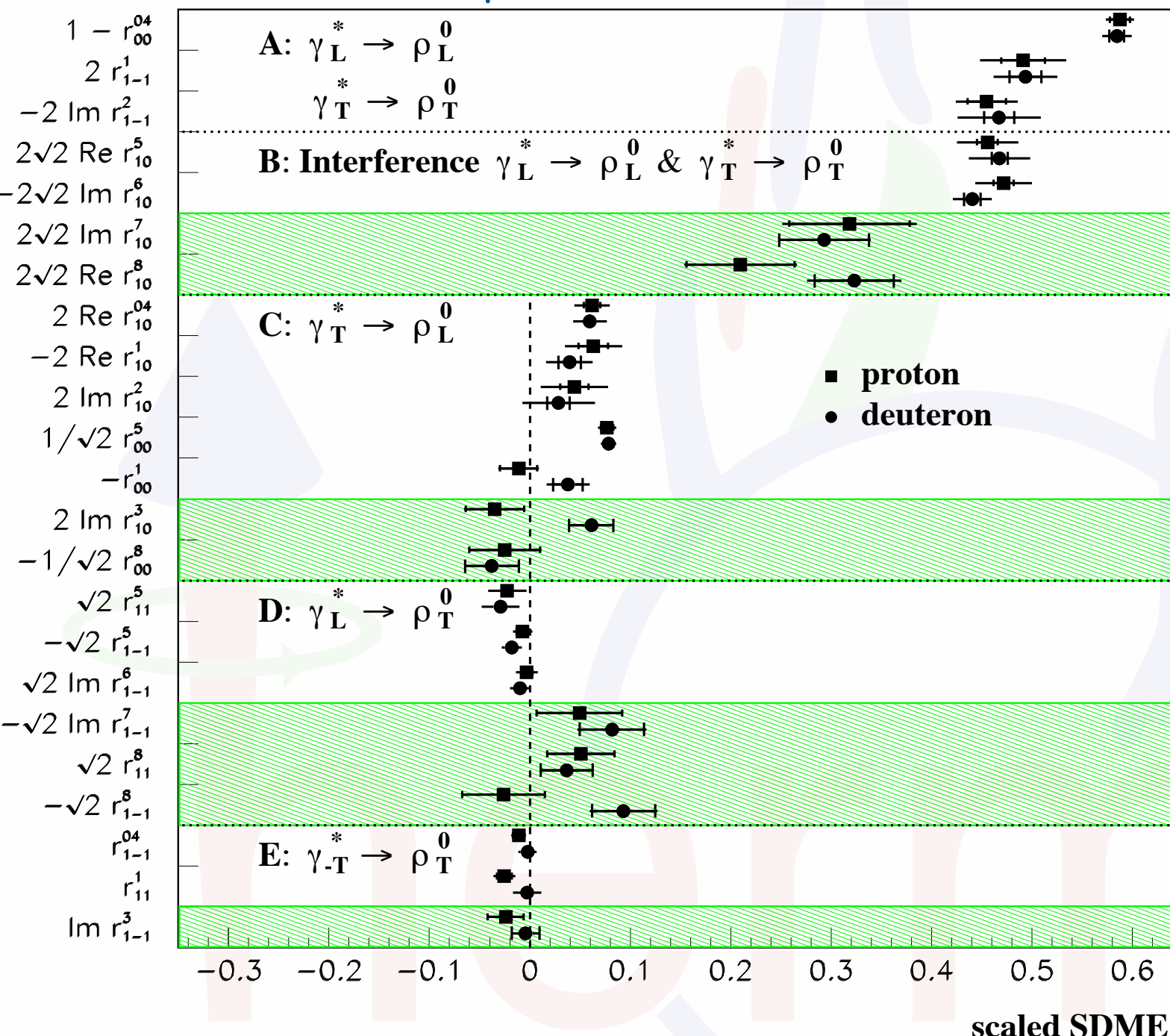
neutrinos

"Regge phenomenology"



ρ^0 SDMEs from HERMES

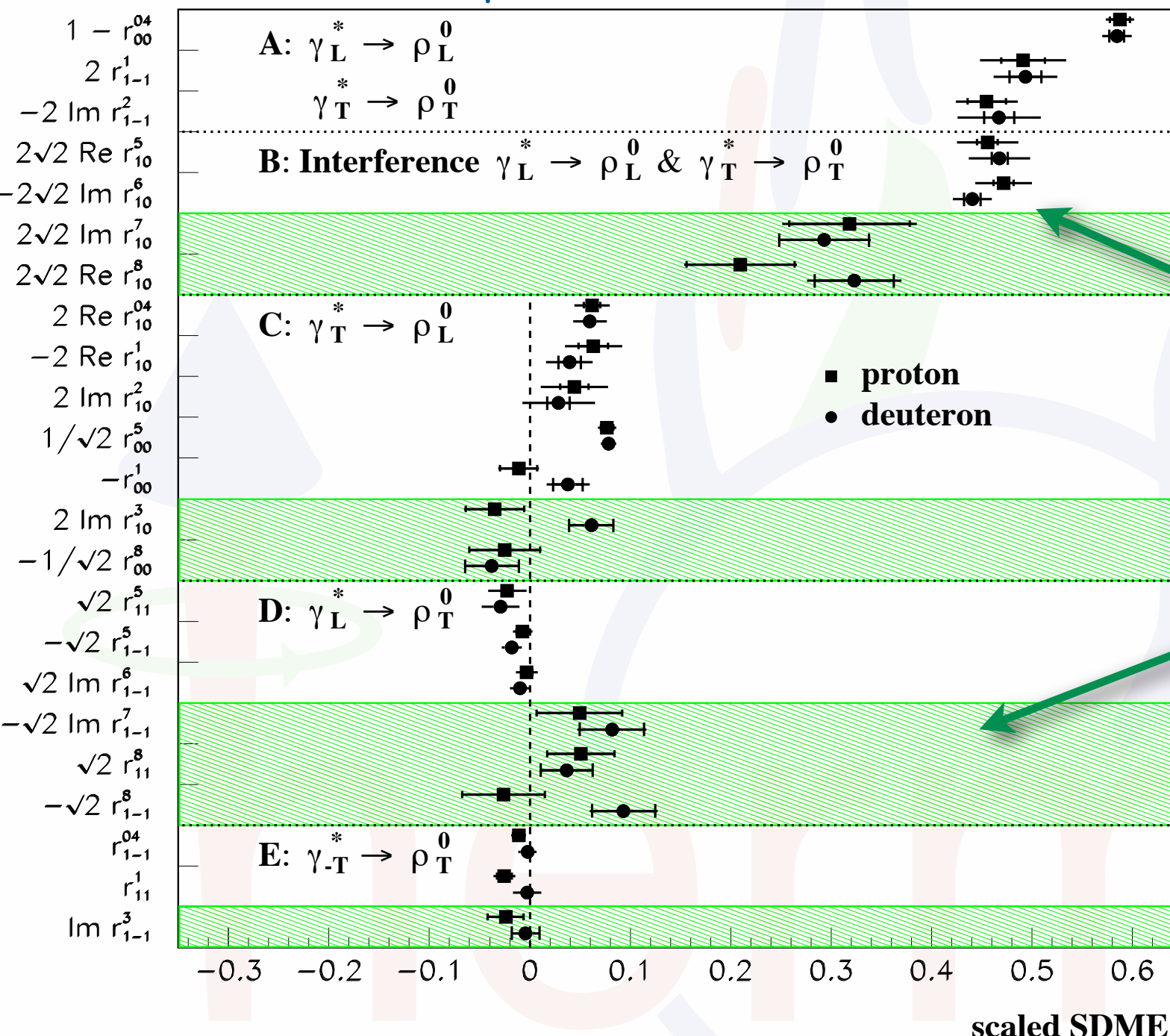
[A. Airapetian et al., EPJ C62 (2009) 659]



target-polarization independent SDMEs

ρ^0 SDMEs from HERMES

[A. Airapetian et al., EPJ C62 (2009) 659]

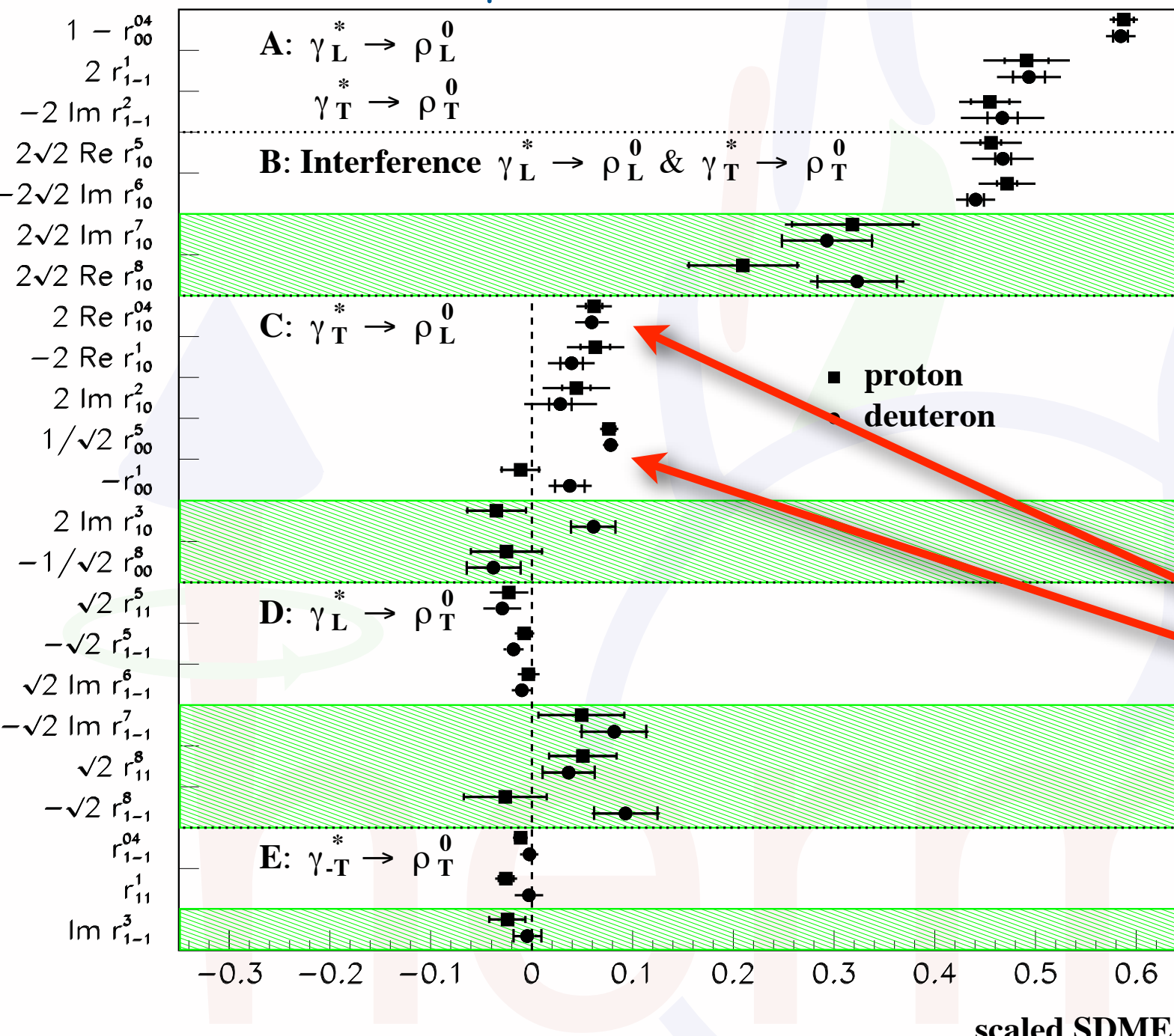


target-polarization independent SDMEs

helicity non-flip much larger than helicity-flip and double helicity-flip

ρ^0 SDMEs from HERMES

[A. Airapetian et al., EPJ C62 (2009) 659]



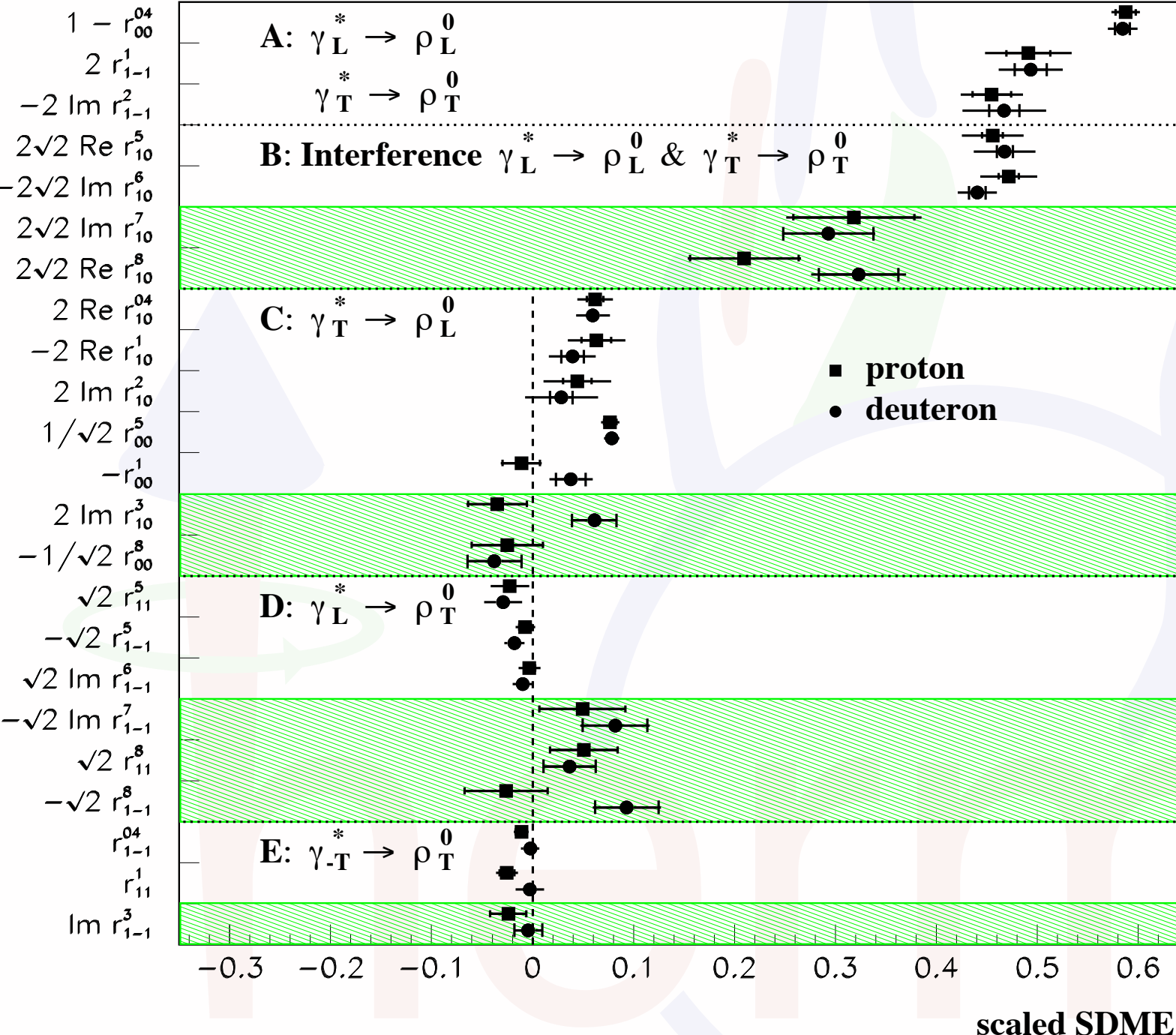
clear breaking of s-channel
helicity conservation

target-polarization independent SDMEs

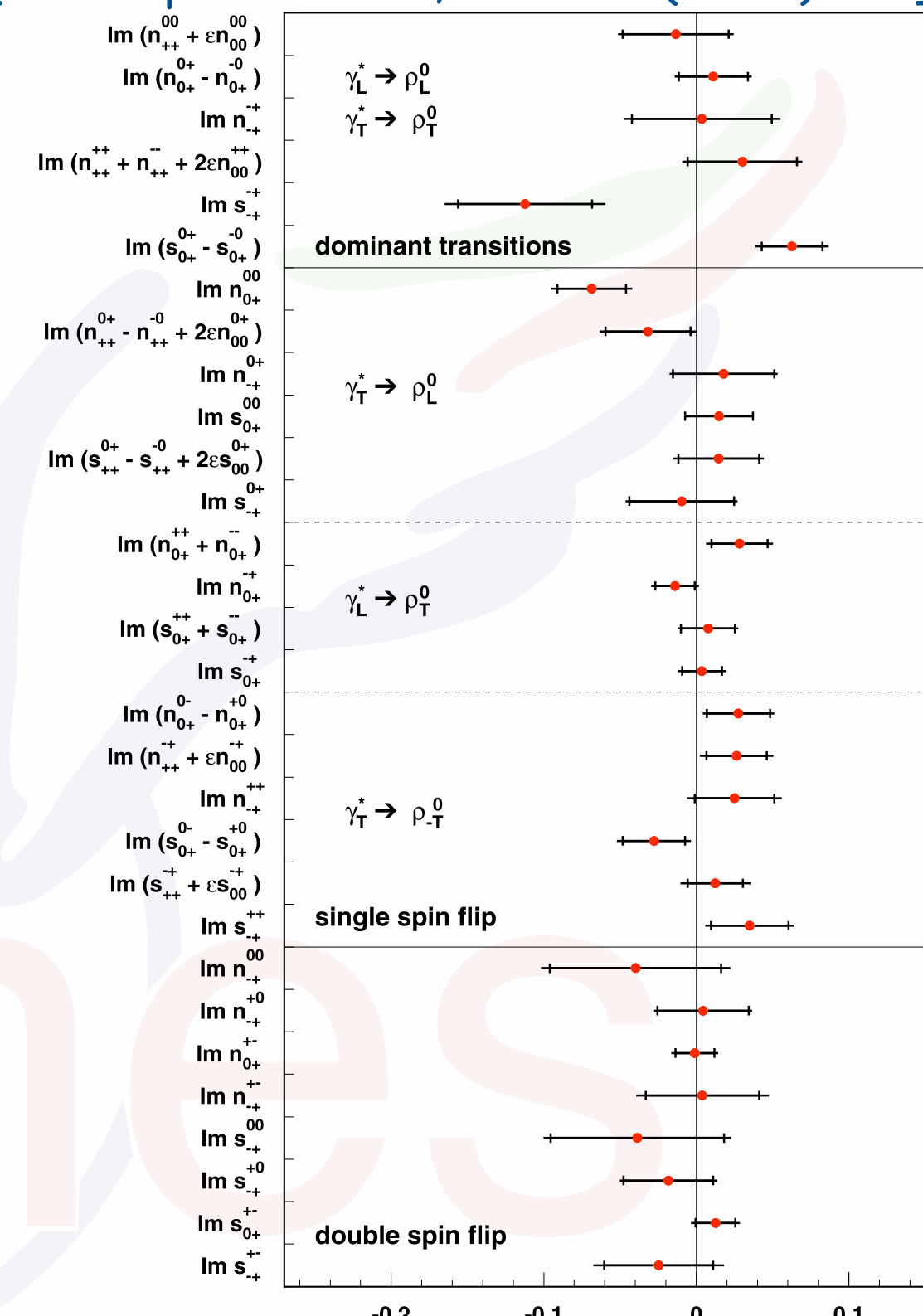
ρ^0 SDMEs from HERMES

[A. Airapetian et al., PLB 679 (2009) 100]

[A. Airapetian et al., EPJ C62 (2009) 659]



target-polarization independent SDMEs



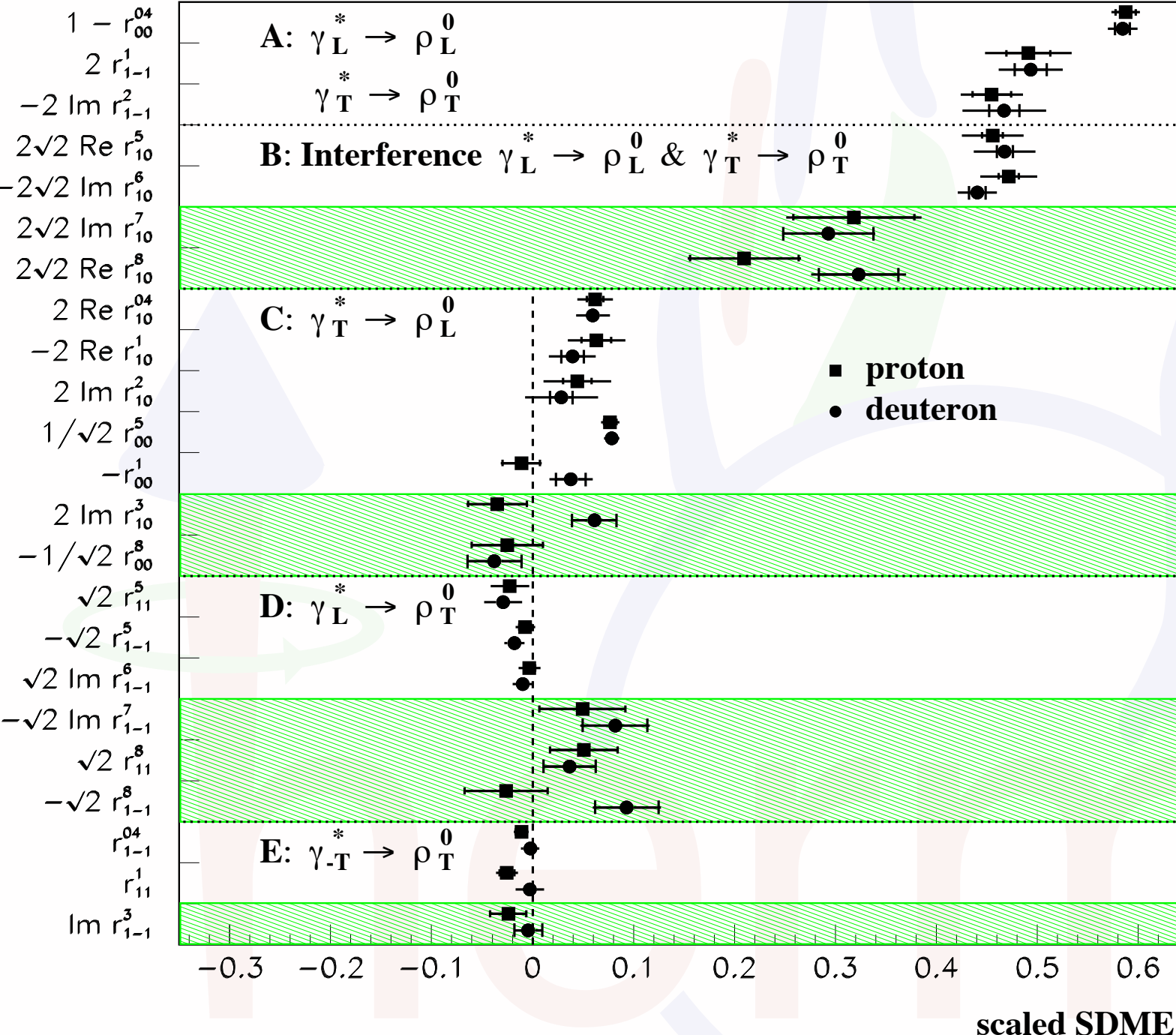
"transverse" SDMEs

SDME values

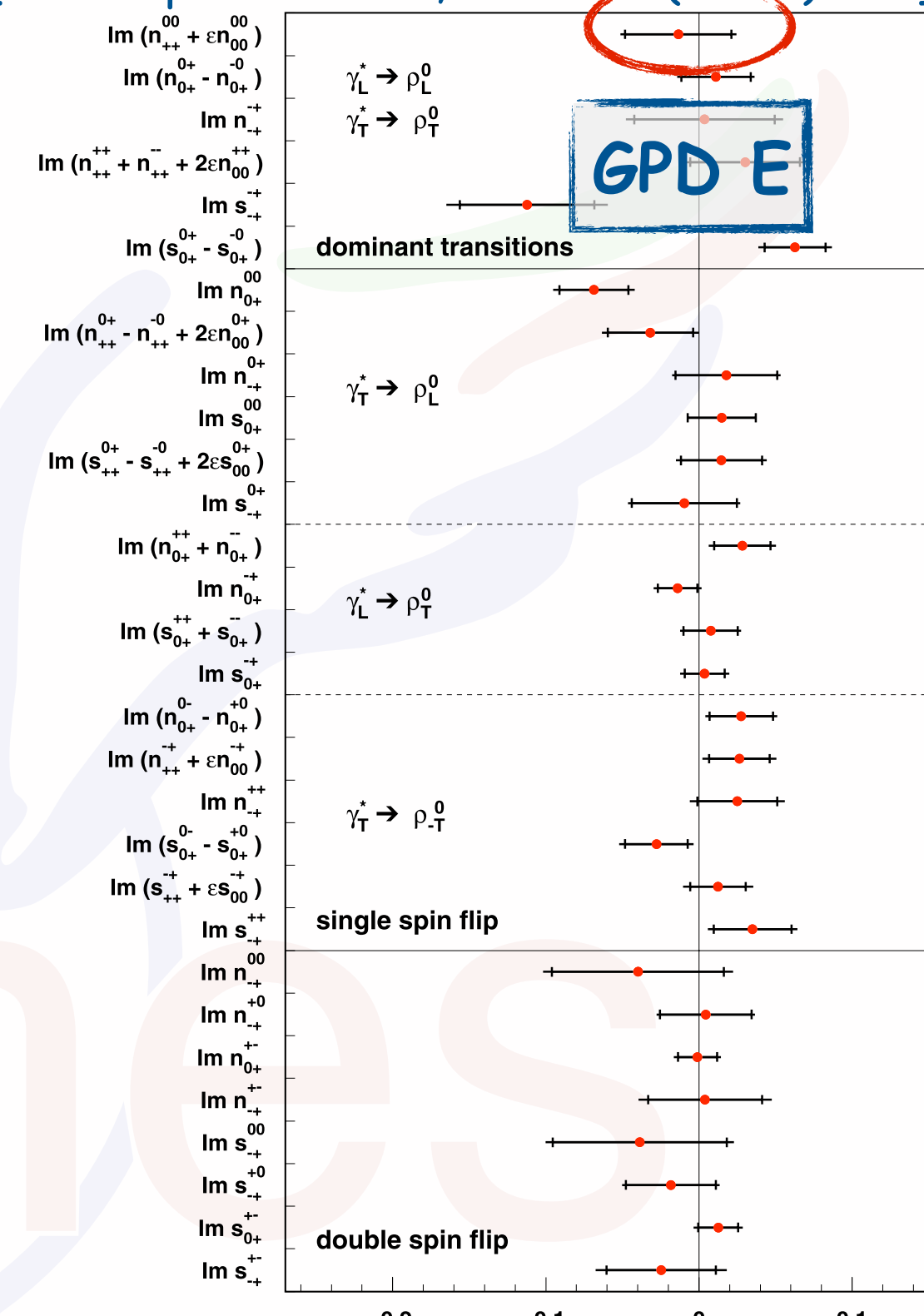
ρ^0 SDMEs from HERMES

[A. Airapetian et al., PLB 679 (2009) 100]

[A. Airapetian et al., EPJ C62 (2009) 659]



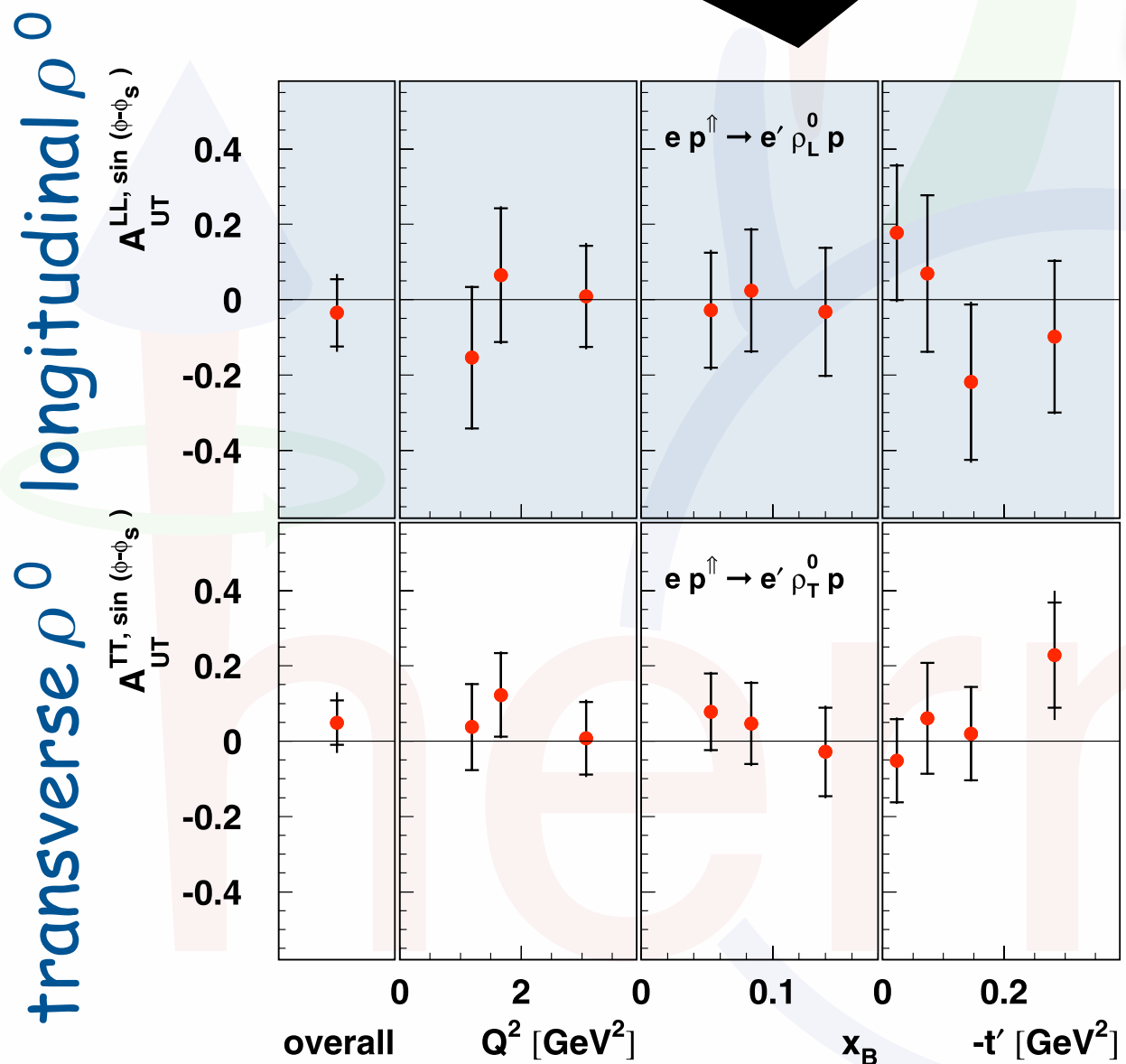
target-polarization independent SDMEs



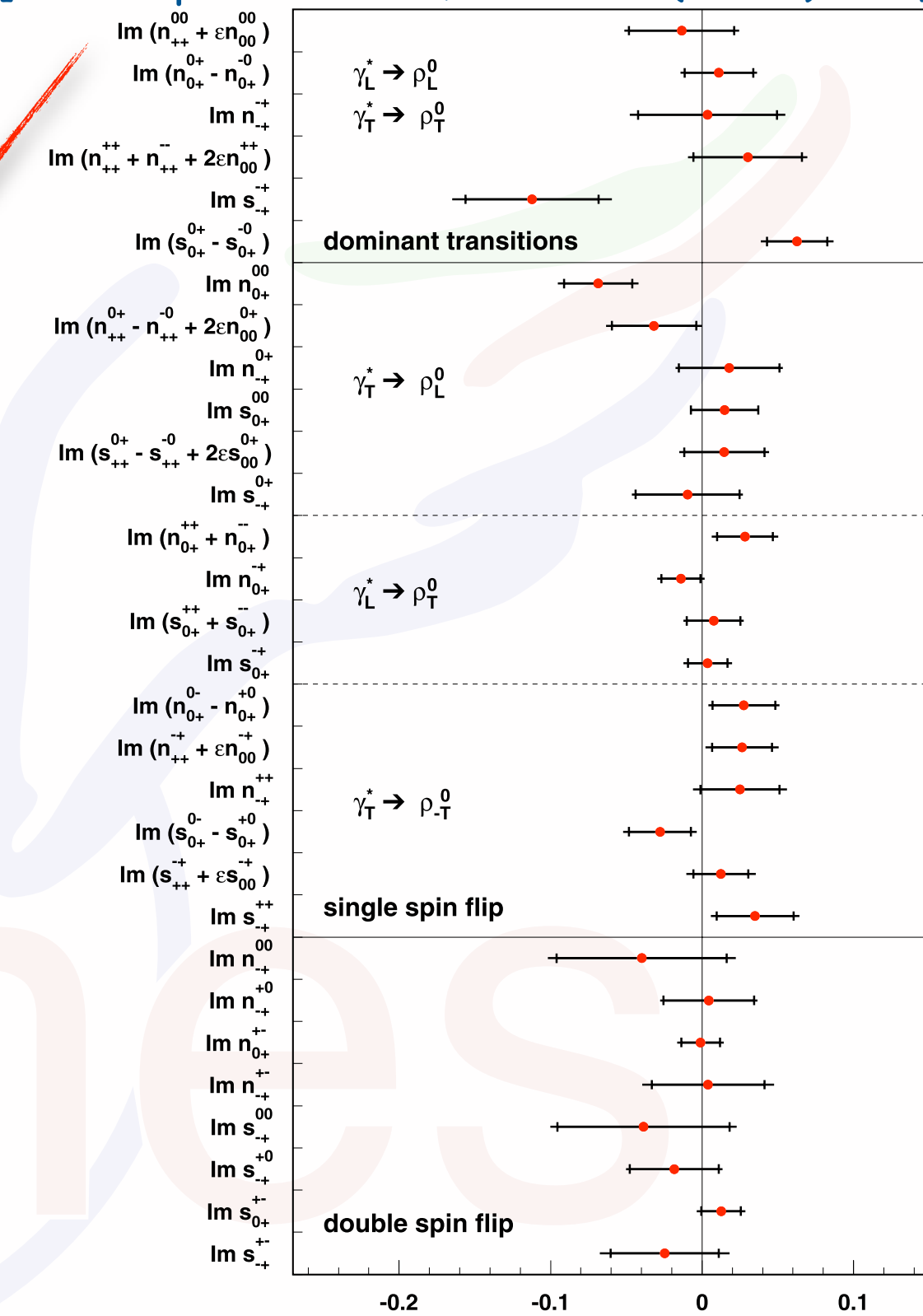
"transverse" SDMEs

SDME values

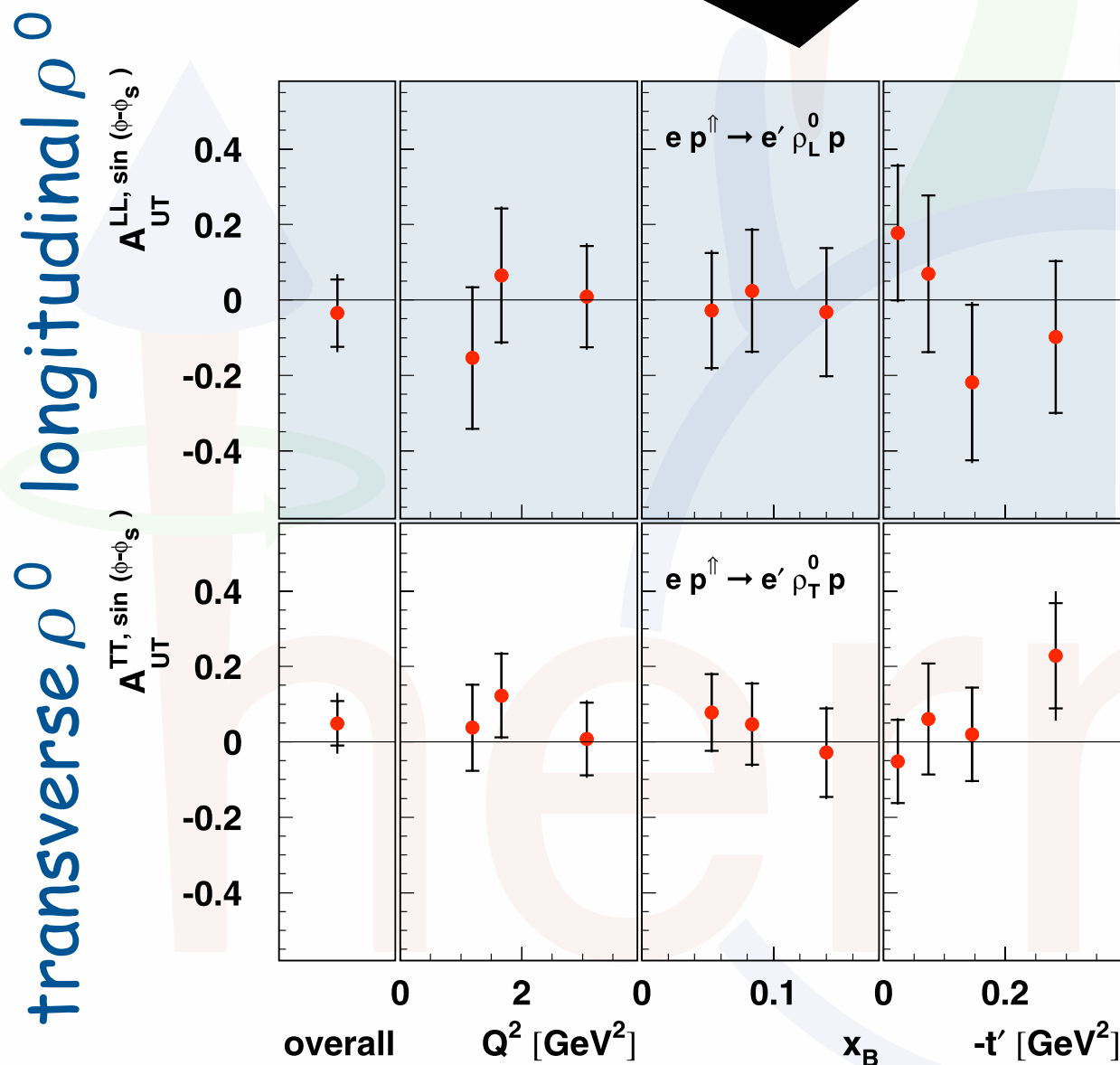
ρ^0 SDMEs from HERMES



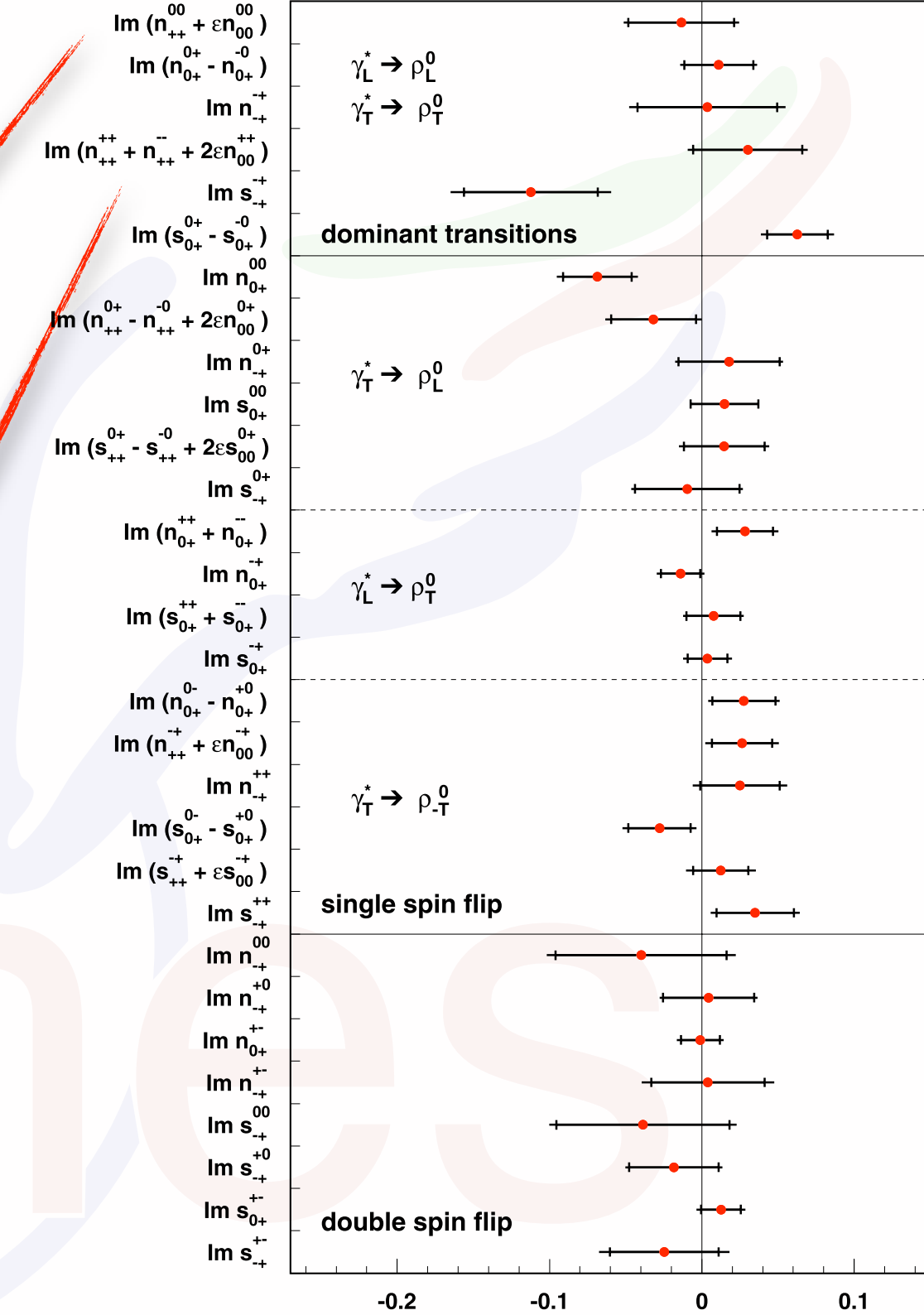
[A. Airapetian et al., PLB 679 (2009) 100]



ρ^0 SDMEs from HERMES



[A. Airapetian et al., PLB 679 (2009) 100]

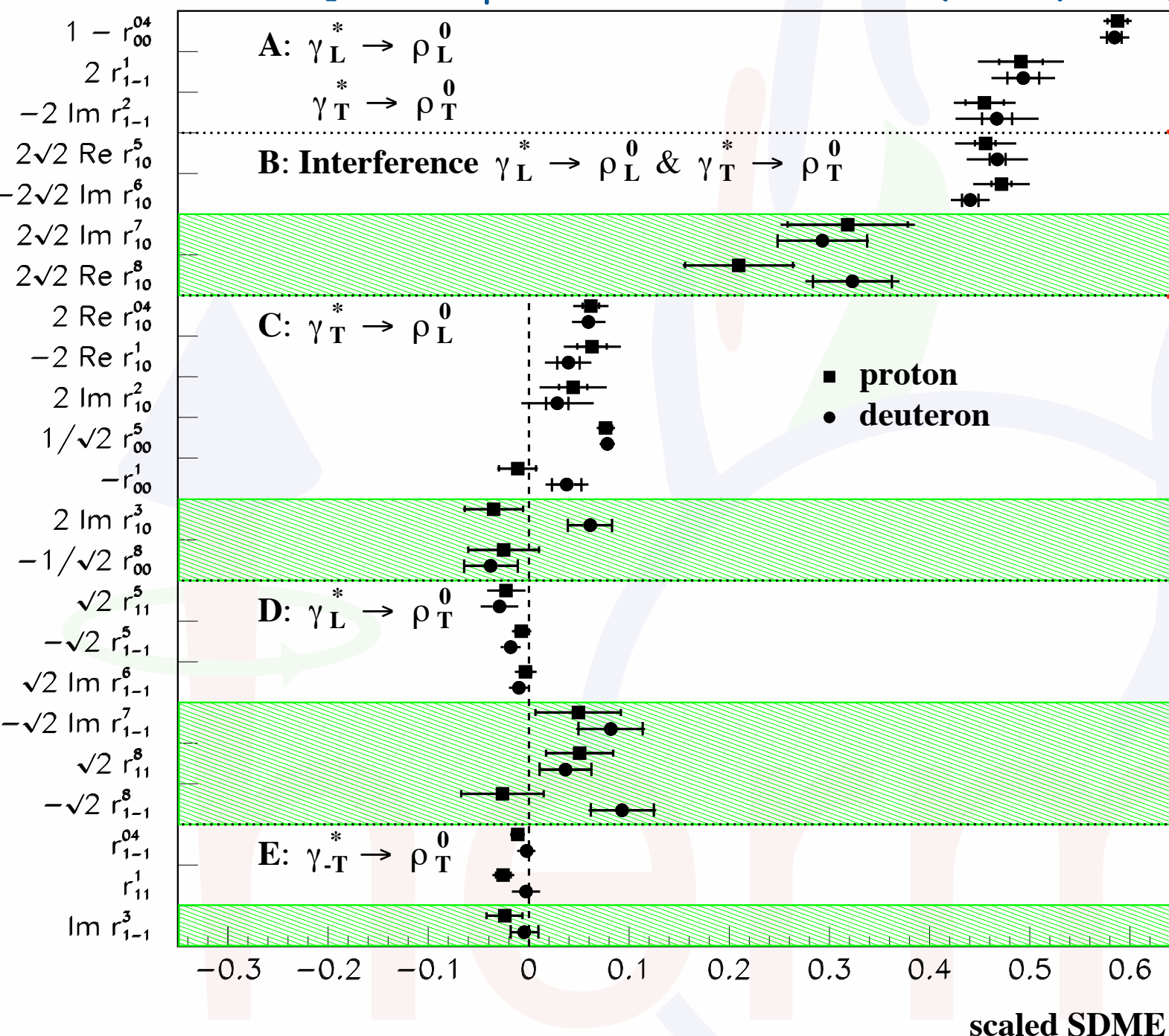


"transverse" SDMEs

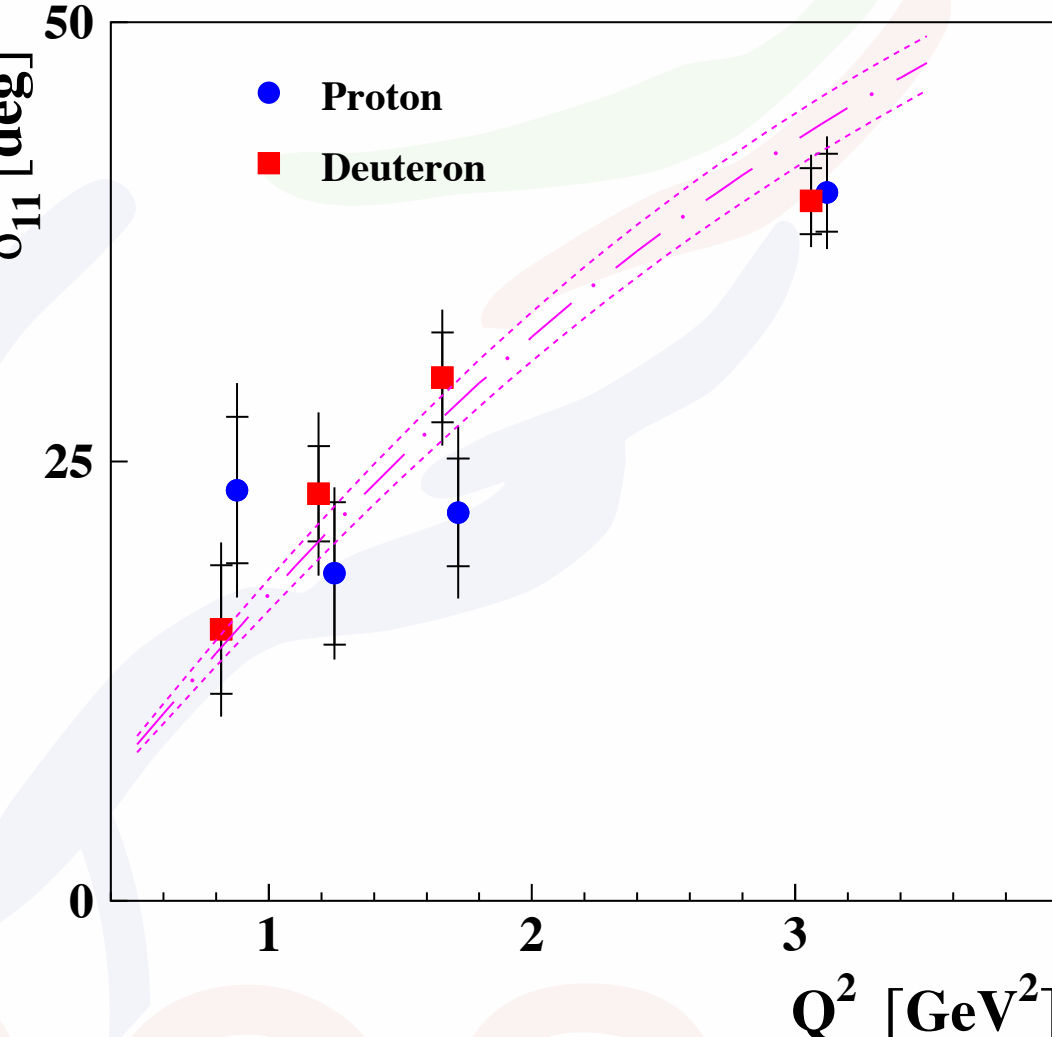
PacSPIN 2015 - Taipei - Oct. 6th, 2015

ρ^0 SDMEs from HERMES: challenges

[A. Airapetian et al., EPJ C62 (2009) 659]



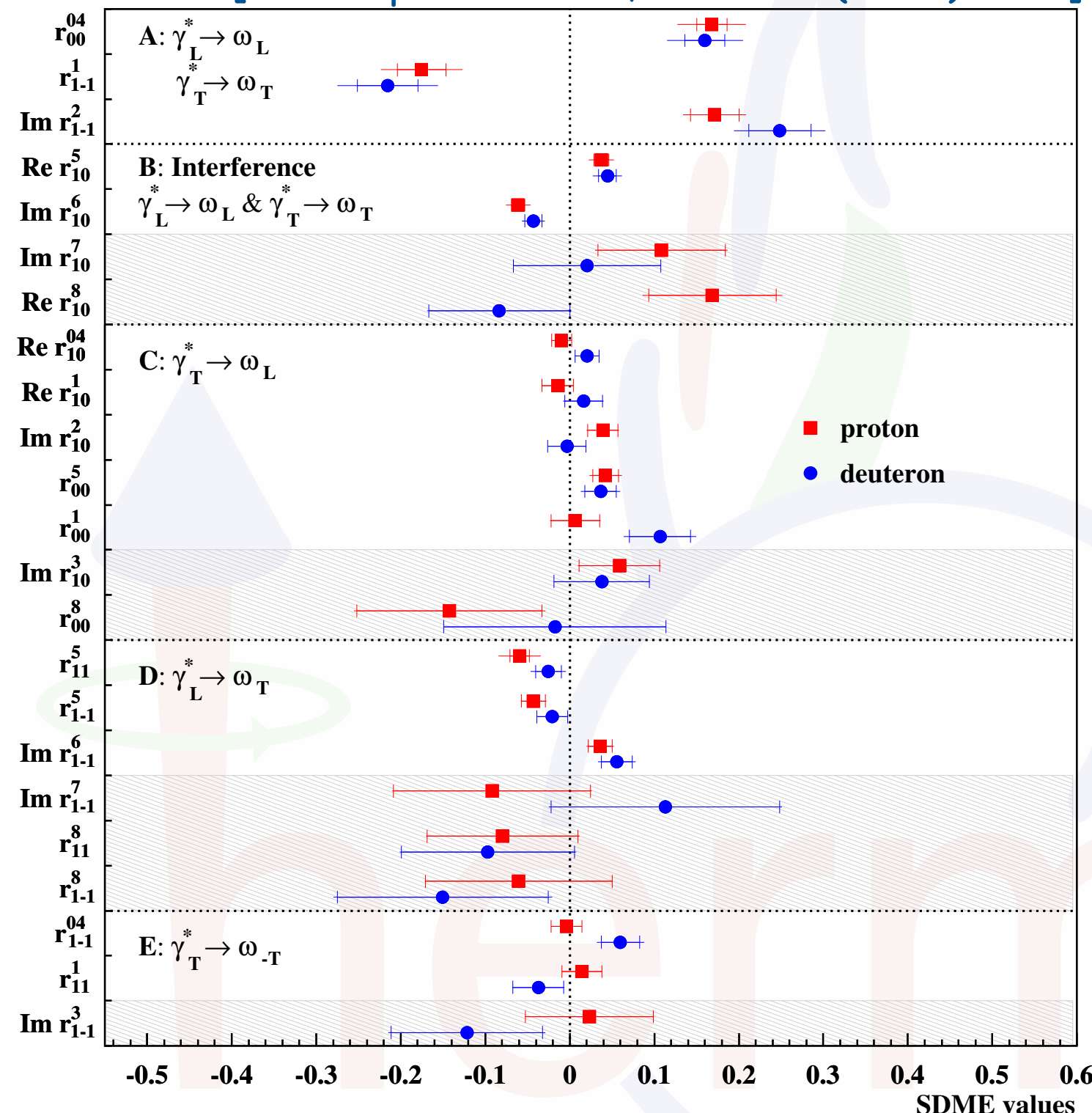
[A. Airapetian et al., EPJ C71 (2011) 1609]



Extraction of SDMEs and helicity amplitude ratios at HERMES for ρ mesons challenges GPD-based calculations (giving small values)

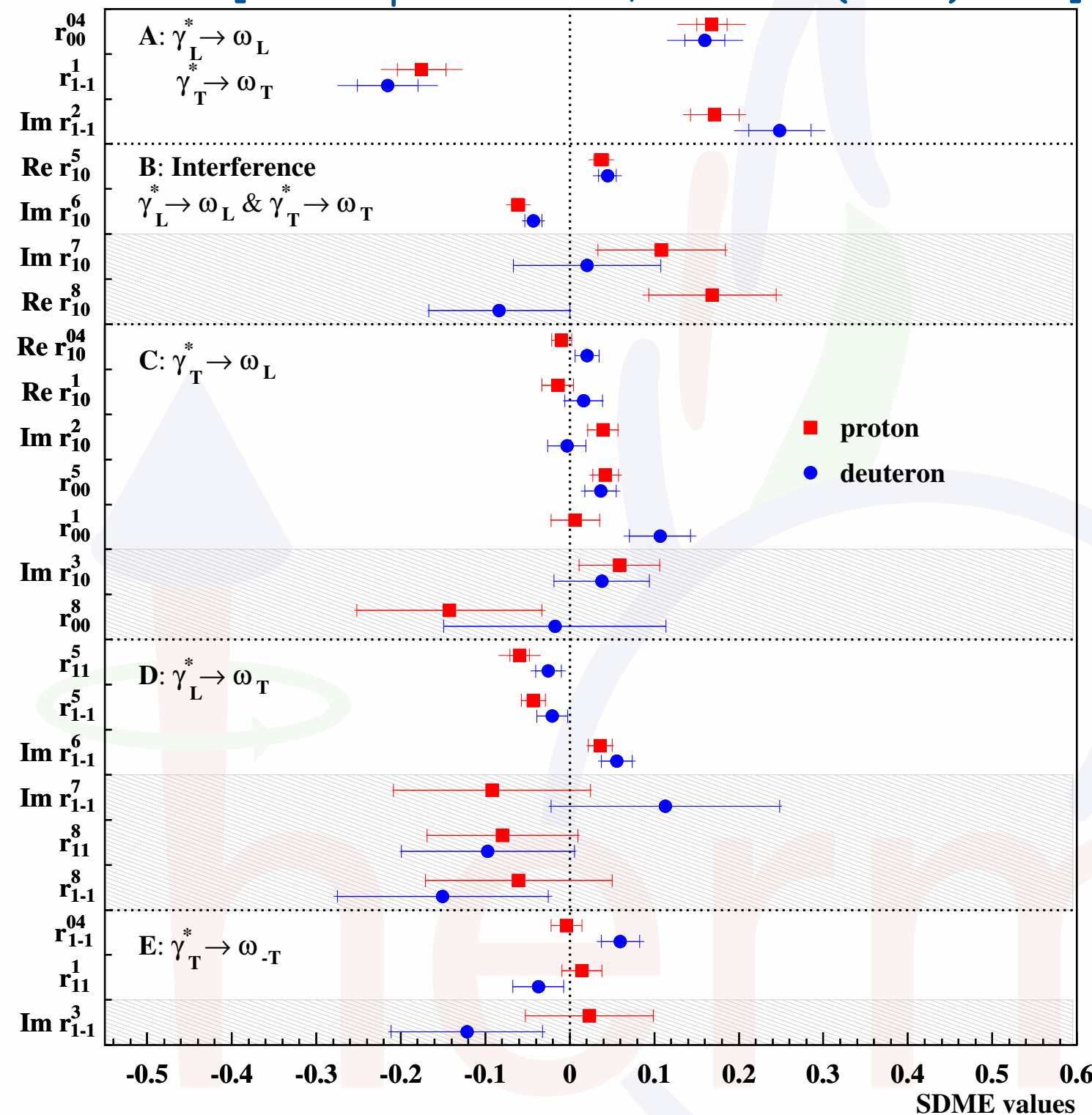
... ω production

[A. Airapetian et al., EPJ C74 (2014) 3110]



... ω production

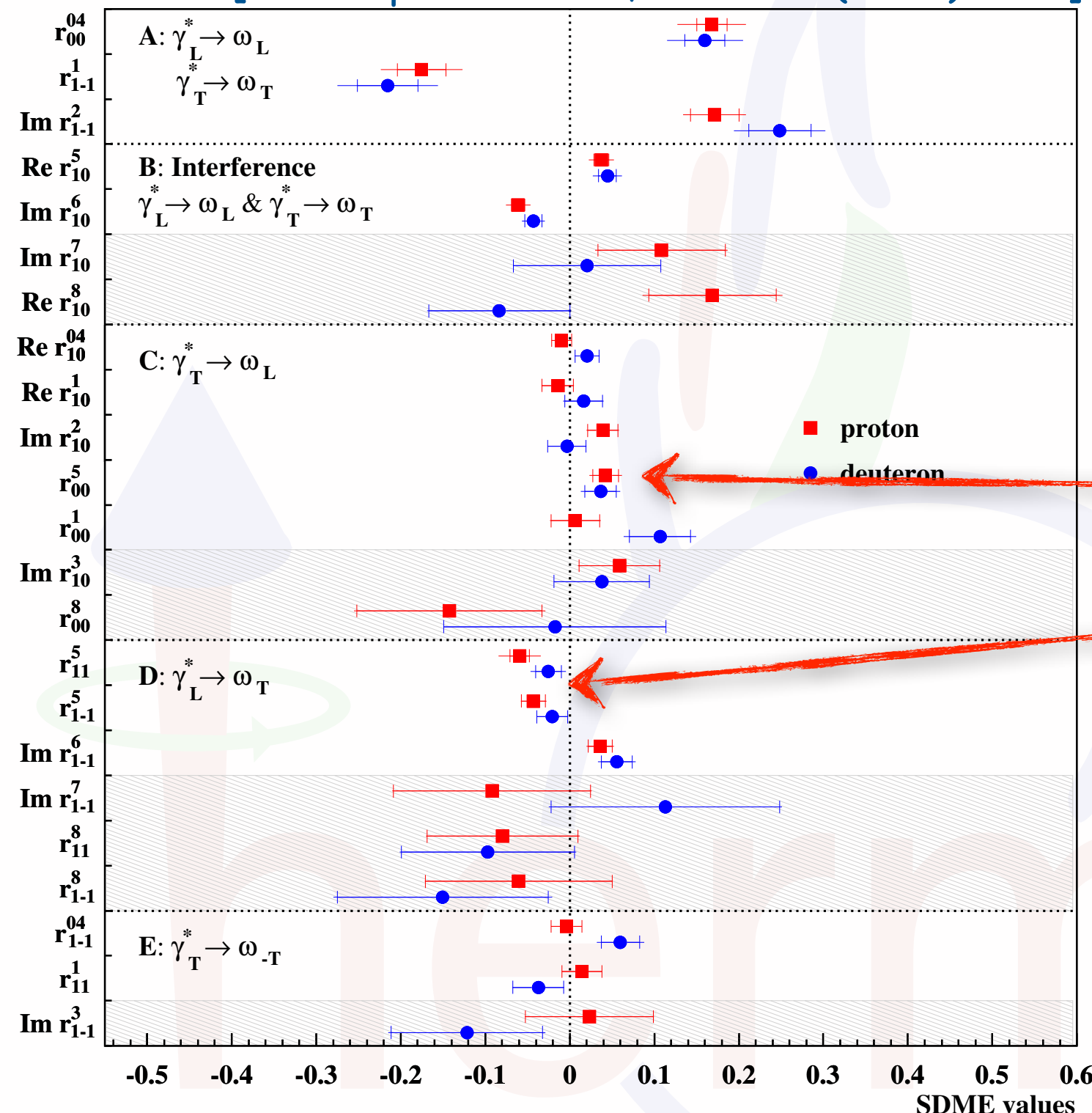
[A. Airapetian et al., EPJ C74 (2014) 3110]



- helicity-conserving SDMEs dominate

... ω production

[A. Airapetian et al., EPJ C74 (2014) 3110]



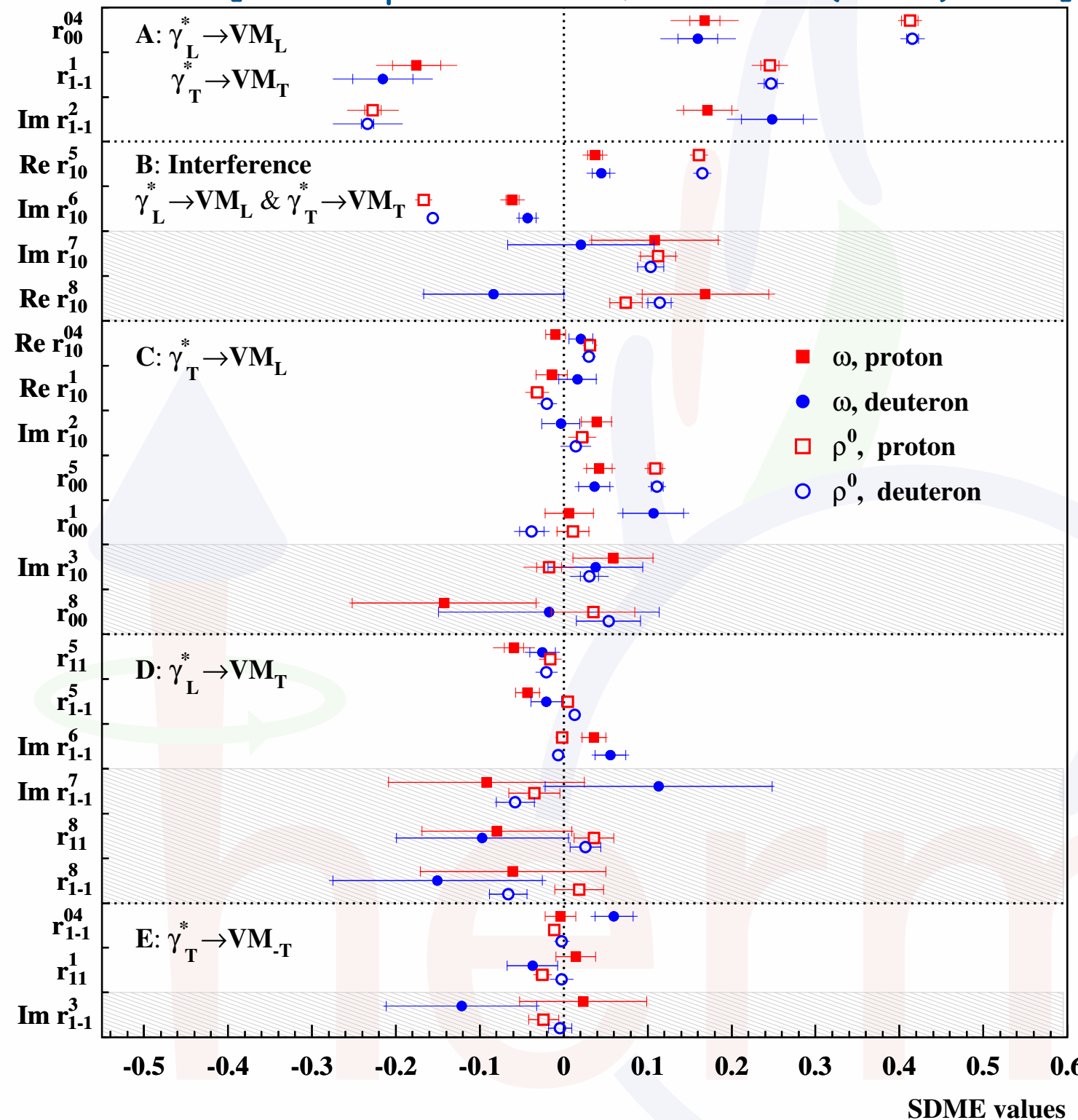
- helicity-conserving SDMEs dominate
- hardly any violation of SCHC, except maybe for

$$r_{00}^5$$

$$r_{11}^5 + r_{1-1}^5 - \Im r_{1-1}^6$$

... ω production

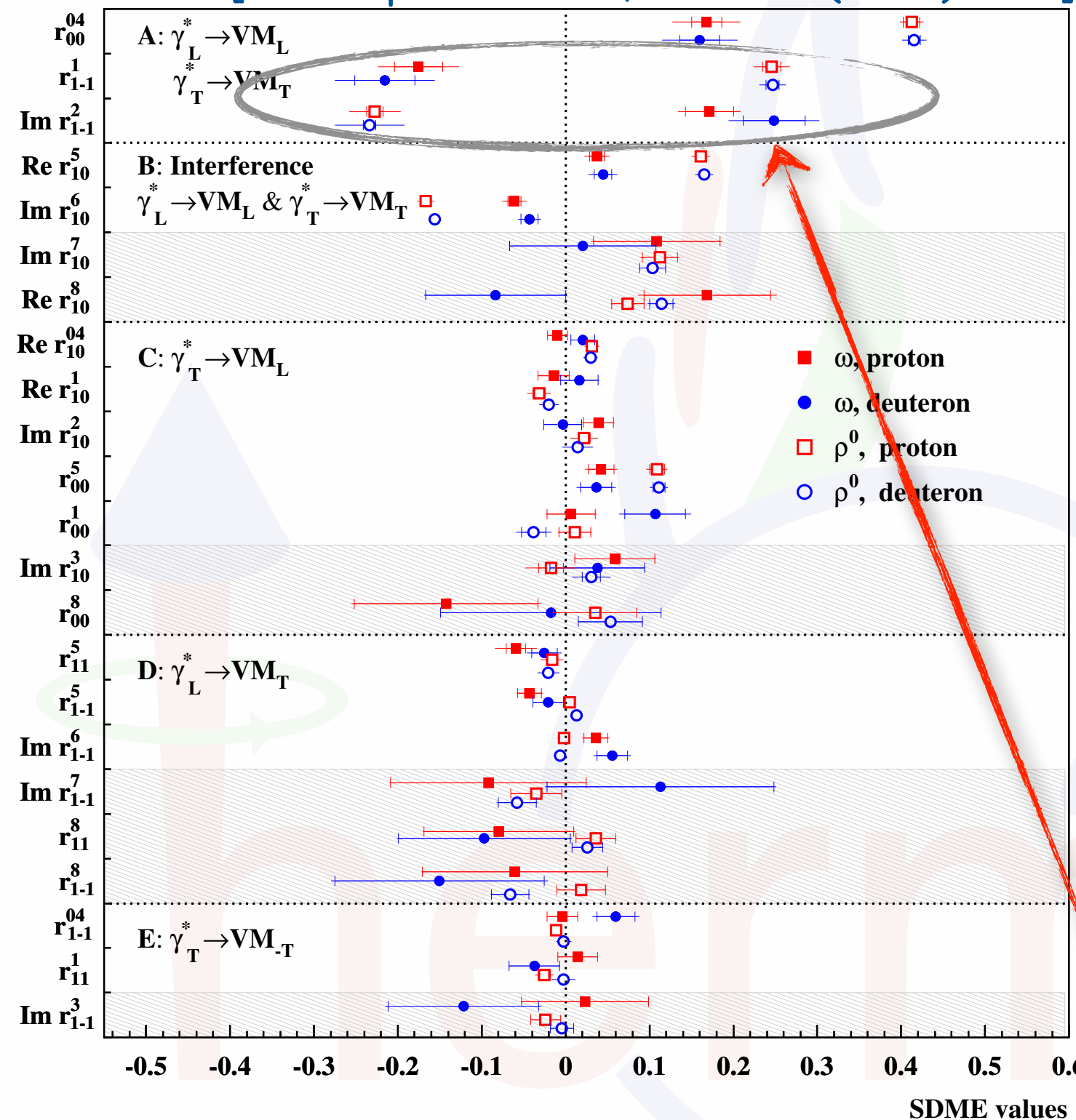
[A. Airapetian et al., EPJ C74 (2014) 3110]



- helicity-conserving SDMEs dominate
- hardly any violation of SCHC, except maybe for r_{00}^5
- $r_{11}^5 + r_{1-1}^5 - \Im r_{1-1}^6$
- interference smaller than for ρ^0 ...

... ω production

[A. Airapetian et al., EPJ C74 (2014) 3110]



- helicity-conserving SDMEs dominate
- hardly any violation of SCHC, except maybe for r_{00}^5 and $r_{11}^5 + r_{1-1}^5 - \Im r_{1-1}^6$
- interference smaller than for ρ^0 ...
... and opposite signs for r_{1-1}^1 & $\Im r_{1-1}^2$

(un)natural-parity exchange contributions

$$\Im r_{1-1}^2 - r_{1-1}^1 = \frac{1}{\mathcal{N}} \widetilde{\sum} (|U_{11}|^2 - |T_{11}|^2)$$

UPE contribution

NPE contribution

- positive for omega \rightarrow large UPE contributions (unlike for rho)
- can construct various UPE quantities:

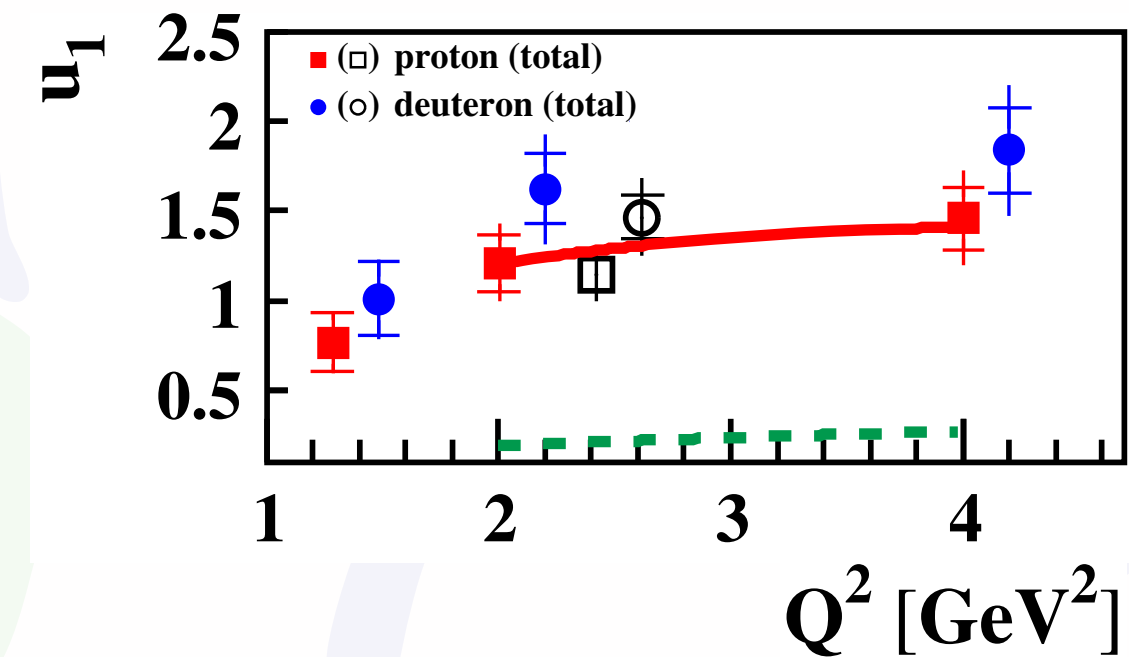
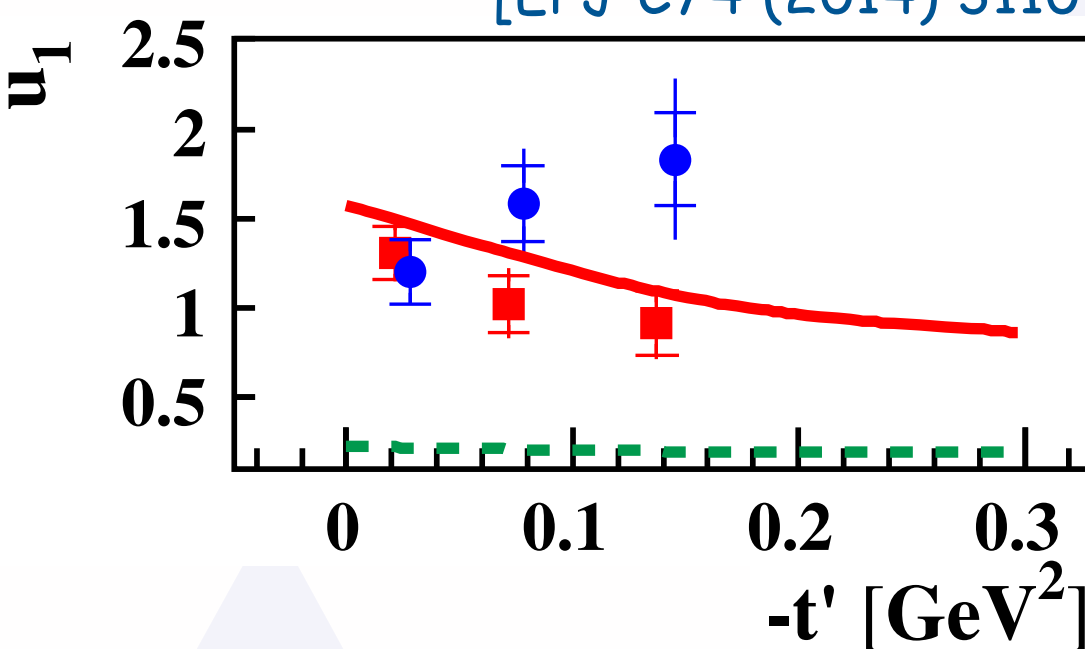
$$u_1 = 1 - r_{00}^{04} + 2r_{1-1}^{04} - 2r_{11}^1 - 2r_{1-1}^1$$

$$u_2 = r_{11}^5 + r_{1-1}^5$$

$$u_3 = r_{11}^8 + r_{1-1}^8$$

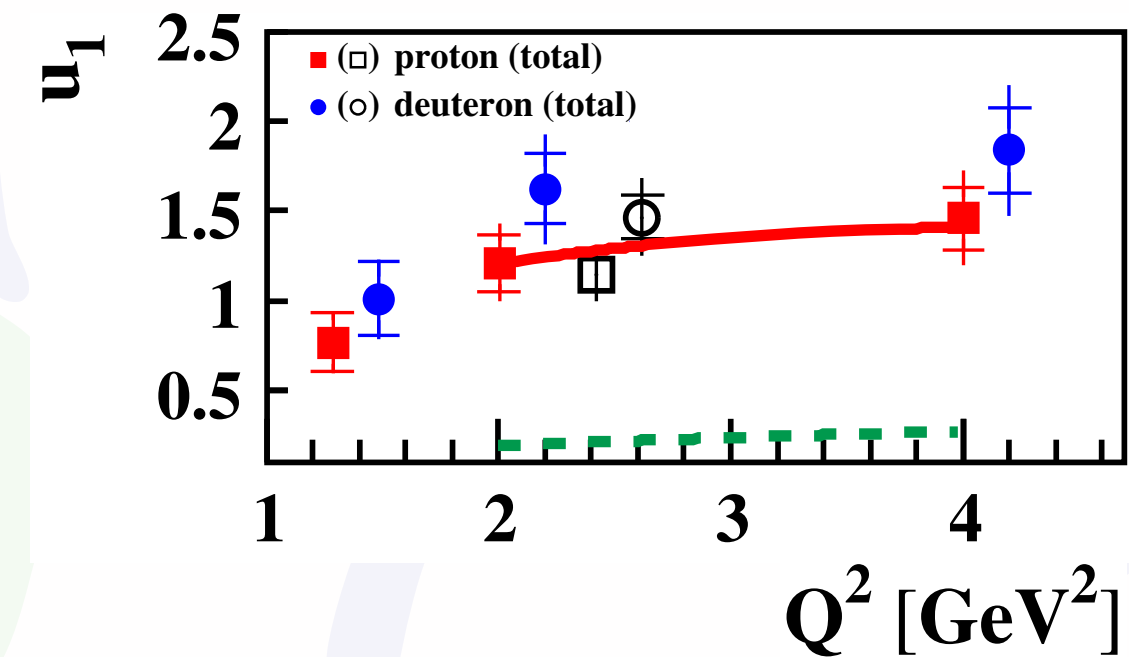
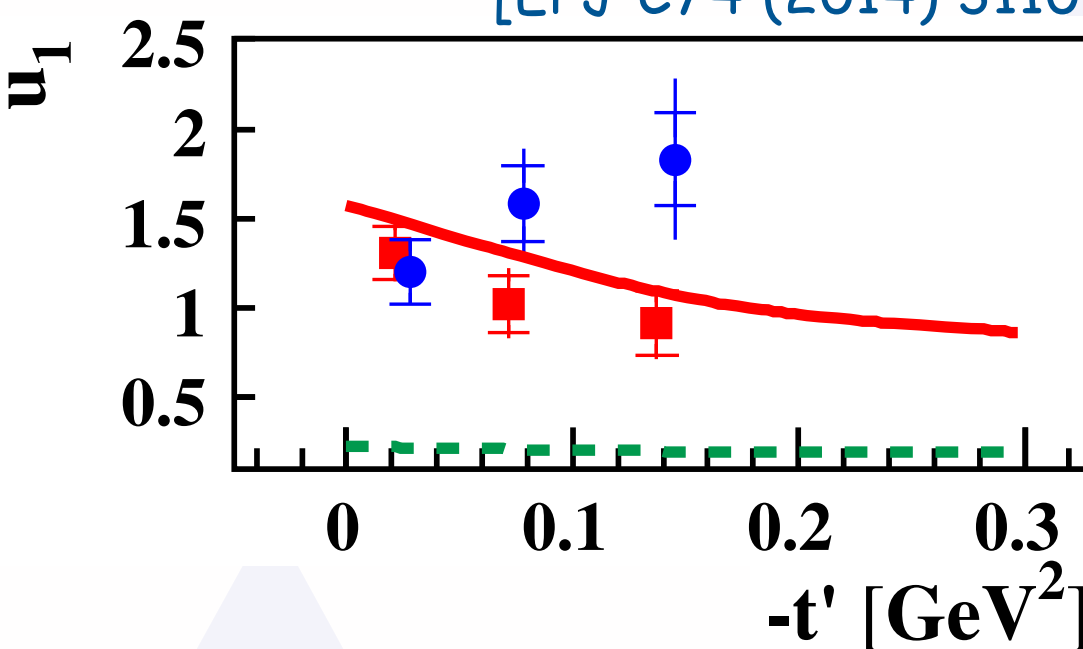
test of UPE

[EPJ C74 (2014) 3110]



test of UPE

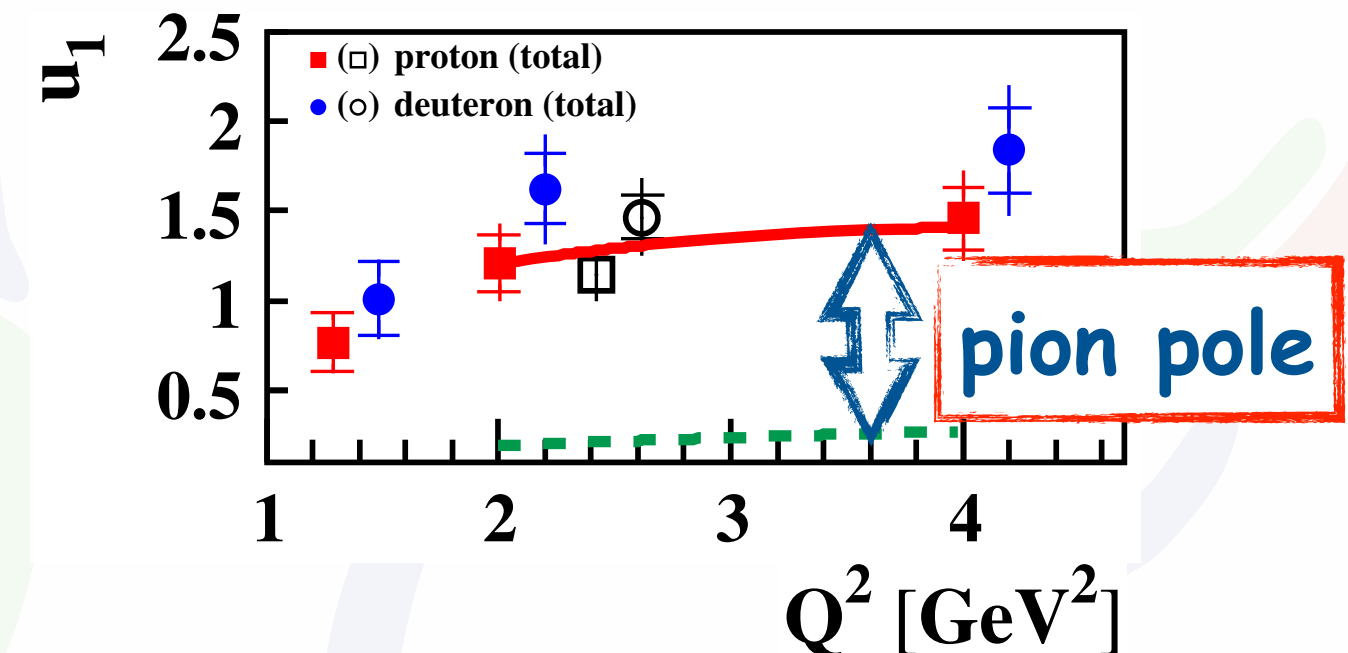
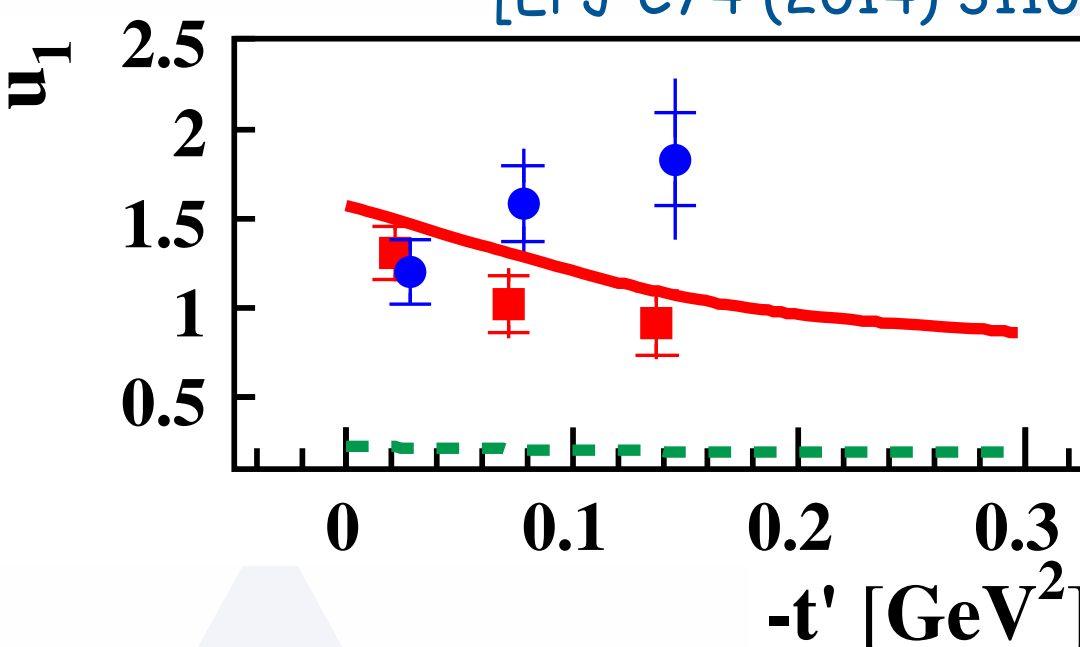
[EPJ C74 (2014) 3110]



- large UPE contributions

test of UPE

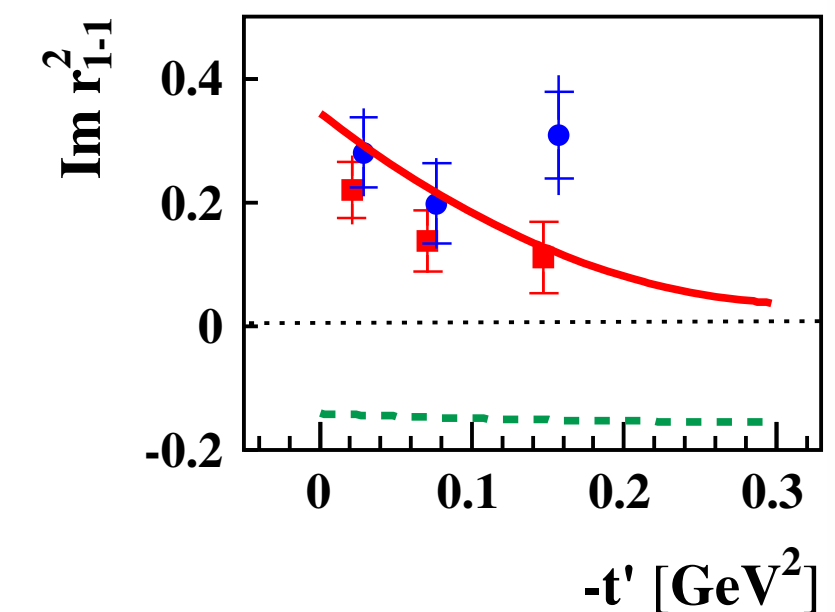
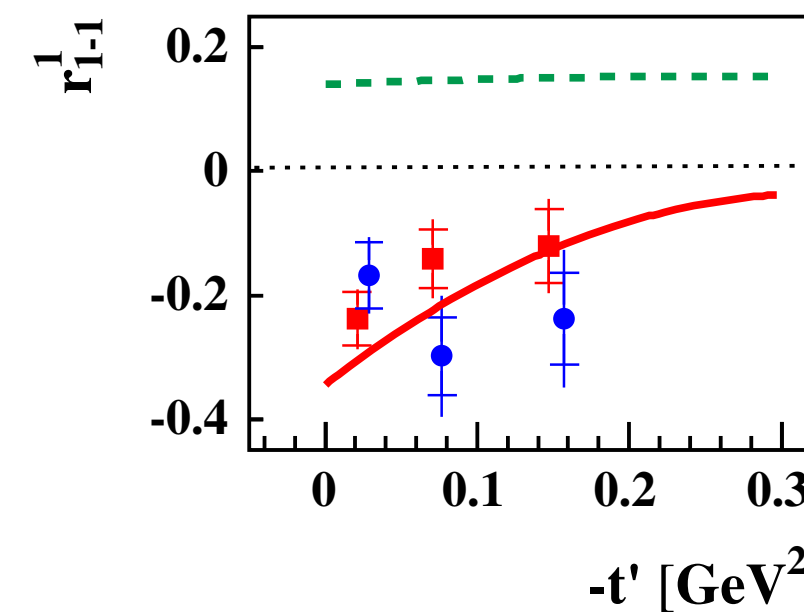
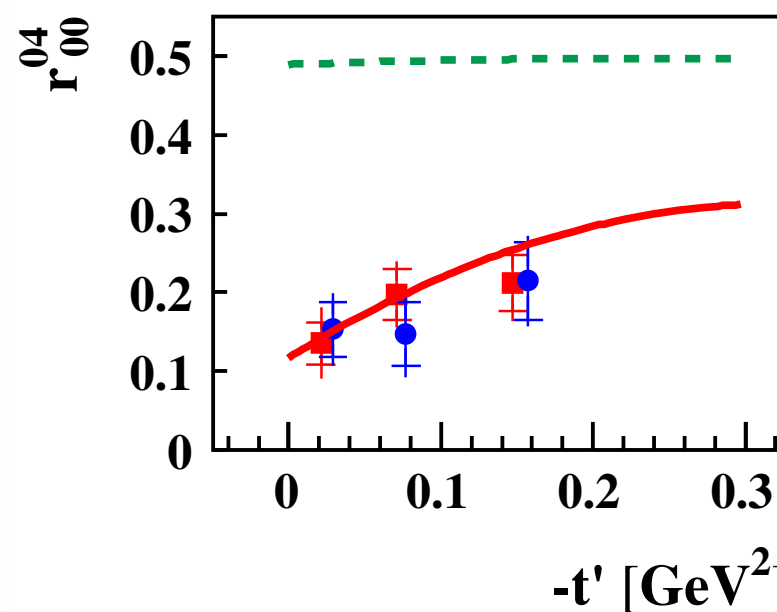
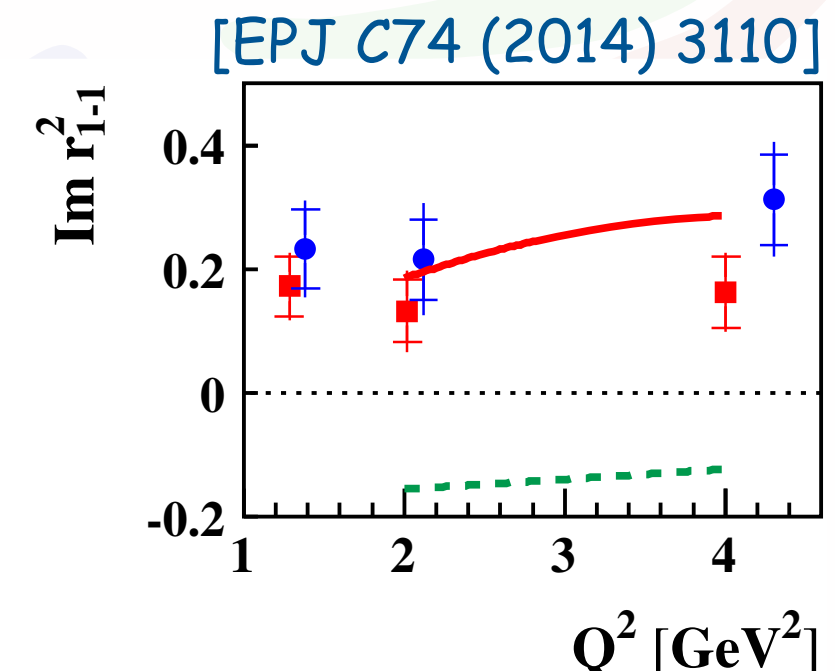
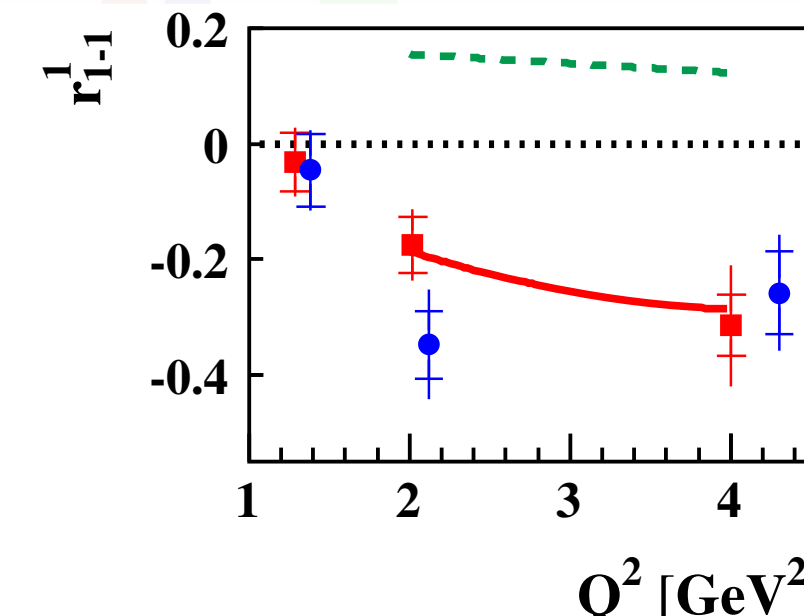
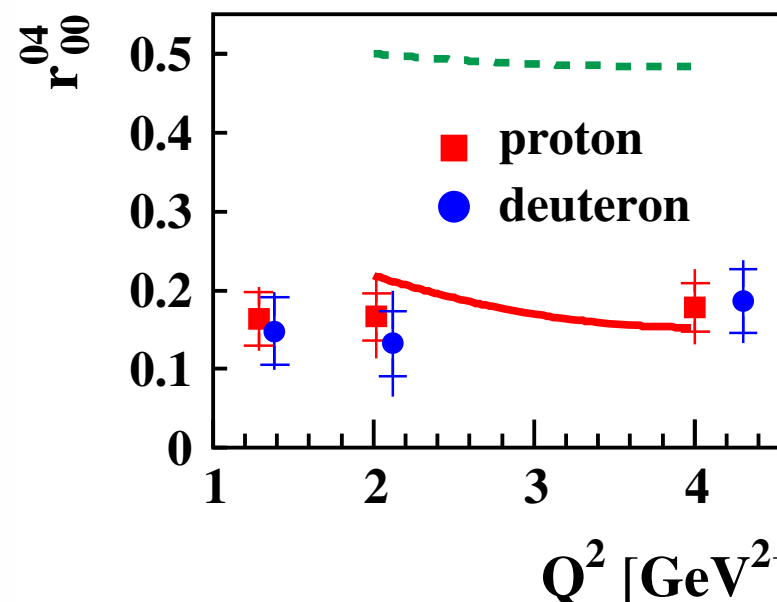
[EPJ C74 (2014) 3110]



- large UPE contributions
- modified GK model [EPJ A50 (2014) 146] can describe data when including
 - pion pole contribution (red curve)
 - corresponding $\pi\omega$ transition form factor (fit to these data)

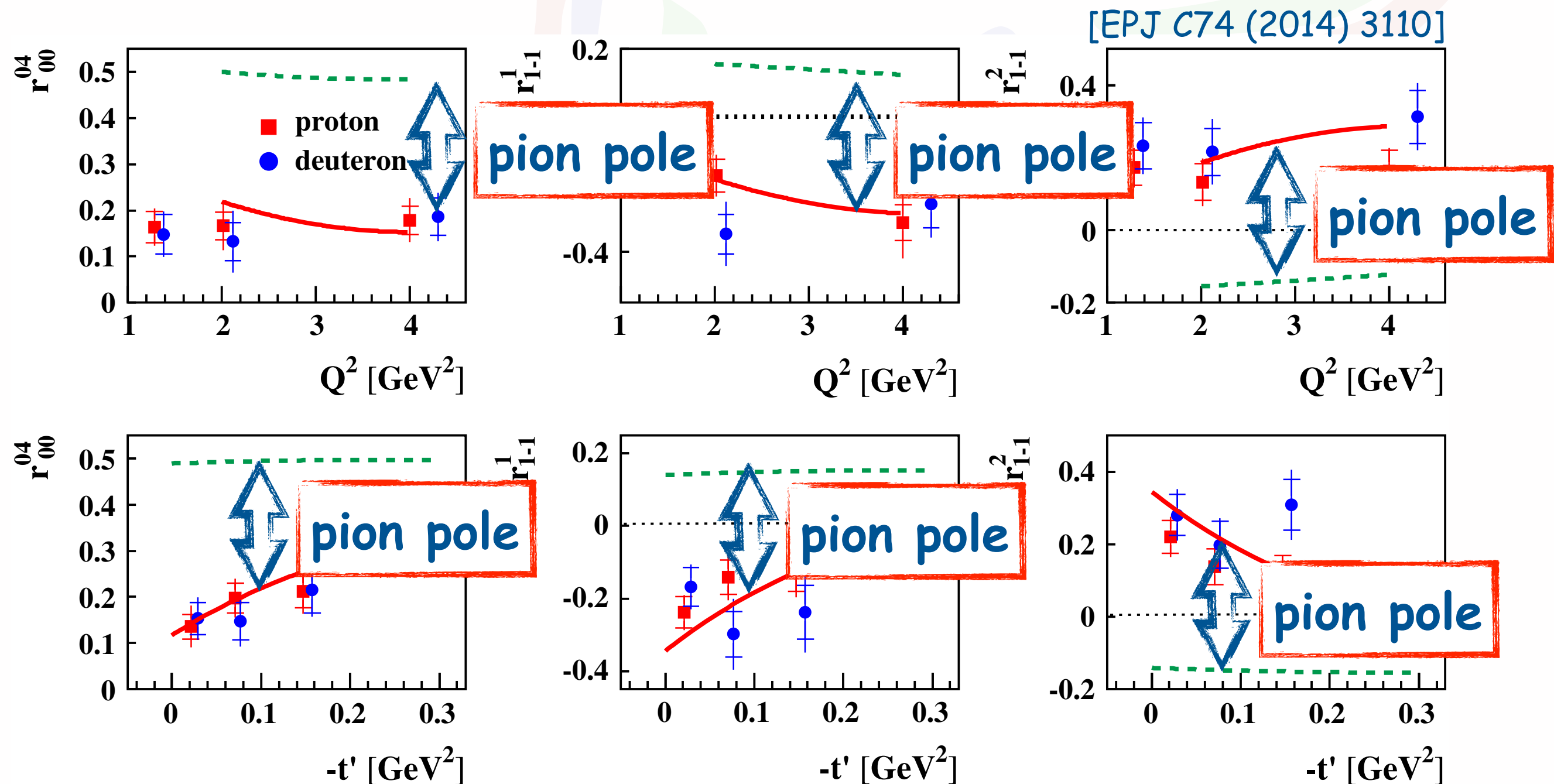
impact of pion-pole contr. on SDMEs

- “class-A” - helicity-conserving transitions



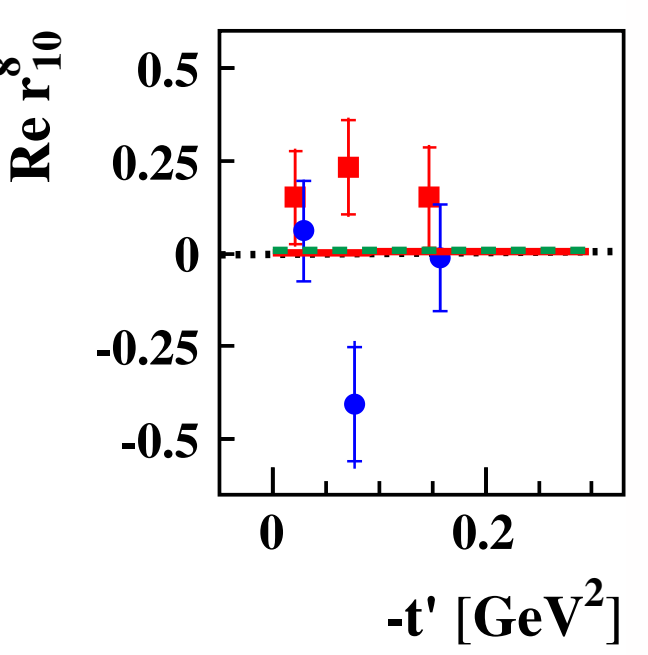
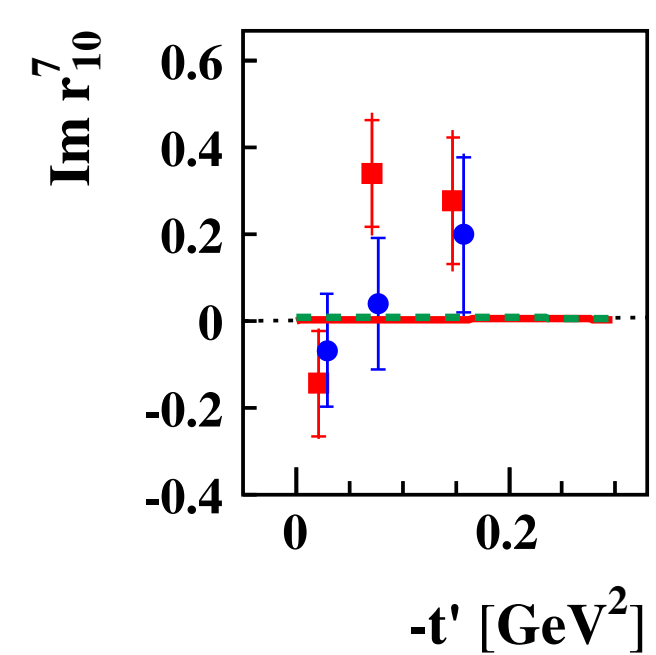
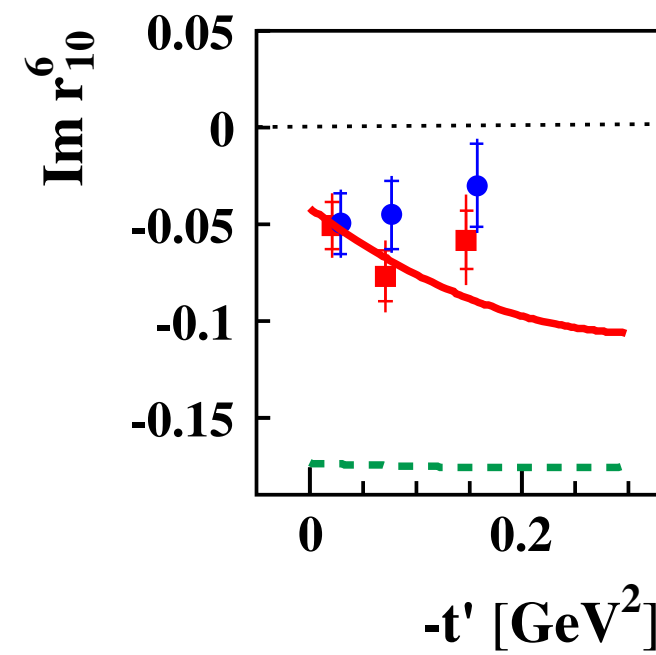
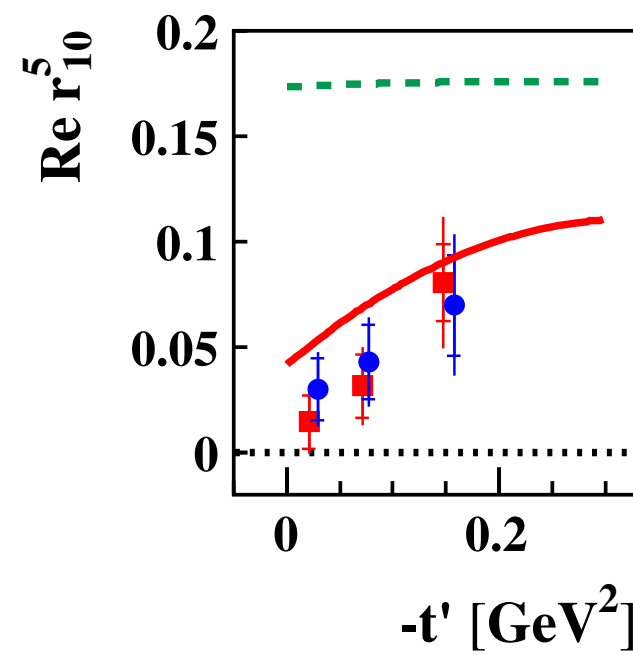
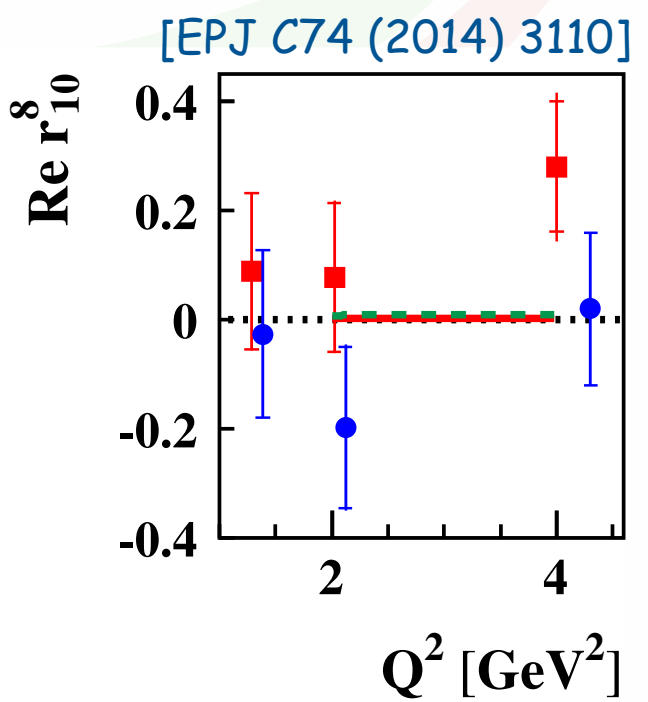
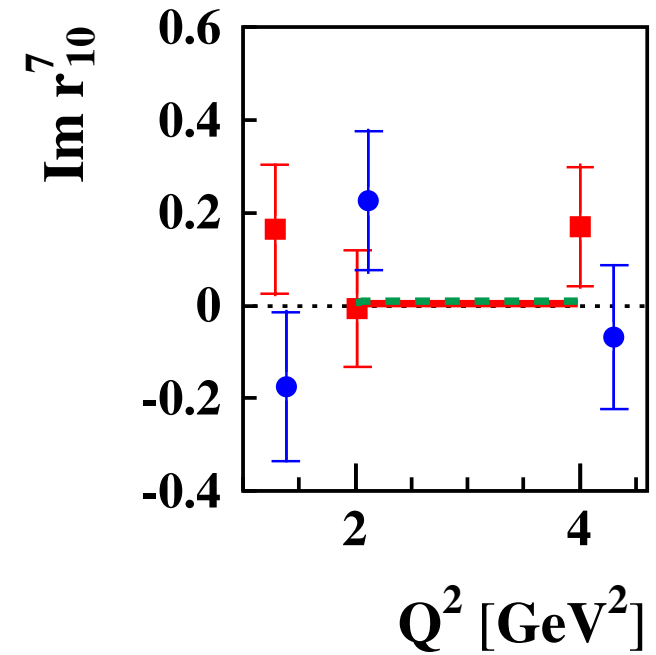
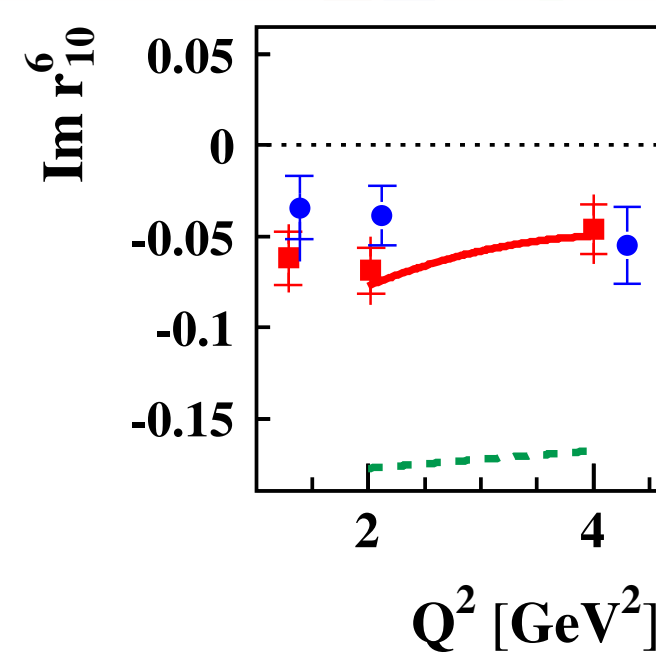
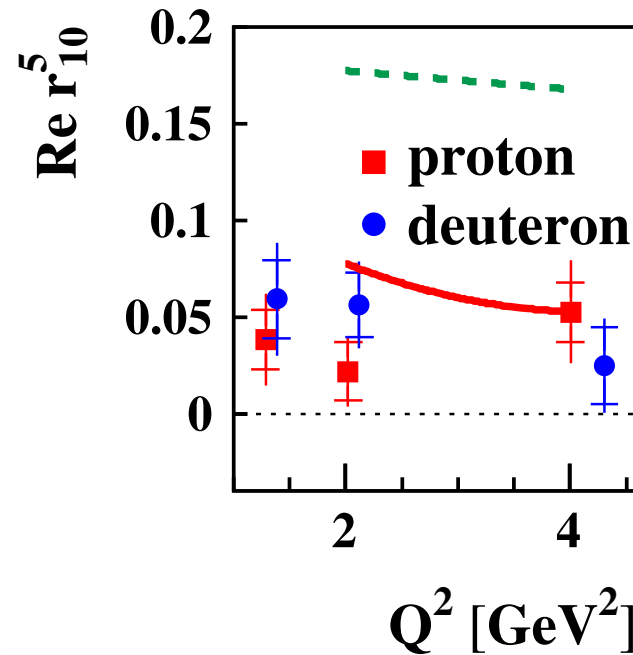
impact of pion-pole contr. on SDMEs

- “class-A” - helicity-conserving transitions



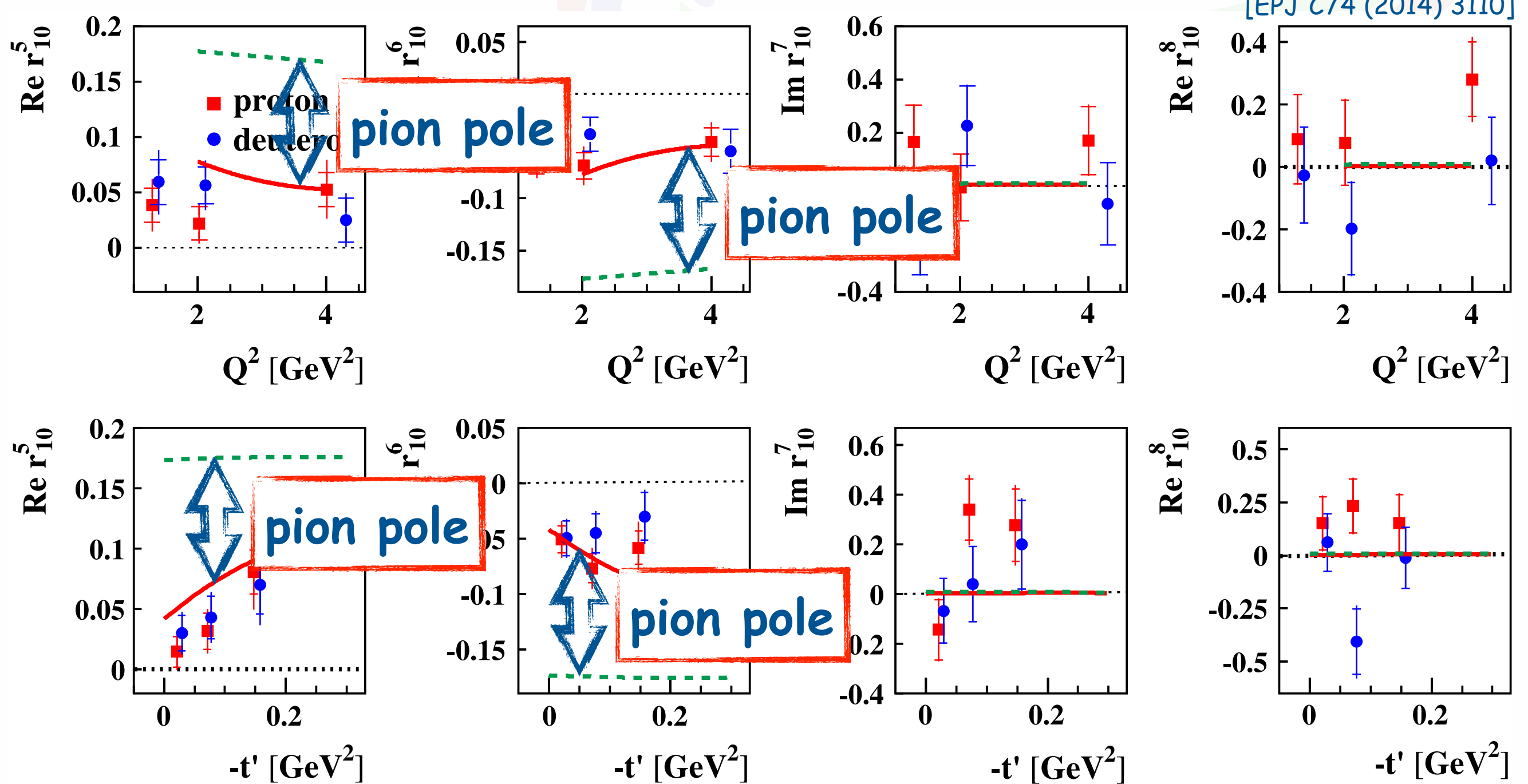
impact of pion-pole contr. on SDMEs

- “class-B” - interference of helicity-conserving transitions



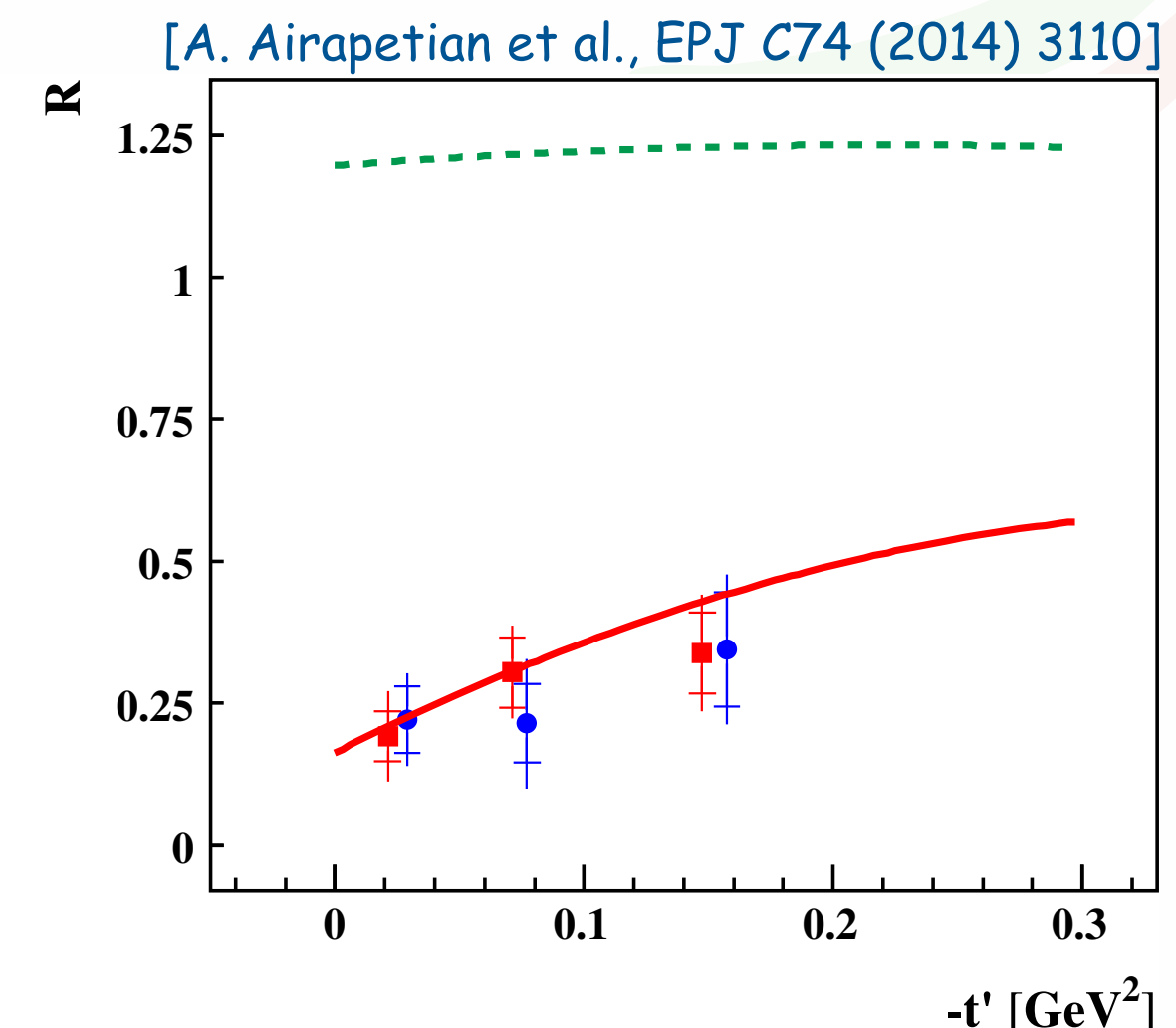
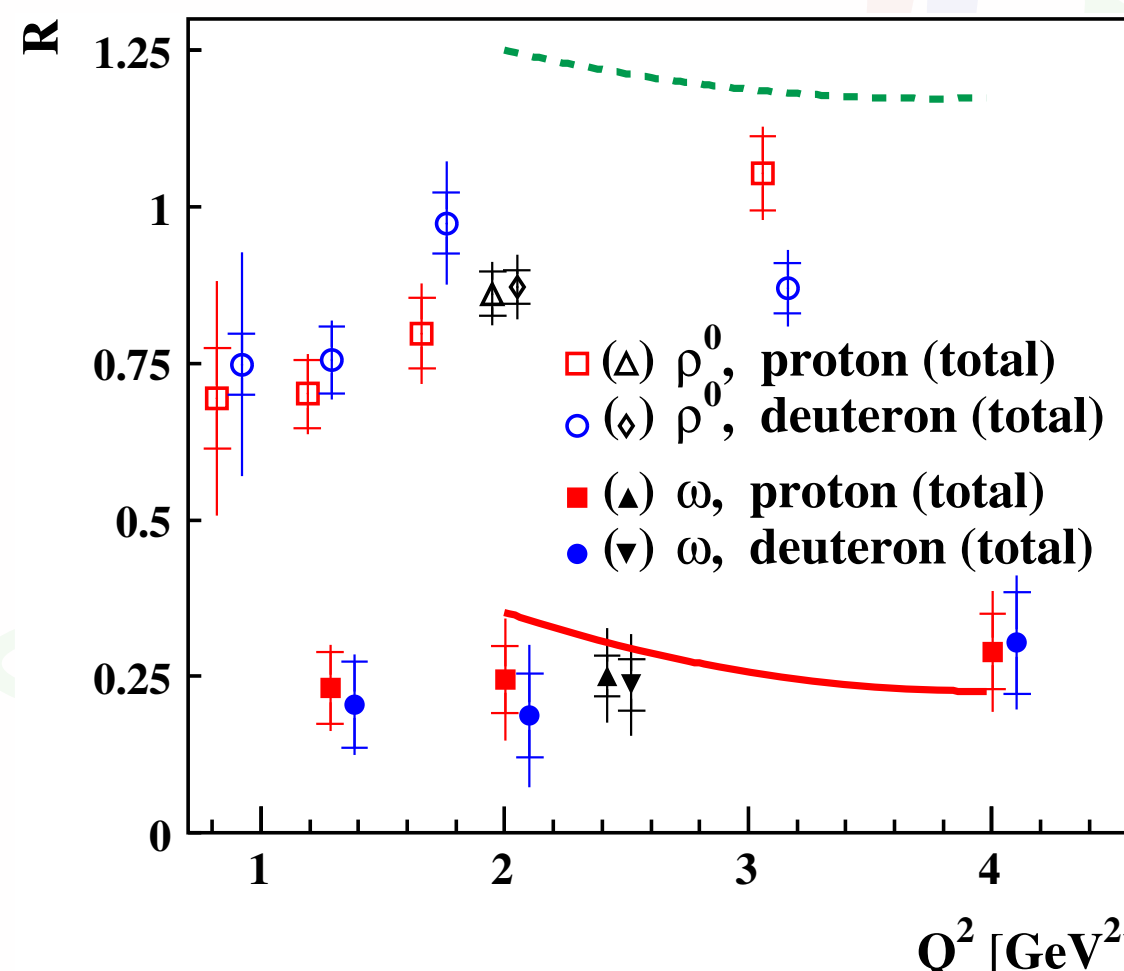
impact of pion-pole contr. on SDMEs

- “class-B” - interference of helicity-conserving transitions



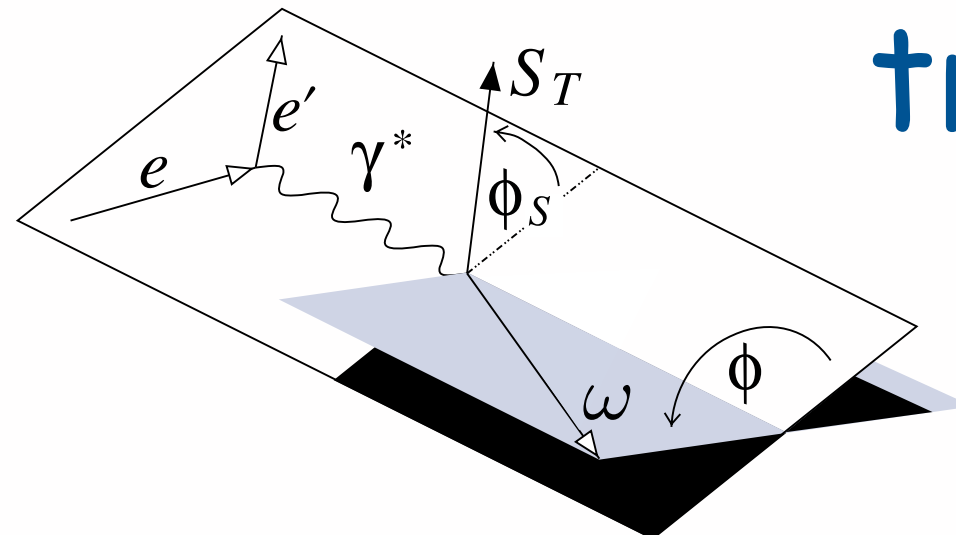
long.-to-transverse cross-section ratio

$$R = \frac{d\sigma(\gamma_L^* \rightarrow \omega)}{d\sigma(\gamma_T^* \rightarrow \omega)} \approx \frac{1}{\epsilon} \frac{r_{00}^{04}}{1 - r_{00}^{04}}$$

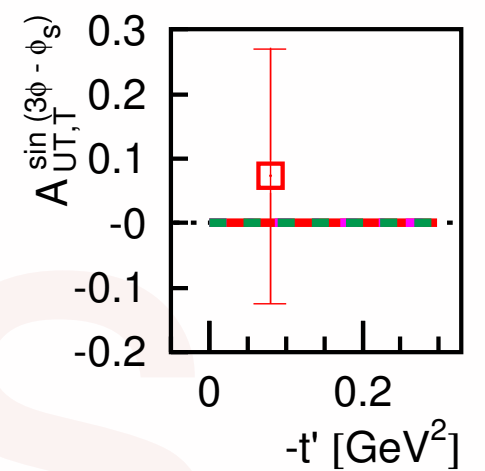
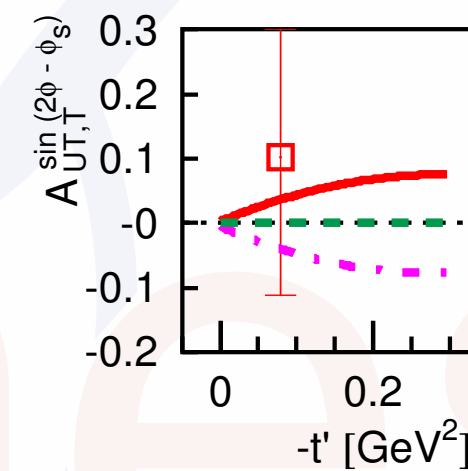
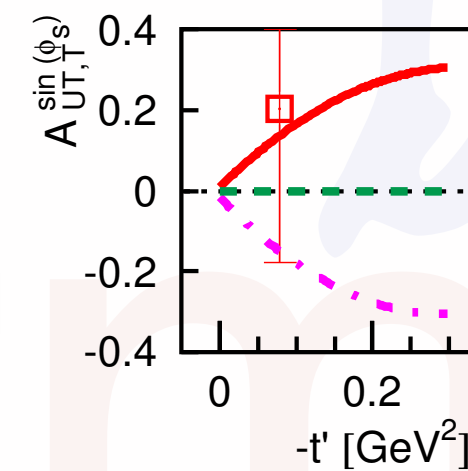
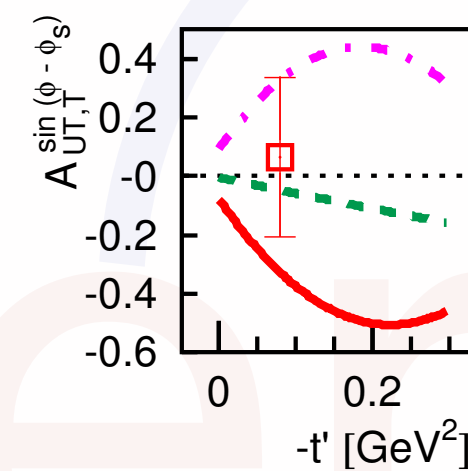
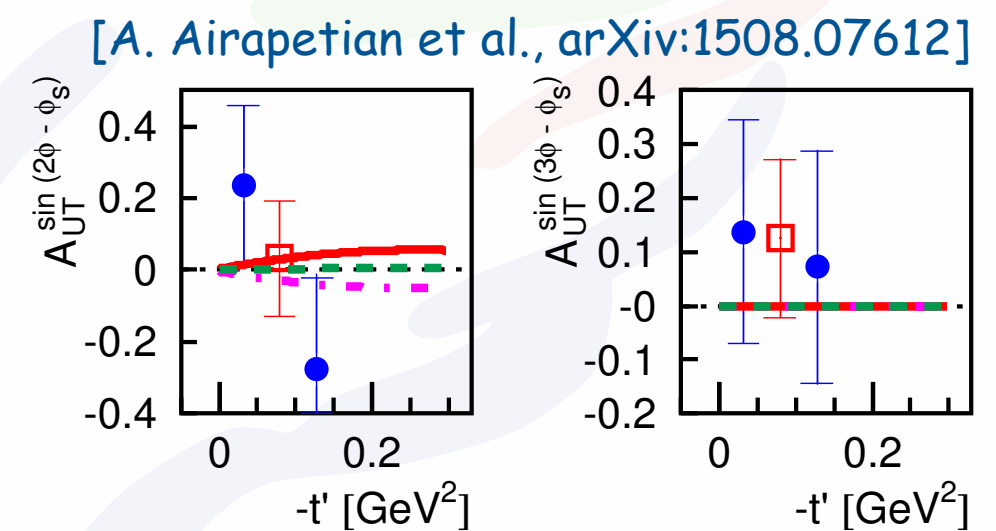
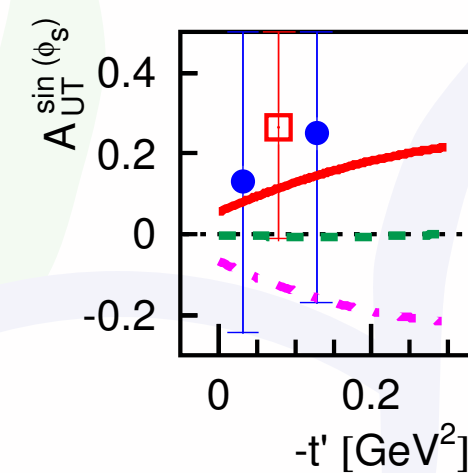
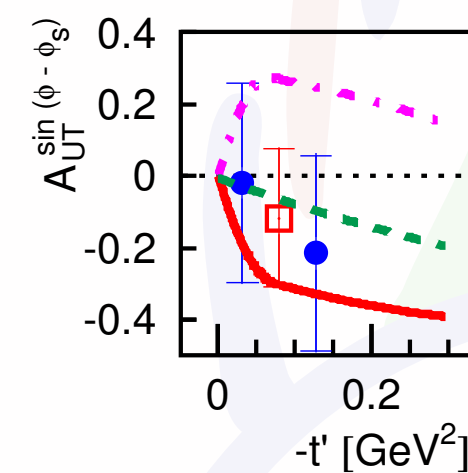
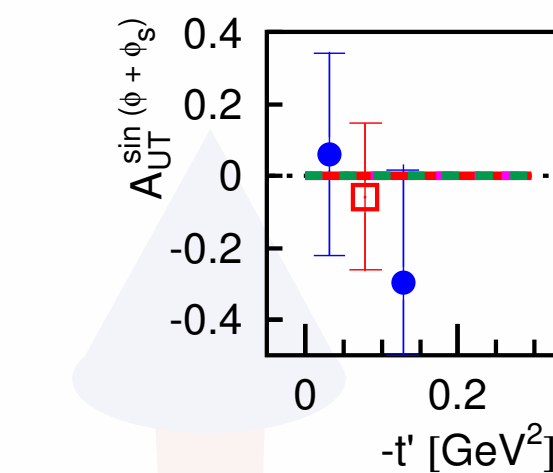


- significantly smaller for ω than for ρ
- important contribution from pion pole

transverse-spin asymmetry



sensitive, in principle, to sign of $\pi\omega$
transition FF



slight preference for positive $\pi\omega$ transition FF (red/full line)
vs. negative one (magenta/dash-dotted line)

summary

DVCS @ HERMES

HERMES analyzed a wealth of DVCS-related asymmetries on nucleon and nuclear targets

data with recoil-proton detection allows clean interpretation

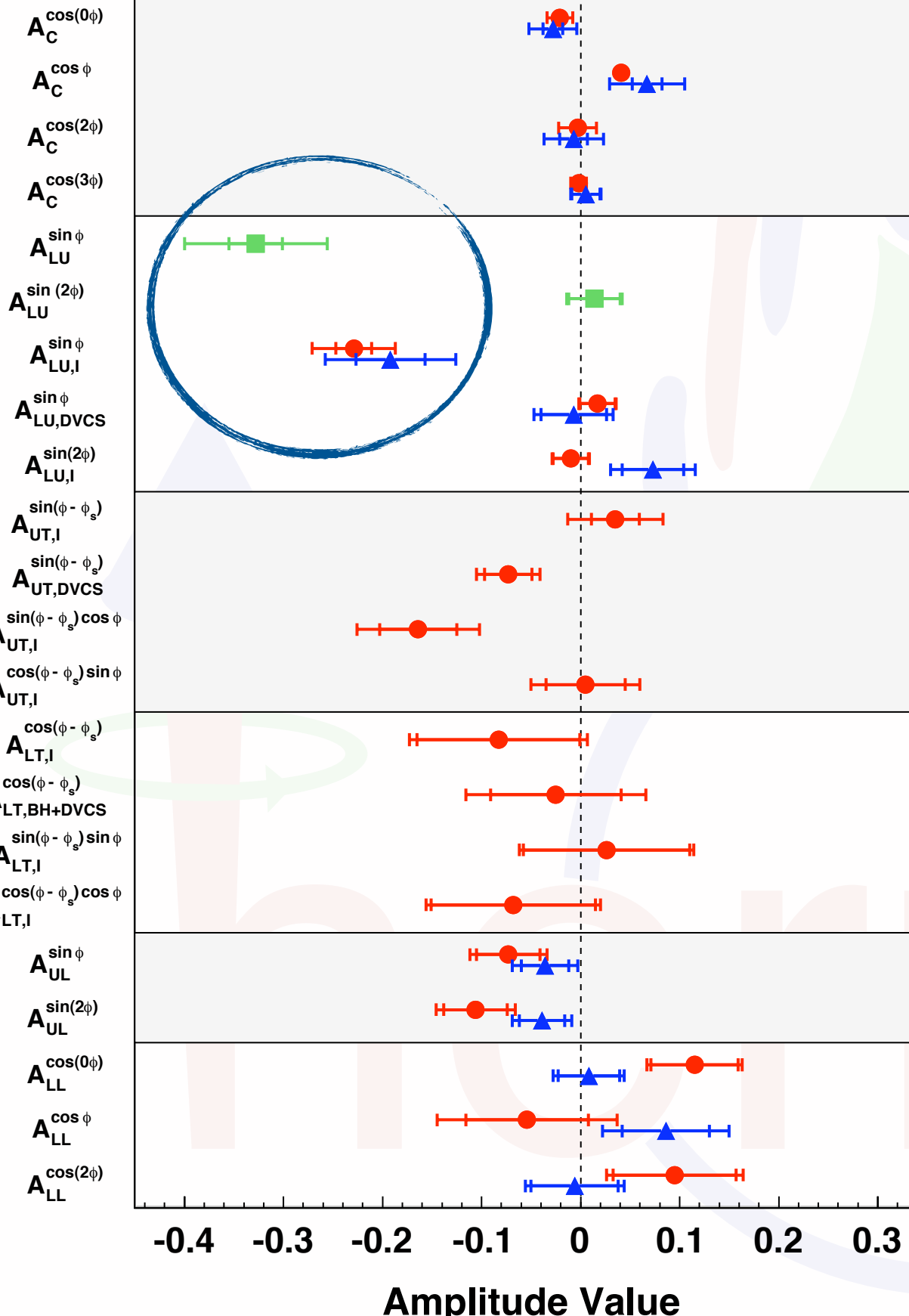
indication of larger amplitudes for pure sample

-> assoc. DVCS in "traditional" analysis mainly dilution, supported by recent results from HERMES
[JHEP 01 (2014) 077]:

assoc. DVCS results consistent with zero but also with model prediction

HERMES DVCS

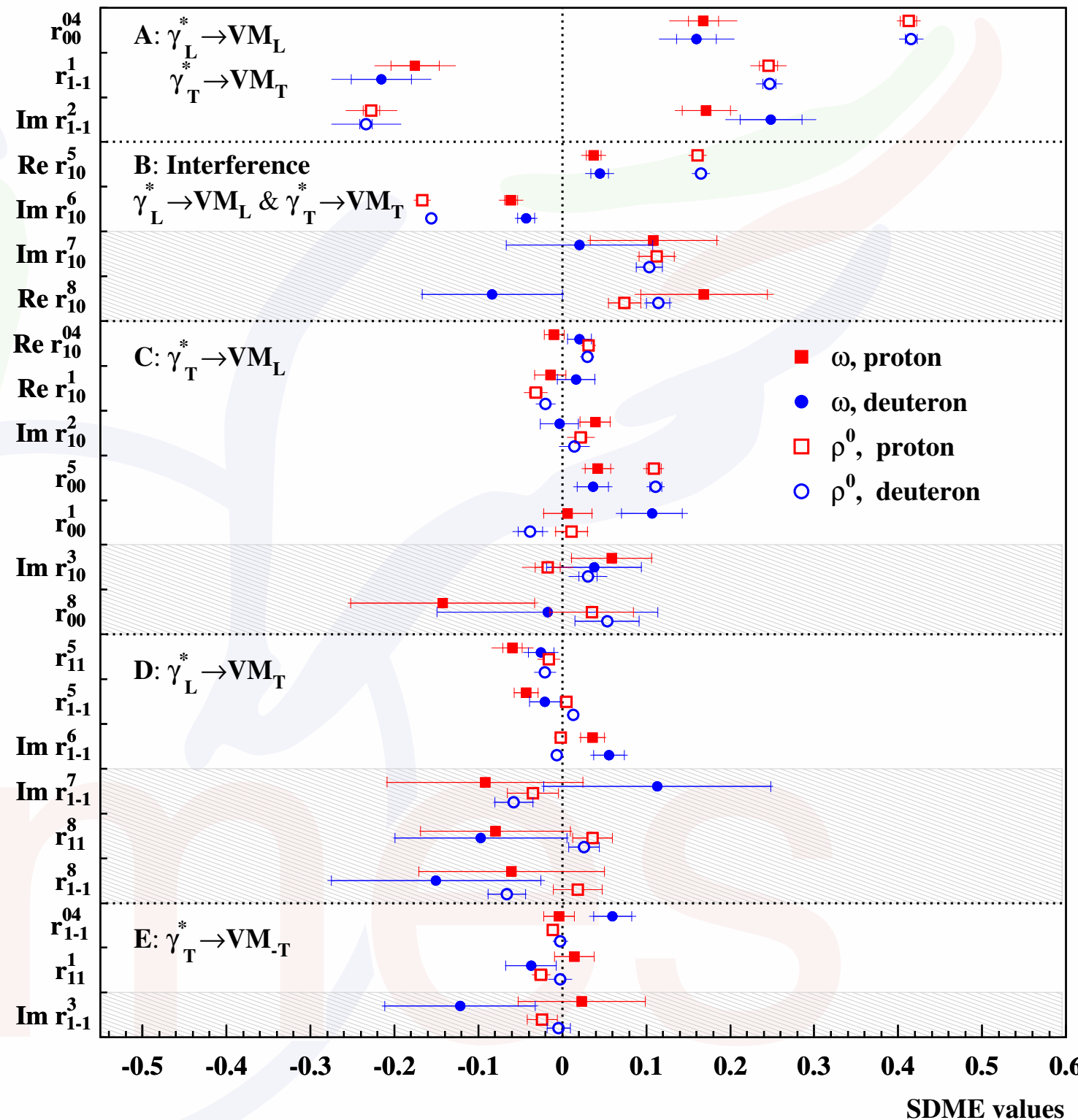
- Hydrogen
- ▲ Deuterium
- Hydrogen Pure



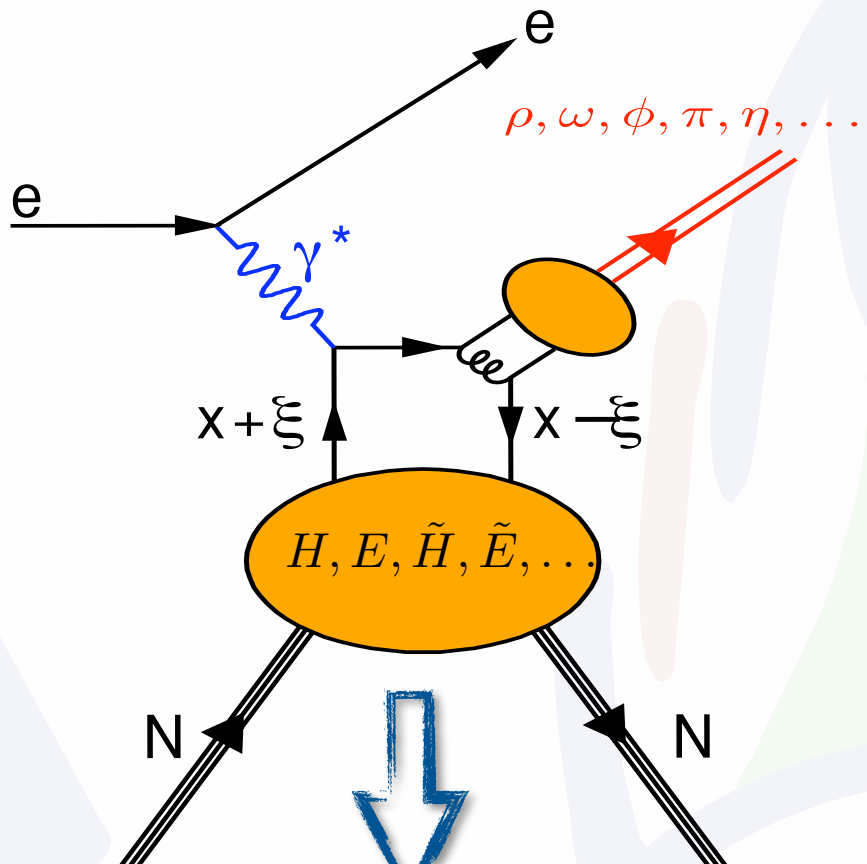
HEMP @ HERMES

- extensive data set on unpolarized and polarized SDMEs in vector-meson production
- (not shown:) cross section and A_{UT} for excl. π^+
- essential input in model building
- recent results on omega production require pion-pole contribution with a preference for positive $\pi\omega$ transition FF

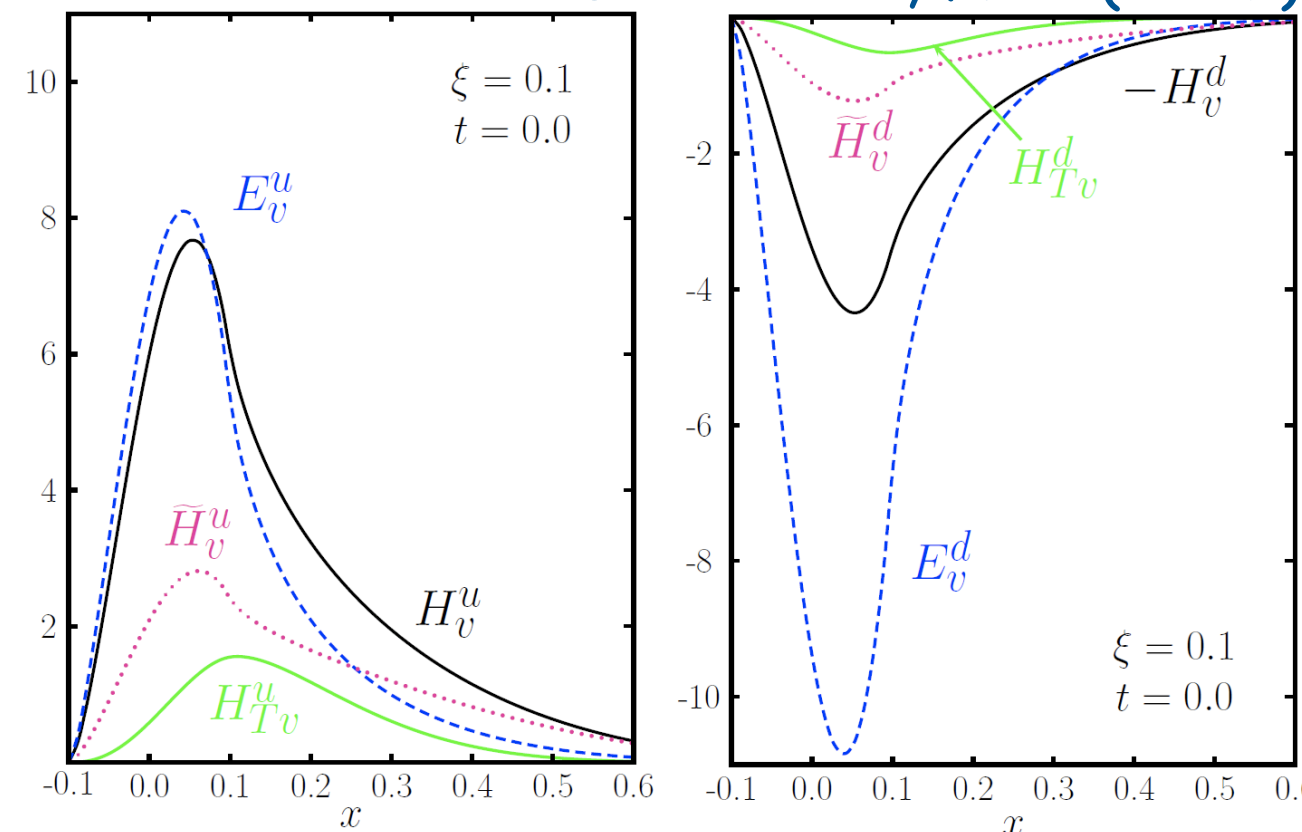
[A. Airapetian et al., EPJ C74 (2014) 3110, EPJ C62 (2009) 659]



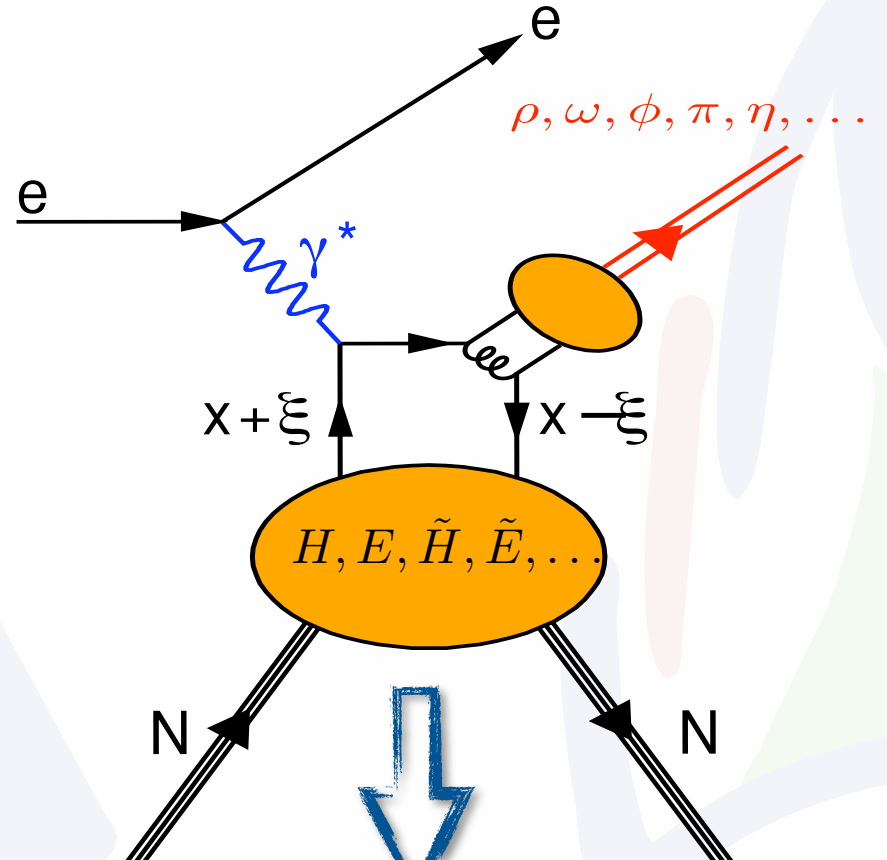
GPDs - a nice success story!



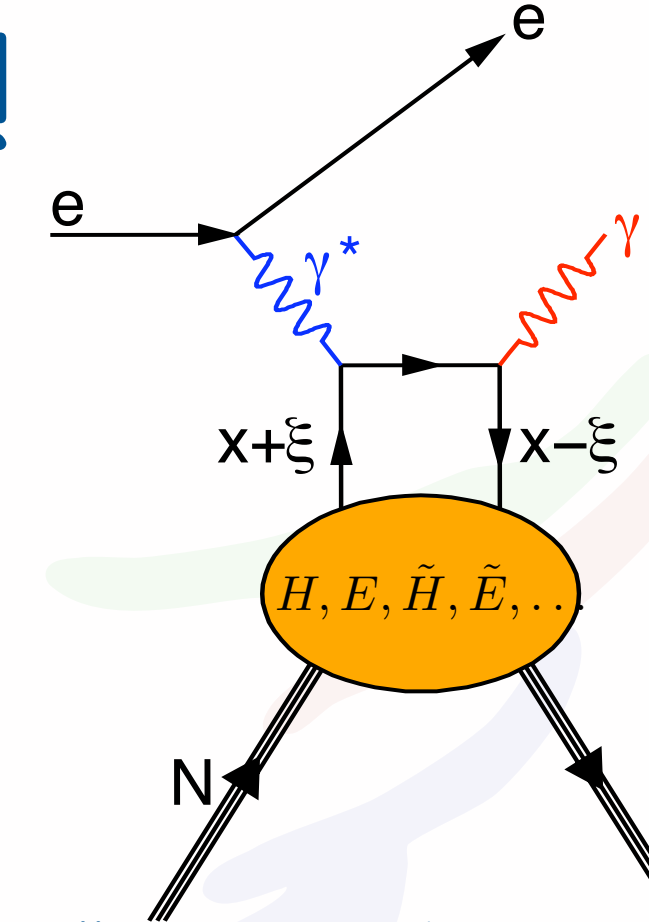
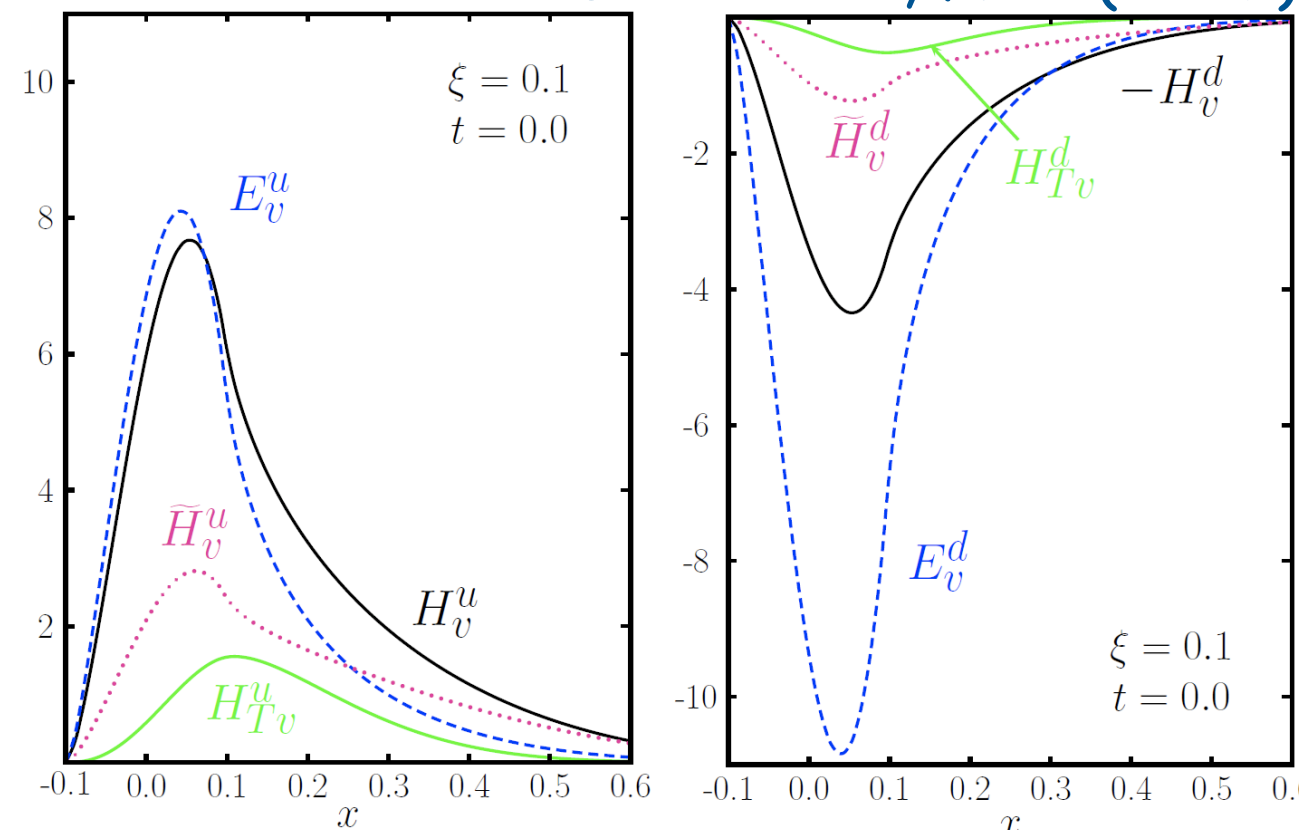
Goloskokov, Kroll (2007)



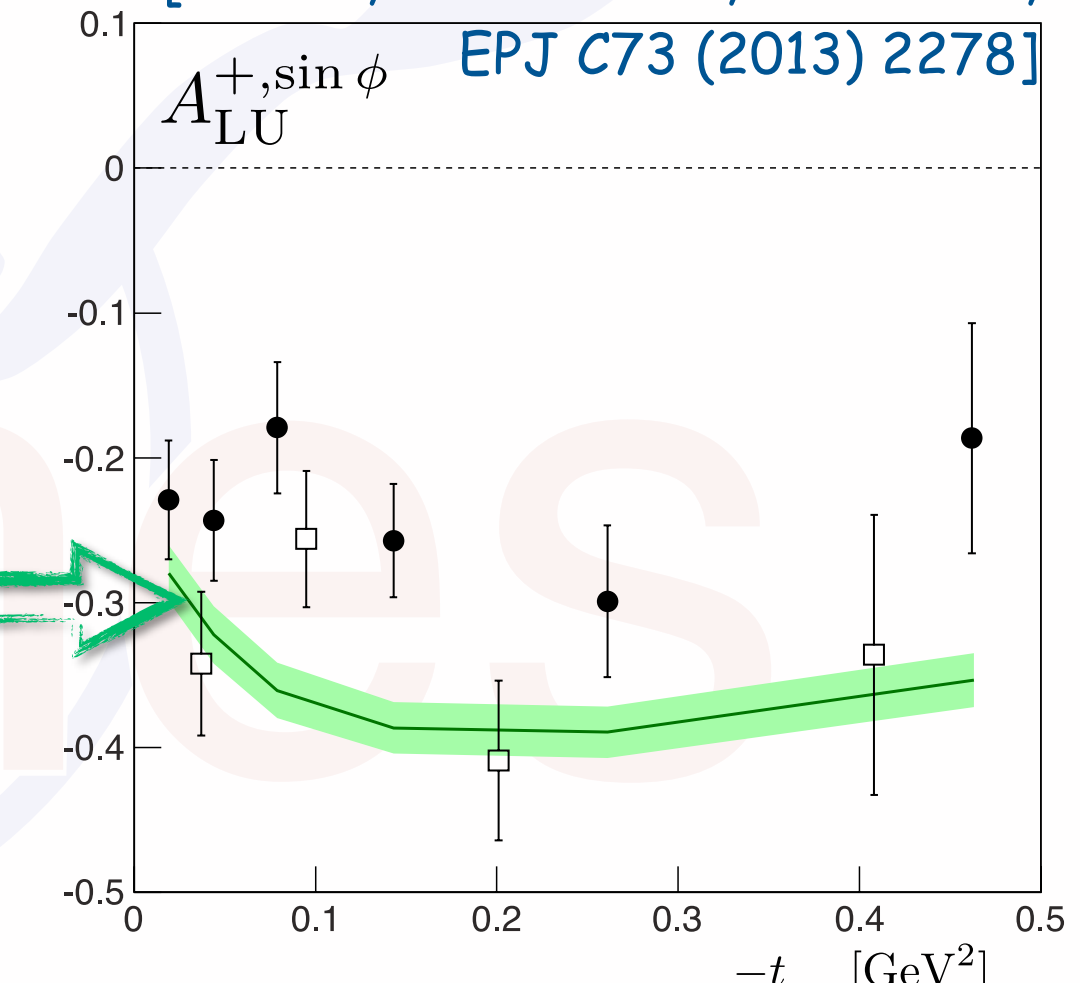
GPDs - a nice success story!



Goloskokov, Kroll (2007)

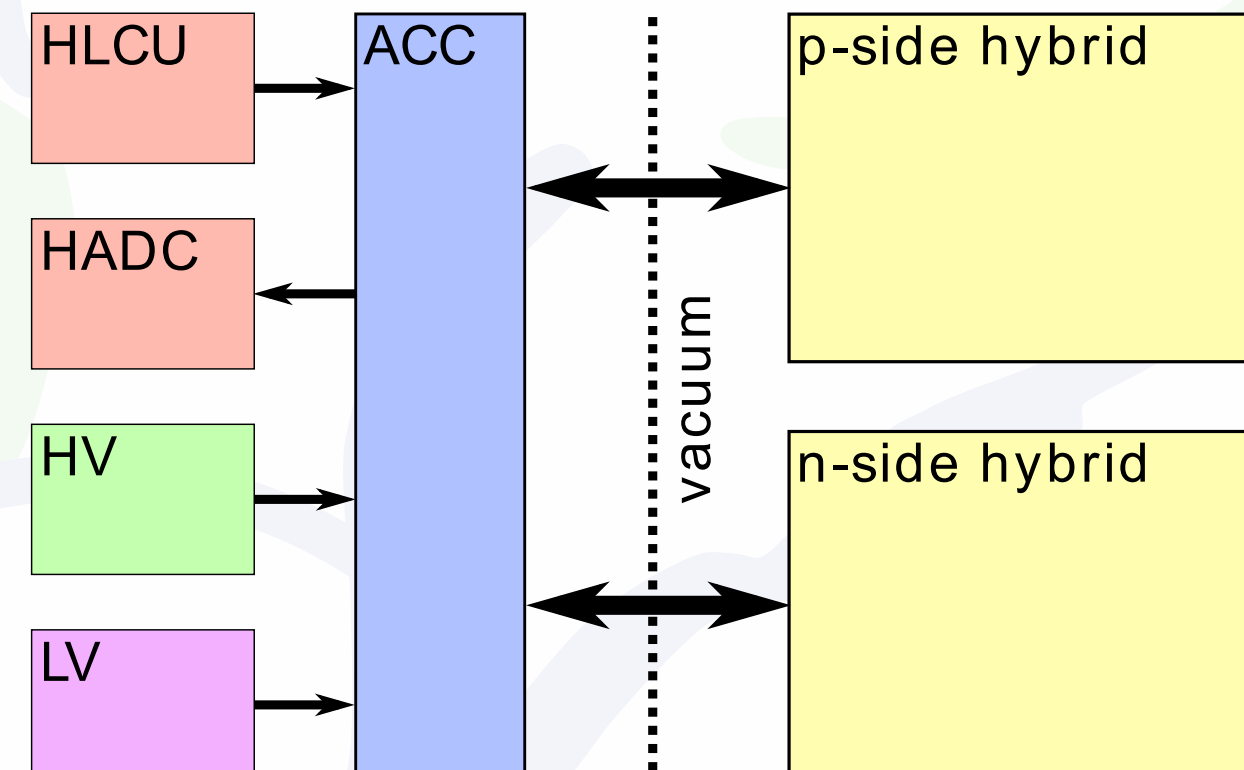
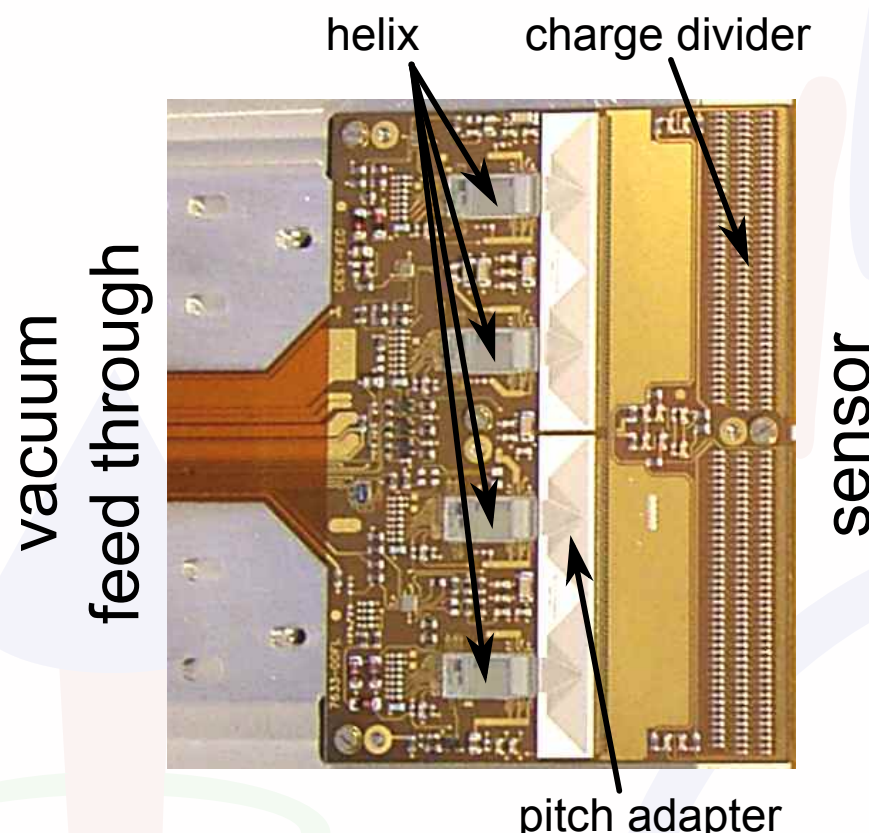


[P. Kroll, H. Moutarde, F. Sabatie,
EPJ C73 (2013) 2278]



backup

SSD (silicon strip detector)



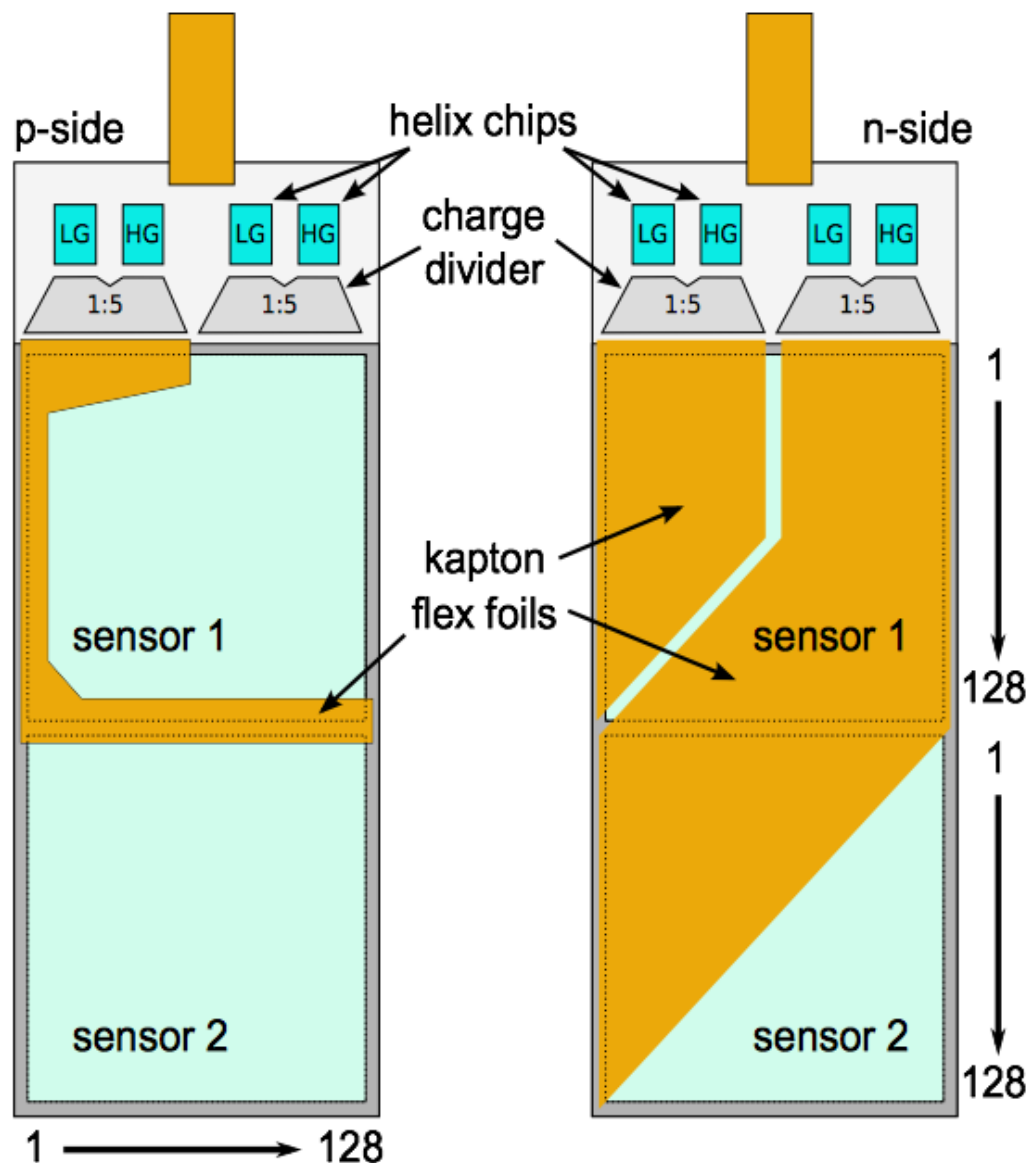
5.8 cm away from lepton beam, 1.5 cm gap

sensor thickness $295 \mu\text{m} - 315 \mu\text{m}$

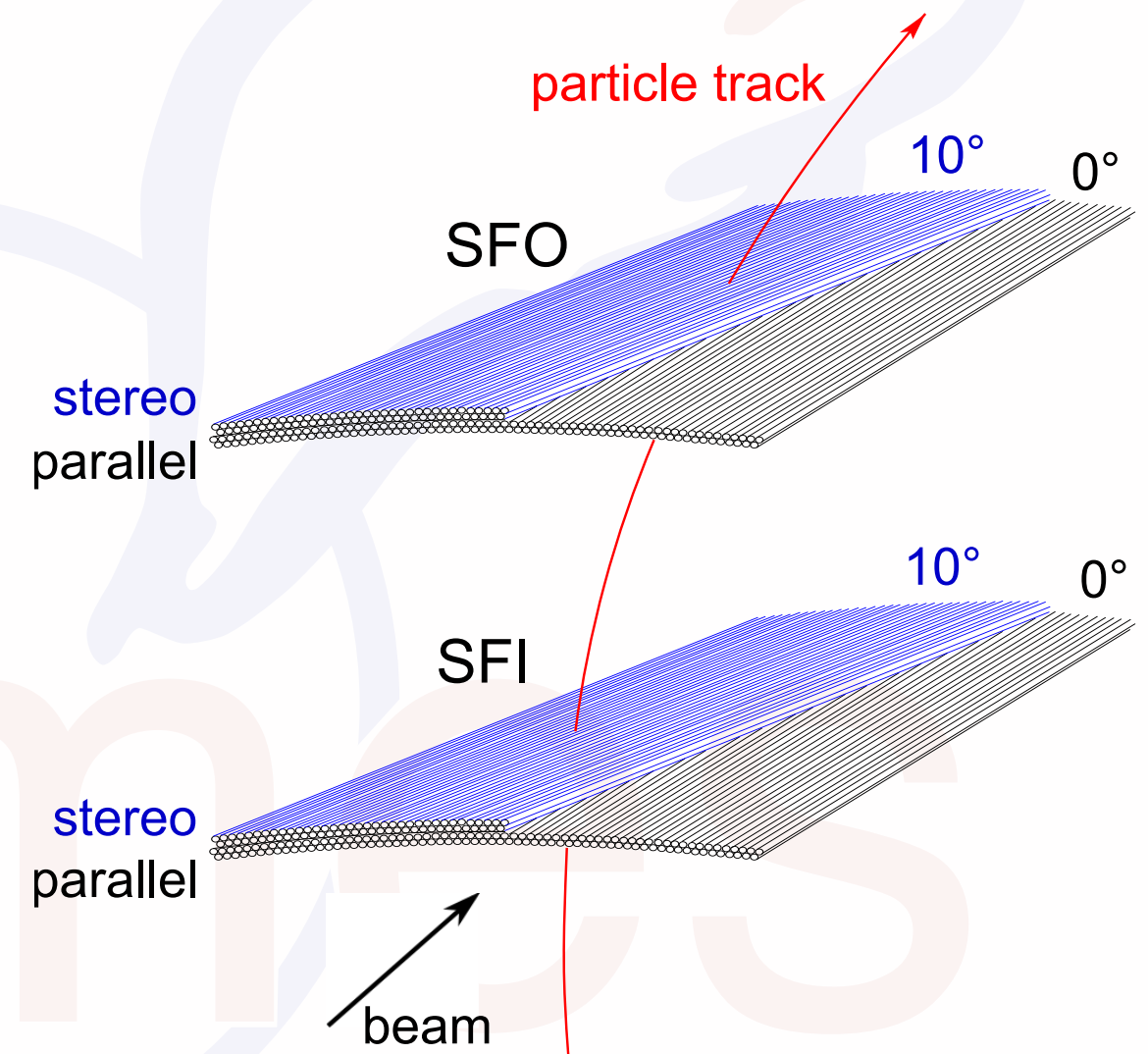
thickness of target cell $75 \mu\text{m}$

The HERMES recoil detector

Sketch of front- and backside of a silicon strip detector module (SSD)

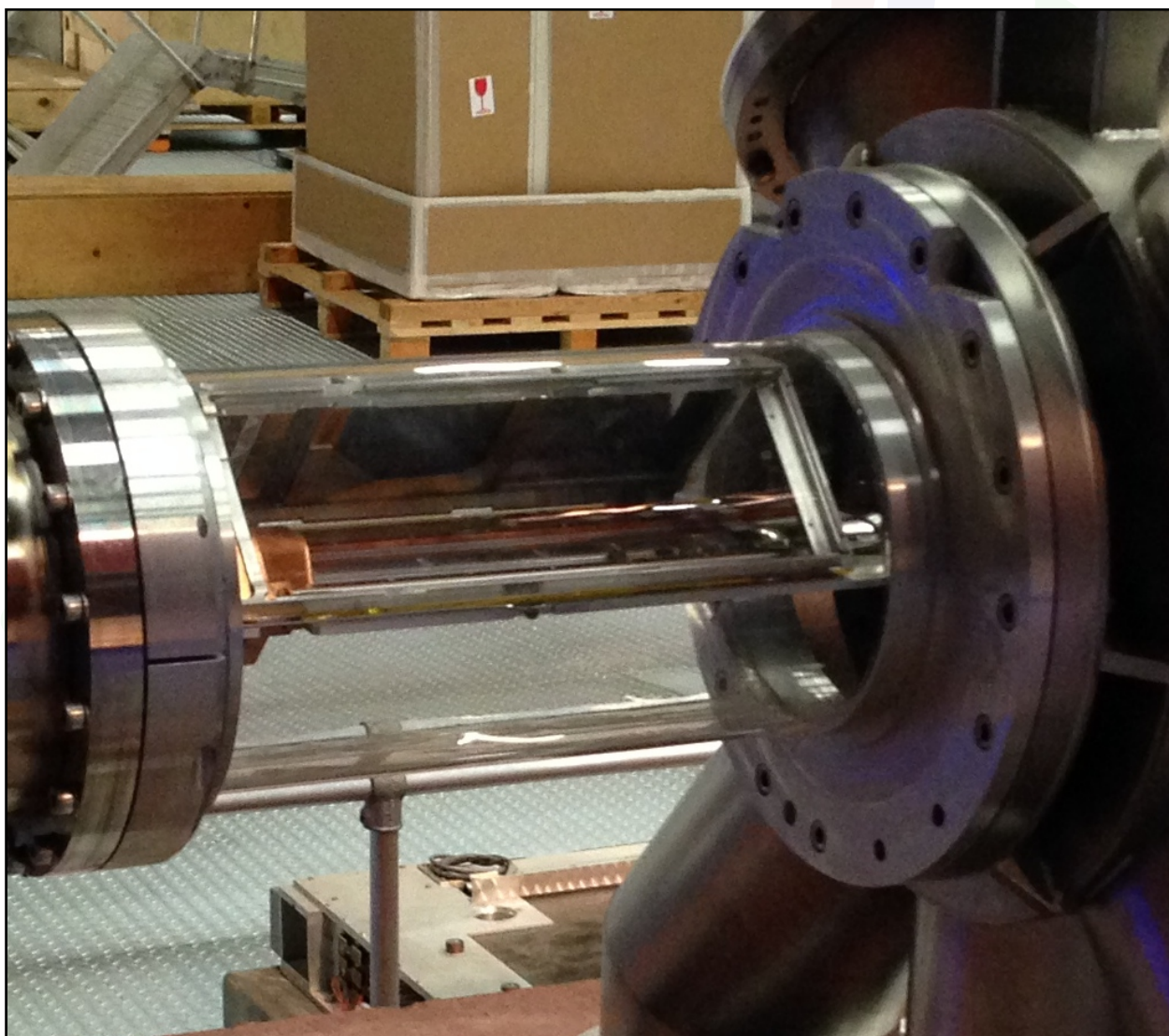


Schematic design of the scintillating fibre tracker (SFT)

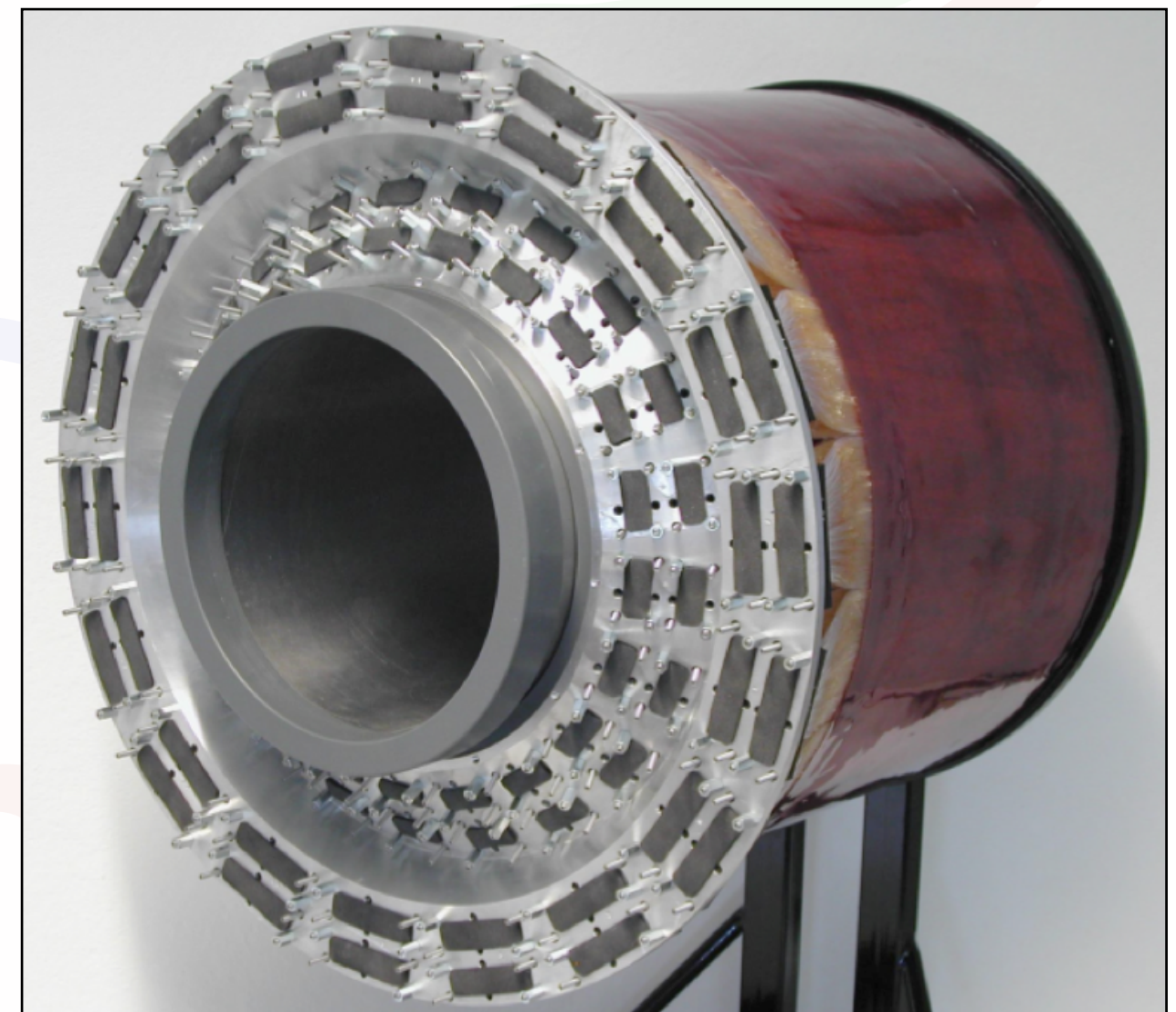


The HERMES recoil detector

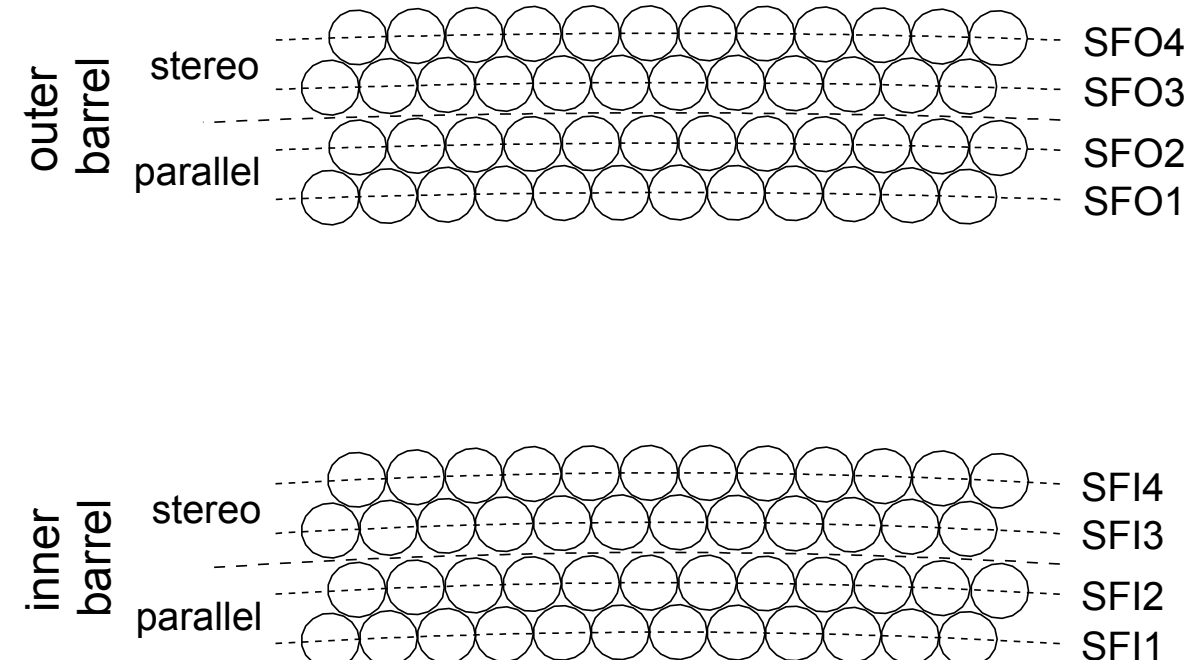
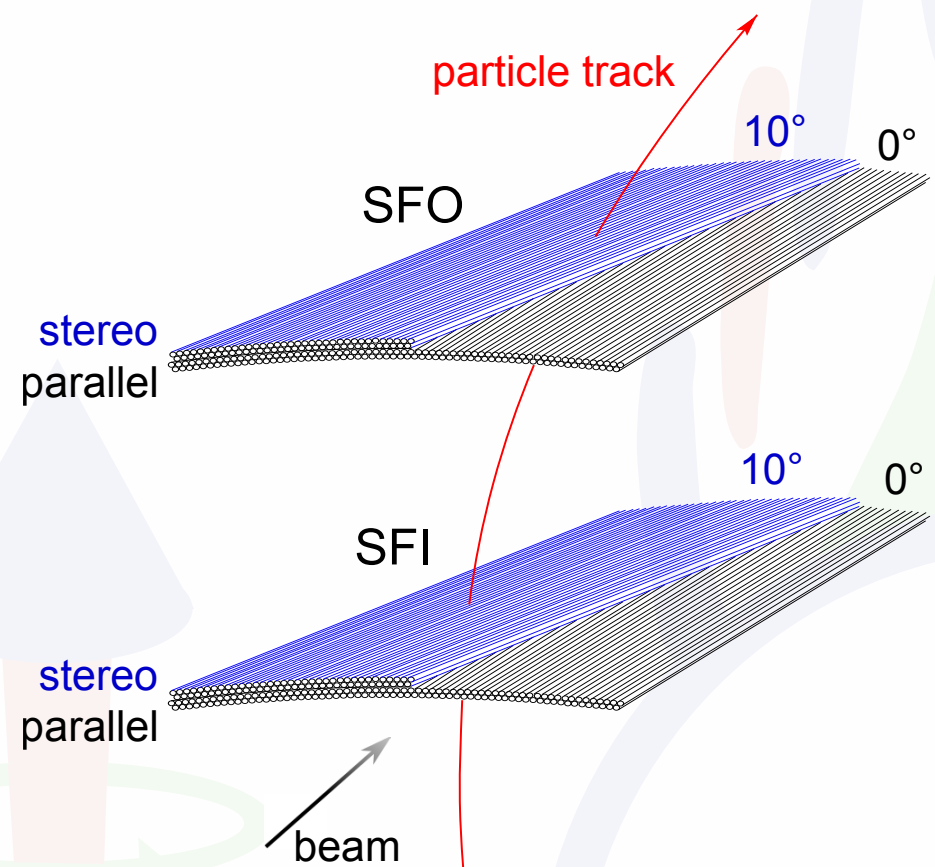
The silicon strip detector (SSD)



The scintillating fibre tracker (SFT)



SFT (scintillating fibre tracker)

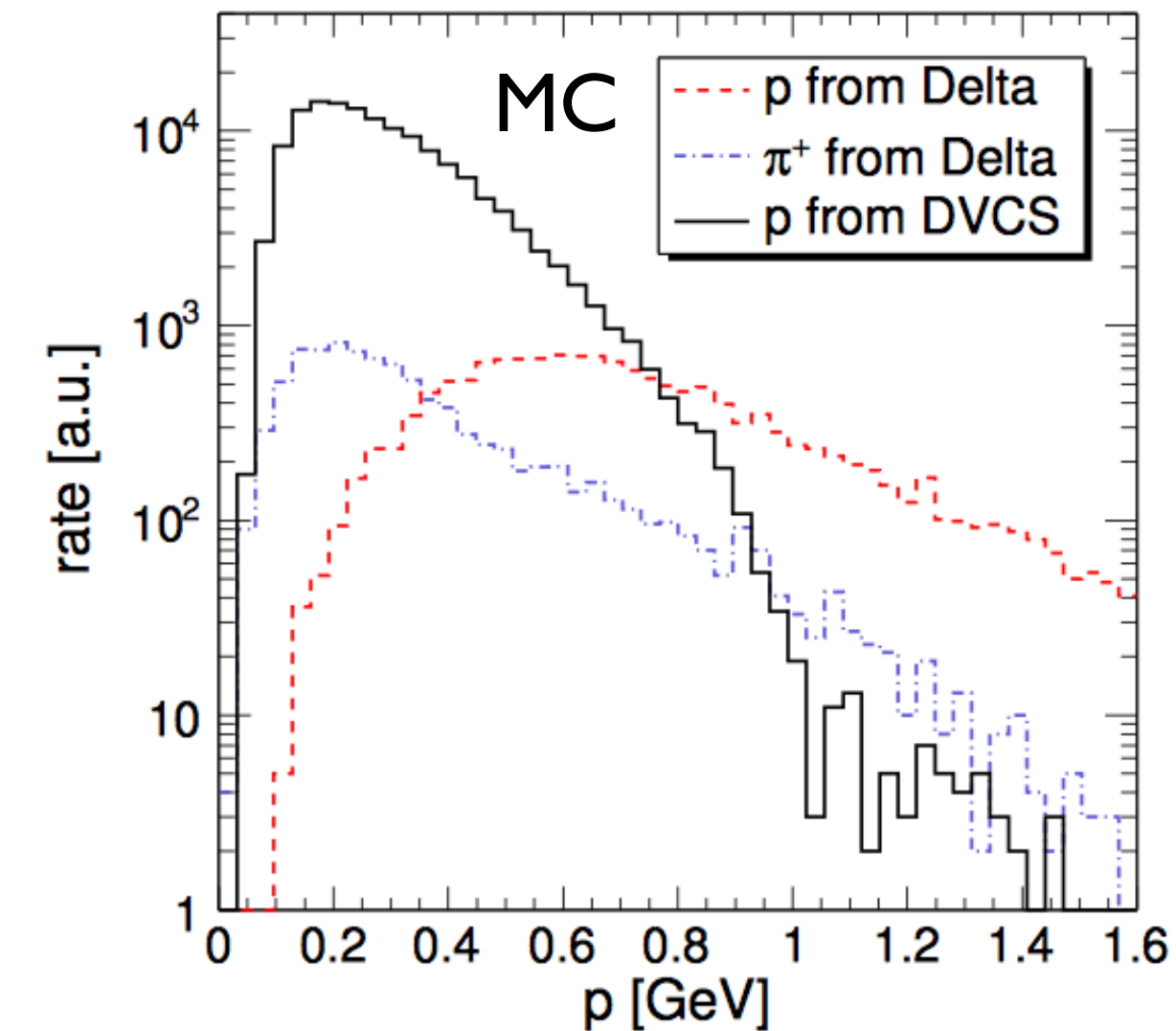
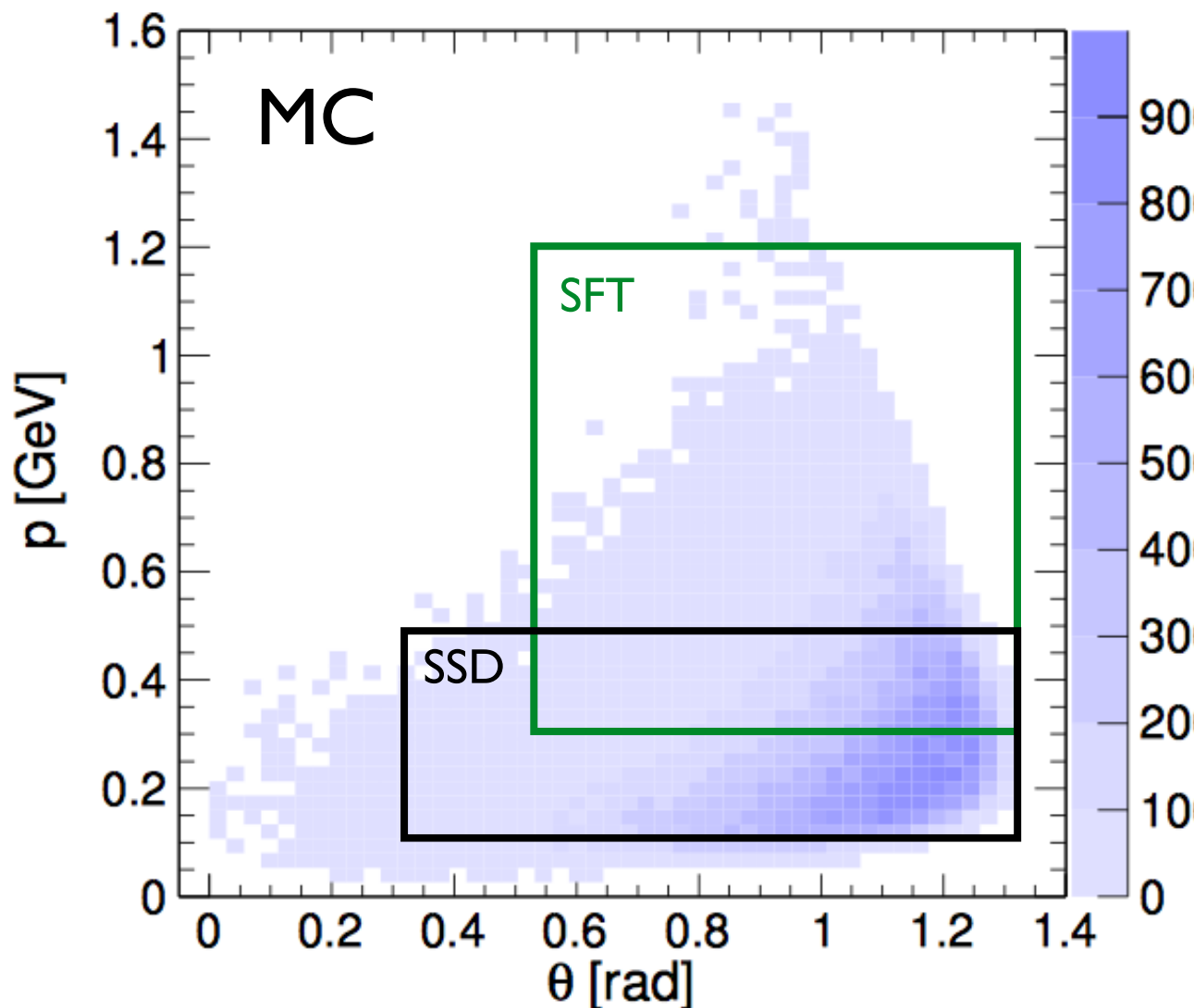


11.5 cm (18.5 cm) inner (outer) radius

1318+1320 (2198+2180) fibers with a diameter of 1 mm each

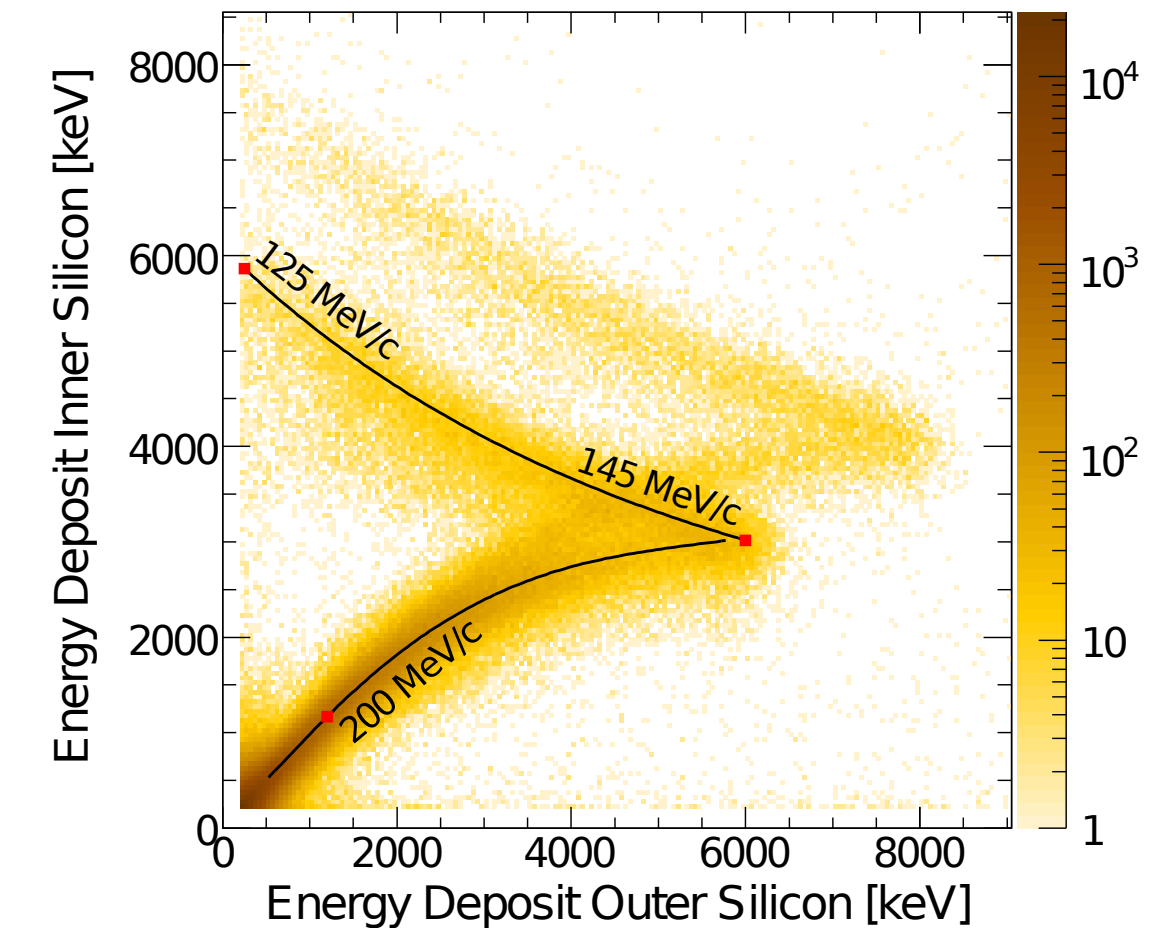
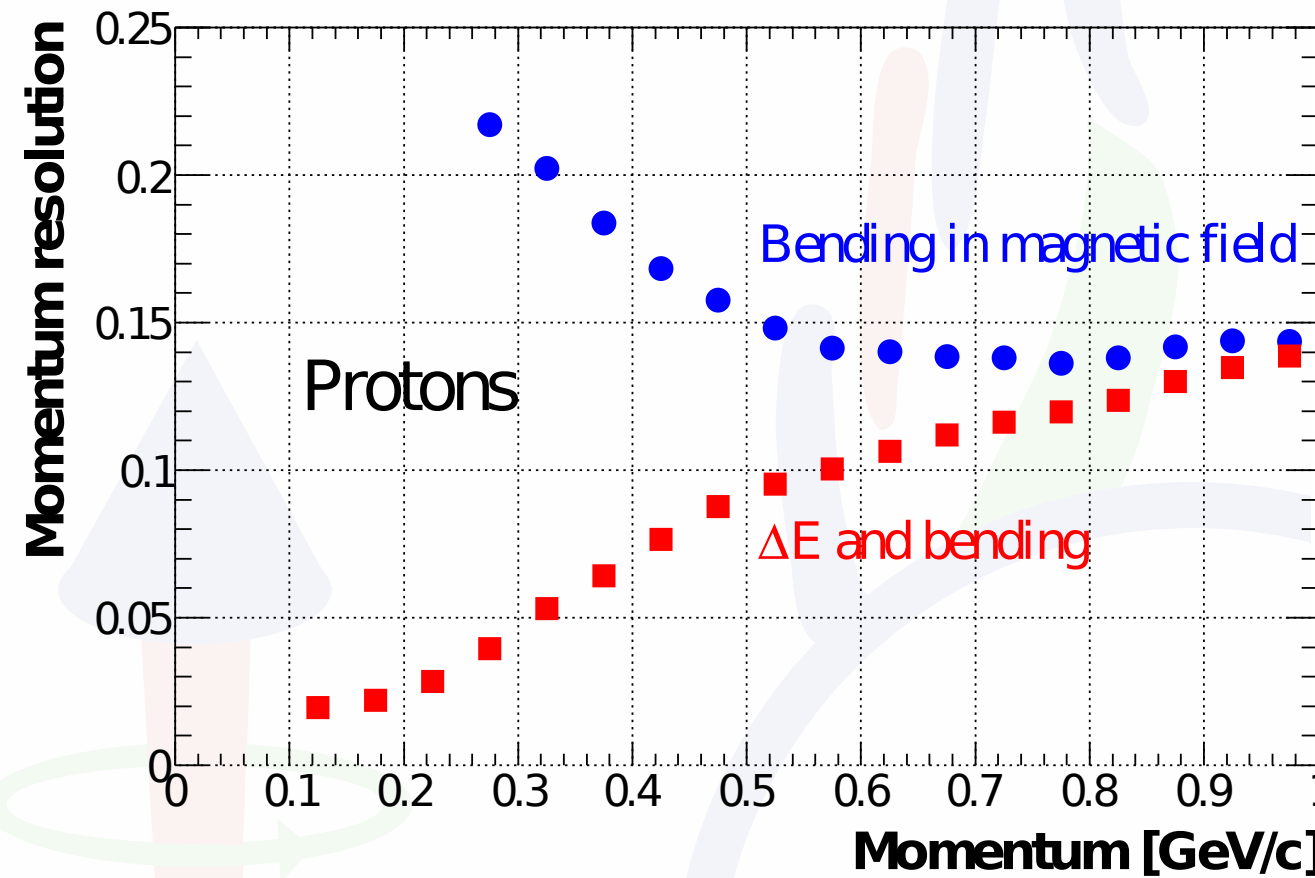
readout by 64-channel Hamamatsu H7546B MAPMTs

Kinematic coverage of the HERMES RD



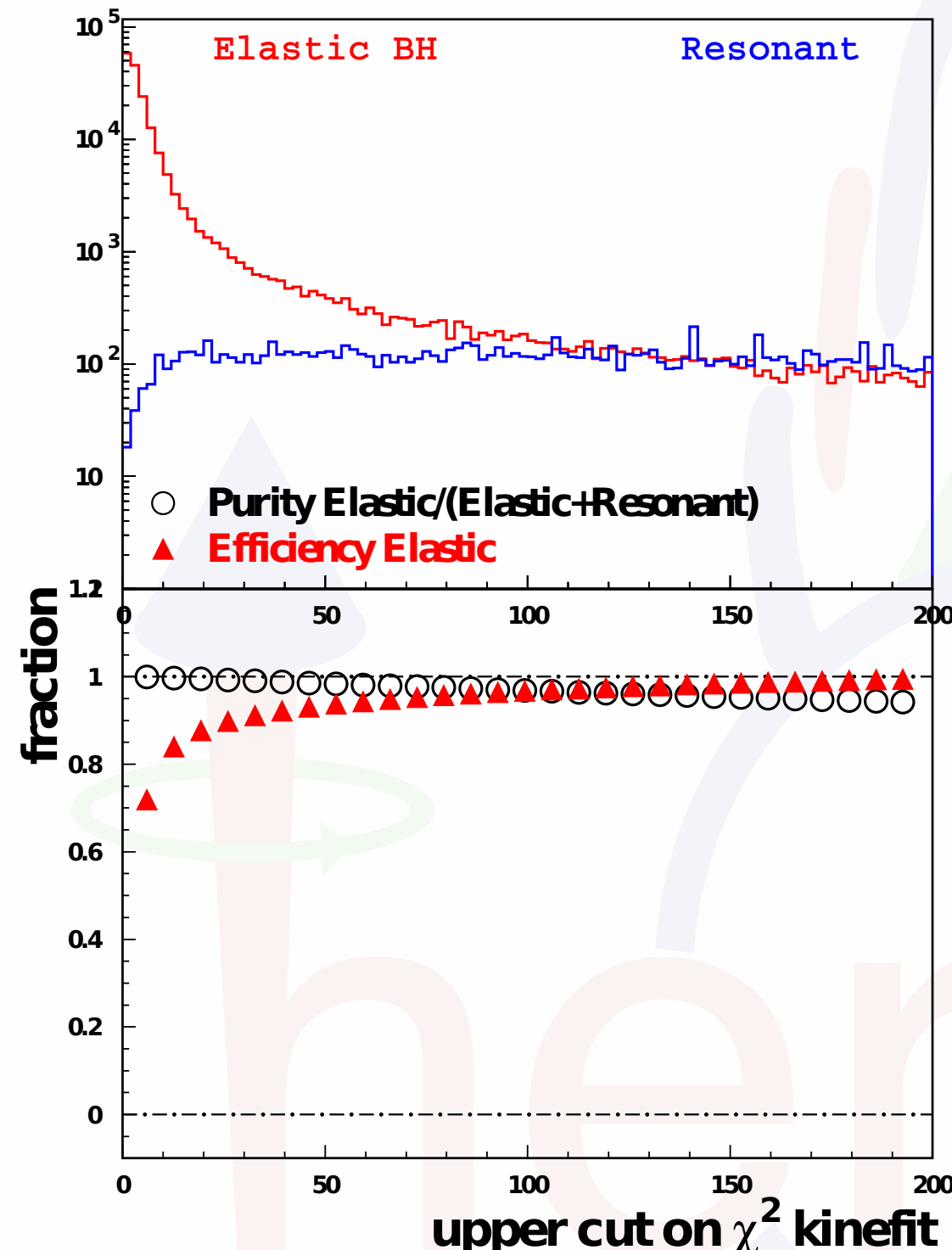
Scintillating fibre tracker (SFT) and silicon strip detector (SSD) complement each other

Recoil-detector tracking



taking energy loss into account improves momentum resolution for low p
azimuthal-angle resolution: 4 mrad
polar-angle resolution: 10 mrad (for $p > 0.5$ GeV)

Kinematic event fitting

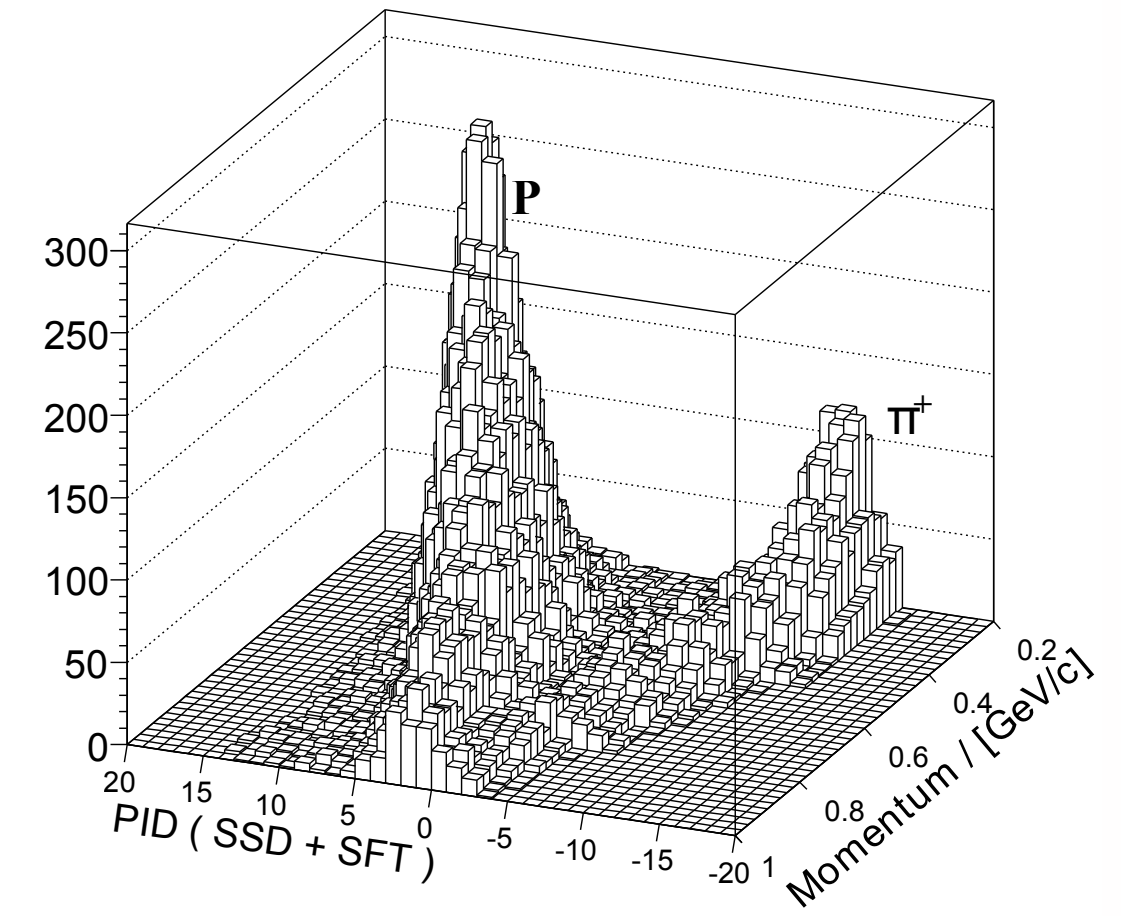
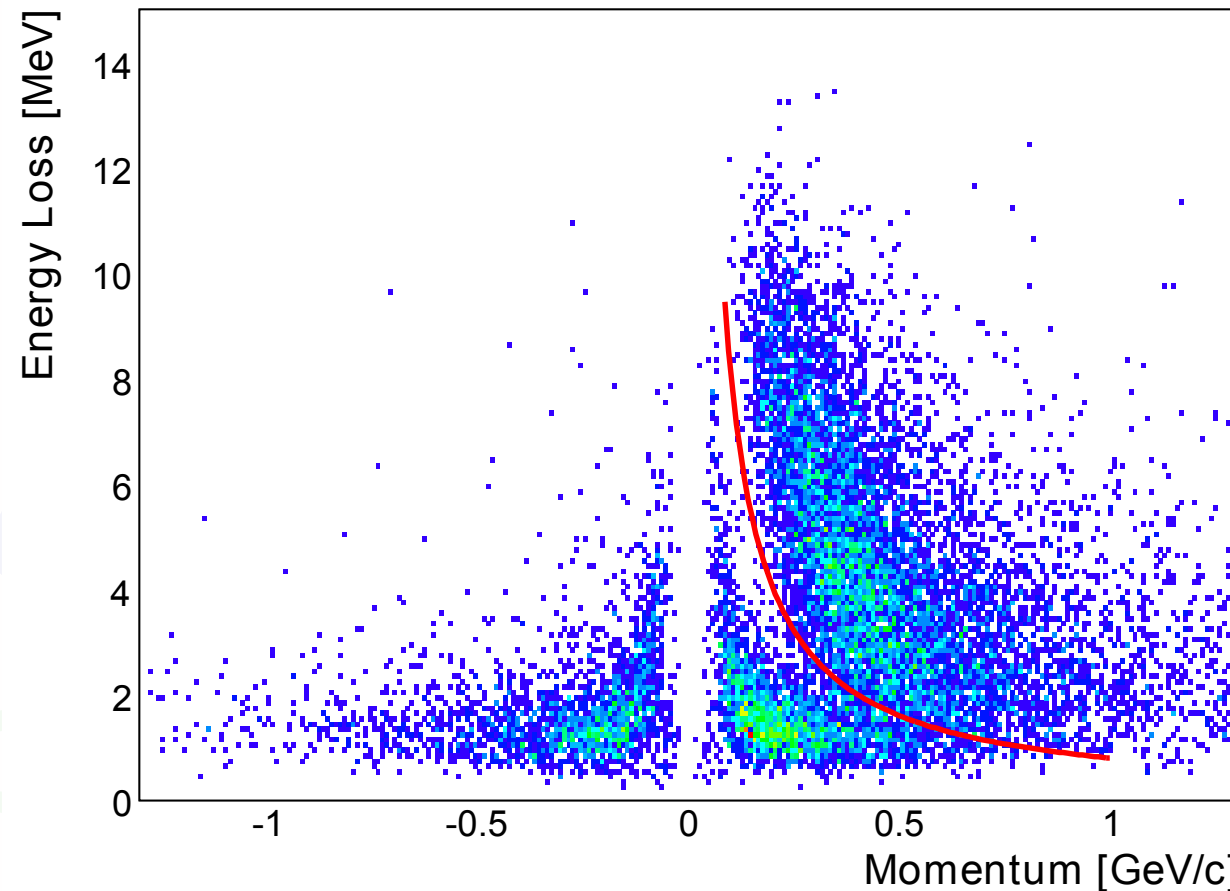


$$\chi^2_{pen} = \sum_{i=1}^9 \frac{(r_i^{fit} - r_i^{meas})^2}{\sigma_i^2} + T \cdot \sum_{j=1}^4 \frac{[f_j(r_1^{fit}, \dots, r_9^{fit})]^2}{(\sigma_j^f)^2}$$

χ^2 -value of interest penalty term constraints

- 4-momentum conservation as constraints
- lowest χ^2 -value in case of multiple recoil tracks per event
- minimum of 1 % fit probability required, which corresponds to $\chi^2 < 13.7$

Recoil PID

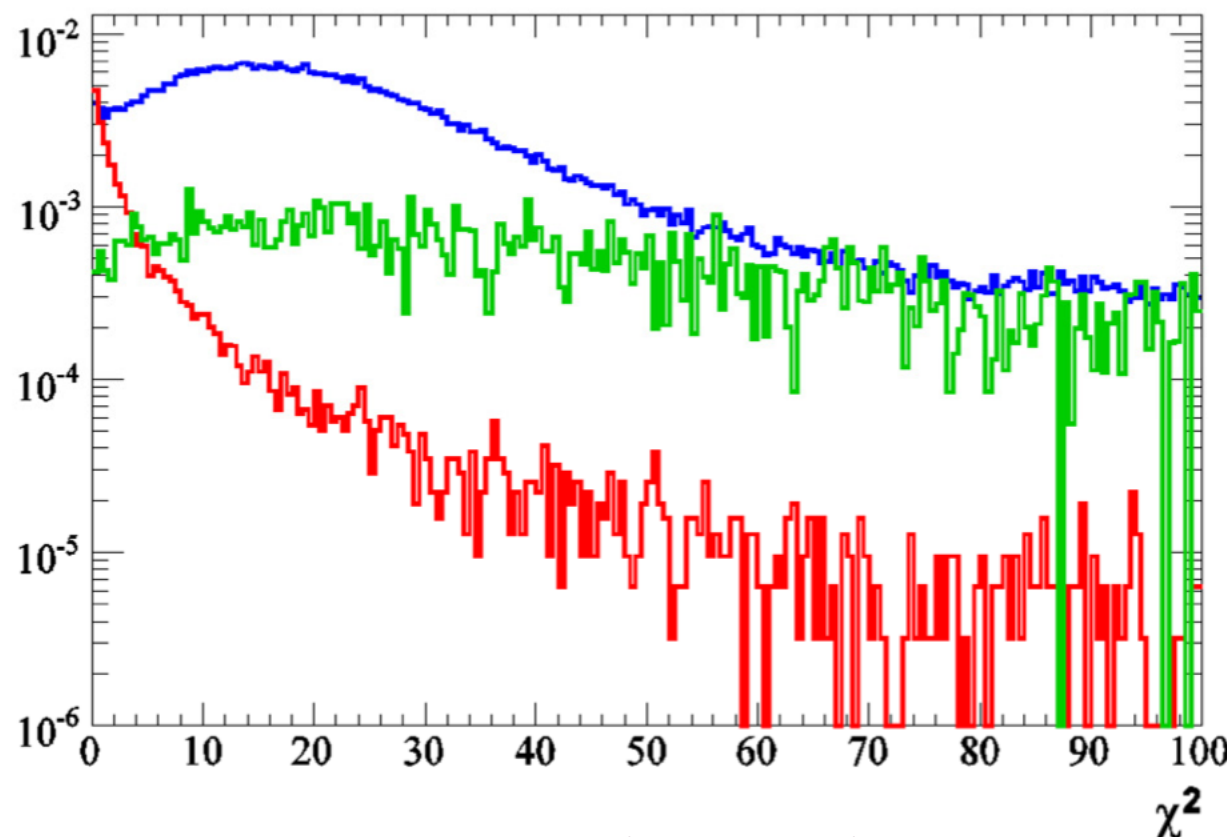


discrimination between protons and positively charged pions

parent distributions were crucial and determined experimentally

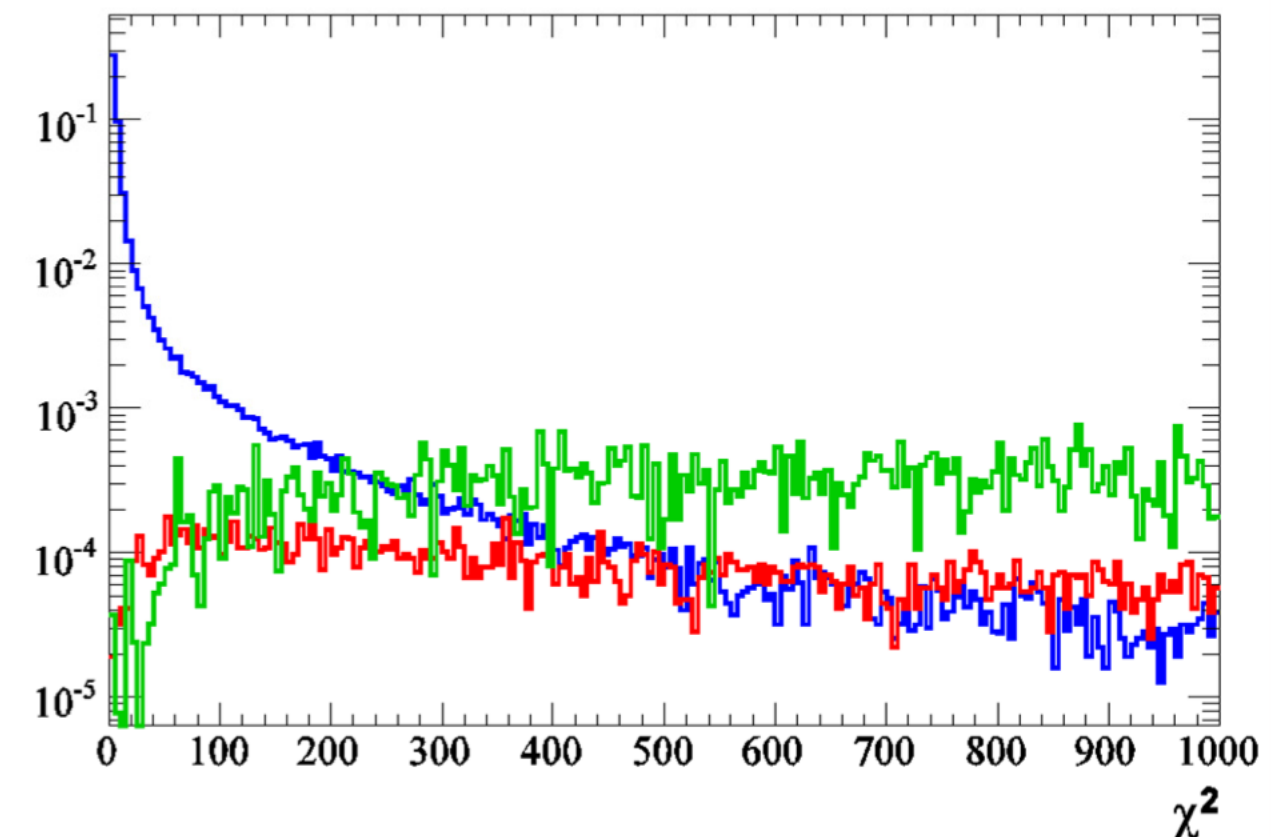
Kinematic fitting for $ep \rightarrow e\gamma p\pi^0$

$ep \rightarrow e\gamma p\pi^0$ $ep \rightarrow e\gamma p$ SIDIS



$ep \rightarrow e\gamma p\pi^0$ hypothesis

$$\chi^2_{ep \rightarrow e\gamma p\pi^0} < 4.6$$



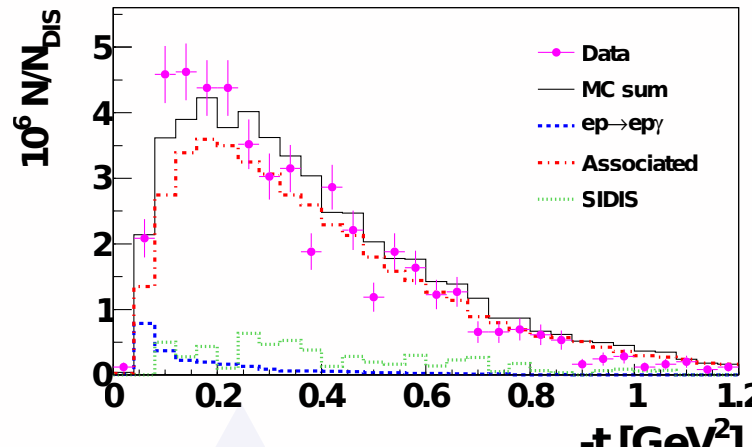
$ep \rightarrow e\gamma p$ hypothesis

$$\chi^2_{ep \rightarrow e\gamma p} > 50$$

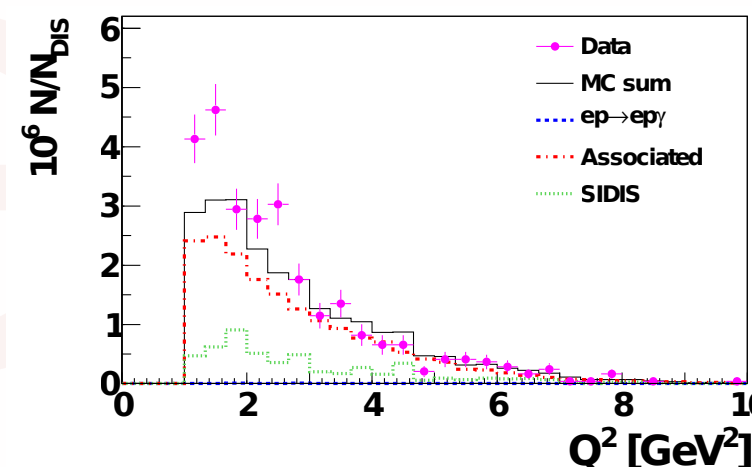
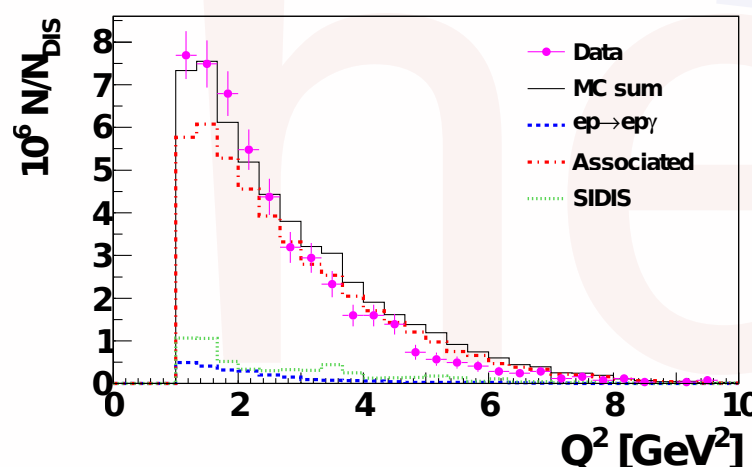
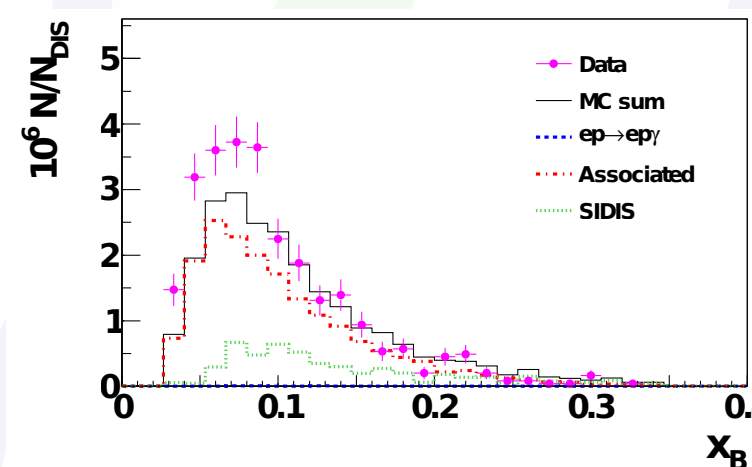
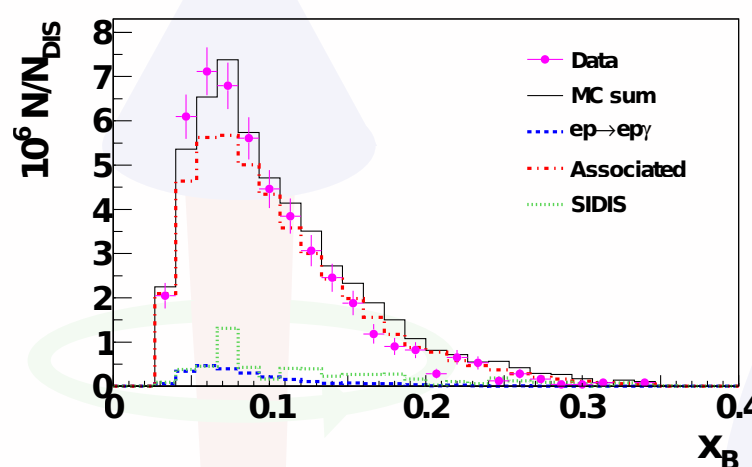
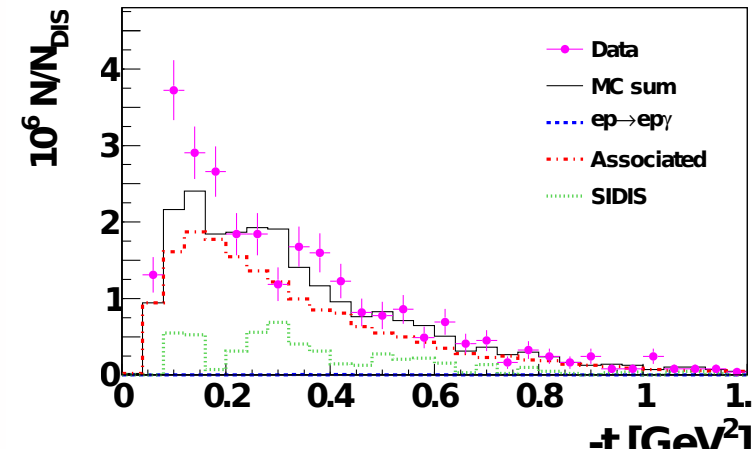
Using powerful kinematic fitting of $ep \rightarrow e\gamma p$ hypothesis
is crucial for the $ep \rightarrow e\gamma N\pi$ analysis

Selection of associated events

$ep \rightarrow e\gamma p\pi^0$



$ep \rightarrow e\gamma n\pi^+$



Uncharged particle
remains undetected

Kinematic fitting in case
of $ep \rightarrow e\gamma N\pi$ hypothesis
therefore not as strong

Additional selection criteria:

- Recoil PID information
- Lower-cut on $ep \rightarrow e\gamma p$ hypothesis